Weather and Climate of Peninsular India Modulated by Extrinsic Factors - Empirical and Numerical Perspectives

RAJESH J.

Thesis submitted in partial fulfillment of the requirement
for the Degree of

DOCTOR OF PHILOSOPHY
in
ATMOSPHERIC SCIENCES

Department of Atmospheric Sciences

COCHIN UNIVERSITY OF SCIENCE AND TECHNOLOGY
COCHIN - 682 016,
INDIA

AUGUST 2009

To Amma

Achachan

And Appachi

COCHIN UNIVERSITY OF SCIENCE AND TECHNOLOGY
DEPARTMENT OF ATMOSPHERIC SCIENCES

Lakeside Campus, Fine Arts Avenue, Cochin - 682 016, India.

Dr. K. Mohankumar M.Sc., Ph.D.
Dean, Faculty of Marine Sciences

CERTIFICATE

This is to certify that the research work presented in this thesis *Weather and Climate of Peninsular India Modulated by Extrinsic Factors-Empirical and Numerical Perspectives* is the original work done by Mr. Rajesh J under my guidance and has not been submitted for the award of any Degree or Diploma by any other University or Institution.
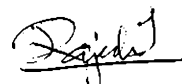
Certified that Mr. Rajesh J. has passed the Ph. D. qualifying examination conducted by the Cochin University of Science and Technology in August 2006.

Cochin 682 016

August 21, 2009

Prof. K. Mohankumar

Supervising Guide

DECLARATION

I hereby declare that this thesis entitled *Weather and Climate of Peninsular India Modulated by Extrinsic Factors - Empirical and Numerical Perspectives* is a genuine record of research work carried out by me and no part of this thesis has been submitted to any University or Institution for the award of any Degree or Diploma.

RAJESH J.
Research Scholar,
Department of Atmospheric Sciences
Cochin University of Science and Technology

Cochin 682 016
August 25, 2009

ACKNOWLEDGEMENTS

CONTENTS

PREFACE

The peninsular Indian region exhibits unique characteristics in the distribution and variation in the meteorological fields compared to other parts of the country. In order to obtain a better understanding of the diverse responses of these fields to different forcing factors, a detailed analysis of homogenous zones and subdivisions were carried out. The present doctoral thesis focuses on some of the foremost external factors that influence the weather and climate over the Peninsular India. The methods include both empirical and modeling aspects. The major outcomes of the thesis are summarized as below:

The first chapter provides a general introduction about the climatic features over peninsular India, various factors dealt in subsequent chapters, such as solar forcing on climate, SST variability in the northern Indian Ocean and its influence on Indian monsoon, moisture content of the atmosphere and its importance in the climate system, empirical formulation of regression forecast of climate and some aspects of regional climate modeling.

Chapter 2 deals with the variability in the vertically integrated moisture (VIM) over Peninsular India on various time scales. VIM from surface to various levels over the peninsular India for monsoon and post monsoon seasons was studied for the period 1950-2004. The wavelet spectrum of VIM during the summer monsoon (June-August) and post monsoon (September-November) showed an eleven-year mode of variability. The spatial extend of this mode of variability was analyzed by Fast Fourier Transform (FFT) of the VIM for the region 20^0S-50^0N and $0-160^0$ E. Spectral power of frequencies corresponding to 11 and 12 years in FFT were plotted spatially. The Spectral power shows higher values over the

Peninsular India, extending over Bay of Bengal to Indo-China peninsula during the monsoon and post-monsoon seasons. The spectrum for JJA season show highest spectral powers concentrated over regions other than peninsular India. The cross-spectral analysis between solar radio flux and the VIM indices for various seasons indicates that the power spectrum has a peak corresponding to 11-year. Compared to other seasons, monsoon and post monsoon seasons hold the higher spectral power. A possible association between moisture and air temperature in connection with solar activity is also suggested by computing the correlation of monthly solar flux and tropospheric air temperature along vertical sections of 80°E and 10°N. Though the correlations are low, a change in temperature caused by solar variability can amplify similar variability in VIM. Thus it was proposed that the influence of solar flux on the tropospheric temperature is modulating the 11-year variability in the seasonal VIM.

The wavelet analysis of Principal components of VIM for various seasons and various years revealed that the intraseasonal variability in the integrated moisture over the Arabian Sea and Peninsular India is of around 12-32 days. The EOF patterns showed that the third greatest variability over the Indian domain regarding the VIM is over the Arabian Sea and Peninsular India, though the variations account for a small percentage. The zonal coherence in the principal modes of variability over peninsular India and adjoining Seas implies that the first mode of intraseasonal variability over the Indian domain was due to the meridional temperature distribution. While the second and third modes correspond to region over peninsular India.

The third Chapter discusses the influence of solar activity in the low frequency variability in the rainfall of Peninsular India. The study also investigates the

influence of solar activity on the horizontal and vertical components of wind and the difference in the forcing before and after the so-called regime shift in the climate system before and after mid-1970s. The wavelet analysis of high frequency filtered Kerala Summer Monsoon Rainfall showed a significant mode of decadal variability corresponding to 11-12 year period. The cross-spectral analysis between solar radio flux and rainfall of eight subdivisions over peninsular India also showed spectral peeks at a frequency scale corresponding to 11 years. Significant values were obtained for the correlation maps of 4-year running mean Indian summer monsoon rainfall with F10.7 solar radio flux. The vectors of regressed coefficients between F10.7 and horizontal wind indicate that the monsoon flow in the months of July and August is influenced by solar flux and the convection also is very much influenced by solar flux, though there have been significant changes in the regions and intensity in these relations after 1976.

In Chapter 4 on Peninsular Indian Rainfall and its association with meteorological and oceanic parameters over adjoining oceanic region, a linear regression model was developed and tested for the seasonal rainfall prediction of Peninsular India. The parameters used as predictors are (i) lower tropospheric temperature during the month of May over the Peninsular India and adjoining Bay of Bengal (ii) Sea Surface Temperature during the month of March over the mid-Indian Basin over the Indian Ocean (iii) Zonal wind at 700 hPa during February and (iv) meridional wind at 700 hPa during January. The period of analysis was from 1975-2006 of which last nine years were tested against the observed rainfall. The empirical model could explain 77% of the total variance in the PIR and has a RMS error of 7.6%, BIAS of 0 mm and an absolute error of 40.2 mm. Except 2002, the model could capture the extreme years reasonably good.

3

Chapter 5 deals with the effects of Arabian Sea surface temperature on the summer monsoon over peninsular Indian region. The characteristics of circulation, moisture and precipitation during monsoon season over the Peninsular Indian region is investigated on the basis of the sensitivity experiments performed by a regional climate model (RegCM3) for the years 1996, 1997 and 2002. The model is run from 1st May to 30th September except for 2002 for which the ERA40 data is available only till August. The first month is taken for the spin up. The next four months are taken to study the monsoon. RegCM3 has been integrated at 60 km horizontal resolution over the Indian domain. The experiments were carried out by changing the initial conditions of sea surface temperature by 0.1^0 C steps *i.e.* 0.1, 0.2, 0.3, etc. to 1^0 C maximum. The RegCM3 model successfully simulates some important characteristics of the Indian summer monsoon such as the 850-hPa westerlies and precipitation. Even though the precipitation is overestimated the model is found to be capable of simulating the monsoon rainfall to a reasonable degree in spatial distribution, particularly the large-scale precipitation zones owing to the southwesterly monsoon flow.

The influence of moisture over the Northern Indian Ocean on the climate of Peninsular India has been studied and reported in Chapter 6. In this chapter, the influence of moisture in the low-level monsoon flow through the western and southern lateral boundary of the model domain on the vertically integrated moisture, precipitation, surface air temperature and integrated moisture transport are studied using RegCM3. In the southern boundary experiment EXP_SB, when the moisture influx to the domain through the southern boundary was shut down, an increase in the vertically integrated moisture is noted over the southern peninsular India for the wet year 1996, normal year 1997 and dry year 2002. But

4

for the western boundary experiment, EXP_WB, the integrated moisture has substantially reduced implying that the total column moisture is mainly fed by the western boundary stream rather than the compensation by evaporation from the Arabian Sea or the meridional transport through the southern boundary. The largest decrease in moisture fields is noted for the wet year 1996 and the lowest change is for the dry year. A sharp decrease in moisture over the Arabian Sea is also observed. For precipitation, a negative anomaly is noticed for all the three years over the Western Ghats and the Adjoining Arabian Sea, with the greatest decrease for the wet year. Surface temperature anomaly patterns are observed with a decrease in temperature where the moisture was anomalously low. This could be due to the fact that the dry air allows for greater evaporation and thus facilitating cooling in surface air temperature. The vertically integrated moisture transport anomaly vectors for EXP_WB are double the order of magnitude larger than the EXP_SB implying a more significant role of moisture through western Arabian Sea than the moisture advected meridionally through southern boundary. The intraseasonal variability in the zonally averaged precipitation over Peninsular India shows that the precipitation pattern and its distribution in time have been mostly modified for the wet year. In all the three experiments the EXP_WB showed reduction in precipitation for the first half of the season owing to the reduced moisture.

The final Chapter gives the general summary and conclusions about the overall aspects of the study. The major findings of the study are also discussed in this chapter.

CHAPTER 1

INTRODUCTION

1.1   Monsoon

The seasonally varying circulations associated with the annual contrast in heating of the Asian continent are the most important large-scale aspects of the general circulation of the atmosphere, which is called *Asiatic Monsoon*. Figure 1.1 shows the region of global monsoon. The Indian summer monsoon affects the lives and the economies of many countries in Asia. The study of this phenomenon has been mainly limited to the Indian subcontinent whereas it takes place over the entire Indian Ocean. The main aspects of the monsoon are defined as follows. There should be a 120 degree shift in the direction of prevailing wind between January and July. The Average frequency of prevailing wind must be greater than 40% and the mean wind in either January (for winter monsoon) or July (for summer monsoon) must be greater than 3 m/s. It is believed that the differential heating of the land and ocean which leads to the formation of a pressure gradient gives the driving force for monsoon circulation. The Coriolis force deflecting the cross equatorial winds created by the pressure gradient causes the typical monsoon flow. The moist processes such as the release and absorption of latent heat determine the energetics of monsoon.

There are two components of monsoon moisture input; moisture due to actual evaporation from the Arabian Sea and that due to a water vapor flux from the Southern Hemisphere (cross equatorial transport). The greatest amount of moisture flux from the Southern Hemisphere is along the east African coast and is transported due to *low-level Somali jet*, which is a typical feature of the

monsoon. This jet stream originates from a high-pressure system *Mascarene anticyclone,* formed over southeast Indian Ocean. From this high, large outflow of air takes place and it crosses the equator as cross-equatorial Somali jet and due to Coriolis force the wind becomes southwesterly. Reaching at maximum intensity in the summer months, it crosses the southern Arabian Sea and reach over central western and southern coast of India. Variation in the intensity of this jet stream is important in determining the moisture and rainfall over India. The Tibetan high-pressure system, which is an upper level anticyclone found above the surface monsoon trough located over north India is established over Tibetan High lands during July and is well developed at 200hPa level. It remains up to the end of summer season and then moves south-southeast direction with the movement of maximum heating to south. The outflow of air from the southern flank of Tibetan anticyclone gives rise to tropical easterly jet and it remains from June to September
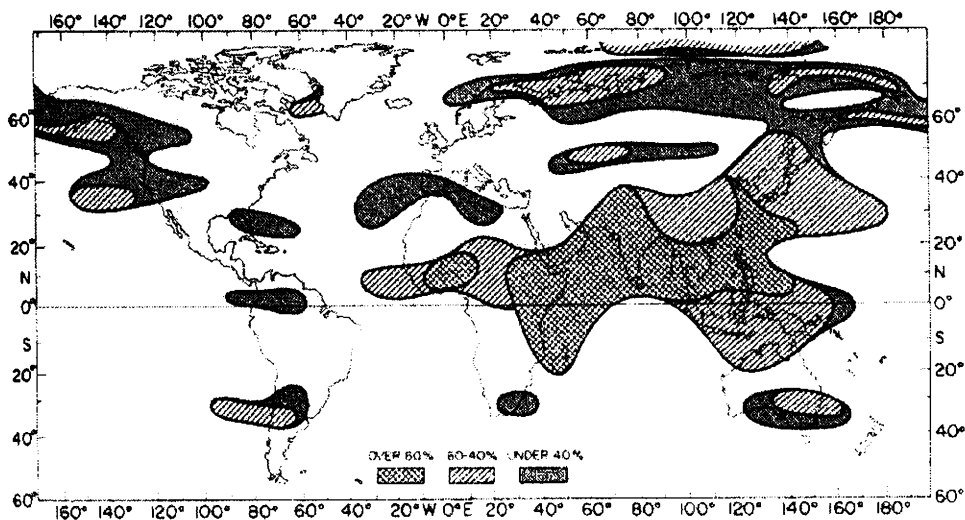
Fig. 1.1 The geographical extend of monsoon. Average frequency of predominant surface wind directions shown in three categories. Unshaded areas are non monsoonal. (Adapted from Ramage 1971)

For India, Monsoons (both southwest and northeast) are responsible for the majority of India's annual rainfall. About 80% of the annual total rainfall is

received between the months of June and September. Orographic effects are important in determining the amount of rainfall at a particular station (*Nair and Mohanakumar, 2009*). Stations on the windward side of mountains receive more rainfall than those in the rain shadow region on the leeside. This factor plays a vital role over the west coast of Peninsular India. The rainfall over Central India is largely affected by monsoon depressions moving in from the Bay of Bengal and also by convergence due to the monsoon trough over central India. It is formed in the summer months as extension of Inter Tropical Convergent Zone (ITCZ) and is the region of low pressure and wind shear at the surface. South of the trough has southeasterly winds and north has northwesterly winds. Monsoon trough during south west monsoon exists parallel to about ~500 km south of the Himalayas. An inversion layer at 800hPa which hinders the instability would produce precipitation. The mean precipitaion and winds over in Indian region during winter and summer are given in Fig 1.2

As the onset vortex moves to the north, westerlies increase sharply on the equatorward (convergent) side of the vortex. Stations on the west coast are influenced by these westerlies as well as the position of the onset vortex. But for the east coast of India, as monsoon depressions moves across, it moves into regions that may not have previously been affected by heavy rains. Stations in central India experience heavier rains than before because they are not as affected by the southwest flow as stations on the west coast. Another characteristic feature of the south west monsoon is the active and break phases. Breaks occur normally in the middle of August. During a break, monsoon trough moves north and the maximum rainfall shifts towards the foothills of the Himalays. Low-level westerlies also move north to the Gangetic Plain and decrease in strength over the Peninsular India.

8

The monsoon usually starts withdrawing during the end of September from North India. Pressure gradient undergoes transition to a winter pattern (reverse conditions of what occurred in the summer pattern) and the easterlies in the upper troposphere weaken. Monsoon trough moves to the south and the westerly jet appears. The Inter tropical convergent zone moves back to the south.
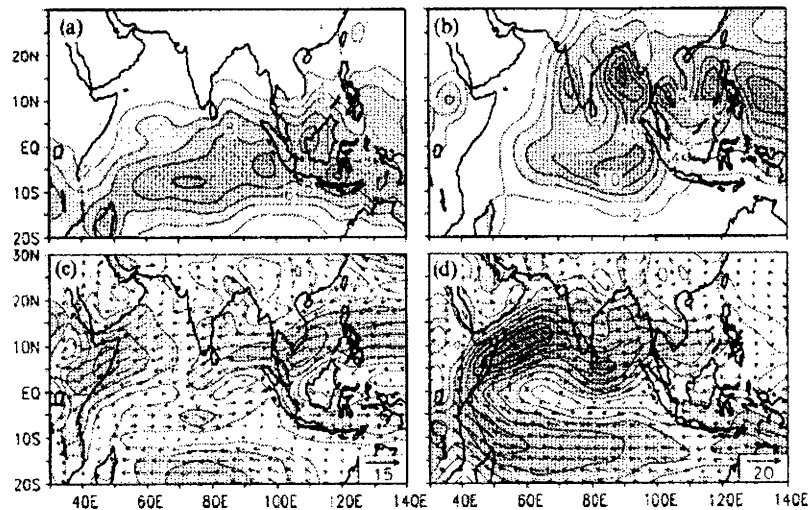
Fig. 1.2 Climatological mean precipitation (unit: mm day-1) during (a) boreal winter (DJF) and (d) summer (JJA). (b) and (c) are the same as (a) and (d) but for winds (unit: ms-1) at 850hPa based on NCEP reanalysis. The contour interval for isotachs is 2 ms-1 with the minimum contour being 2. Adapted from *Goswami, (2005)*.

The monsoon cloud cover is the manifestation of moist convective processes over the Indian subcontinent and it varies both in space and time. During active phase of monsoon, cloud cover is maximum in a belt running from western shore of Bay of Bengal to northern shore of Arabian Sea and minimum over foothills of Himalayas, south India and Sri Lanka. The pattern reverses during break phase and rainfall distribution closely follows the cloud distribution.

Besides possessing the largest annual amplitude of any subtropical and tropical climate feature, the monsoons also possess considerable variability on a wide range of timescales. Within the annual cycle there are large-scale and high-amplitude variations of the monsoon. On timescales longer than the annual cycle the monsoon varies with biennial, interannual, and interdecadal rhythms. In the following sections an attempt is made to describe these variations.

1.1.1 Intraseasonal variability

Intraseasonal variability of the Indian summer monsoon, delineated by active periods of heavy rainfall interrupted by break periods, significantly modulates the seasonal mean monsoon fields *(Krishnamurthy and Shukla 2000; Goswami and Ajayamohan 2001)*. These active and break spells of the monsoon are associated with fluctuations of the tropical convergence zone *(Yasunari 1979, 1980, 1981; Sikka and Gadgil 1980)*. Tropical convergent zone over the Indian monsoon region represents the ascending branch of the regional Hadley circulation. The intraseasonal oscillations (ISOs) of the Indian summer monsoon represent a broadband spectrum with periods between 10 and 90 days but have two preferred bands of periods *(Krishnamurti and Bhalme 1976; Krishnamurti and Ardunay 1980; Yasunari 1980)*, one between 10 and 20 days and the other between 30 and 60 days.

Several recent modeling studies show that a significant fraction of the interannual variability of the Indian summer monsoon is governed by internal chaotic dynamics *(Hazrallah and Sadourny 1995; Goswami 1998)*. Because the separation between the dominant ISO periods and the season is not large, the statistics of the ISOs could, in principle, influence the seasonal mean monsoon and its interannual variability.

Starting from around the mid to late 1970s, a number of studies began to identify intraseasonal fluctuations with periods around 30-60 days, associated with the Asian summer monsoon. These were well observed in both cloudiness *(Murakami 1976; Yasunari 1979, 1980)* and wind variability *(Dakshinamurti and Keshavamurty 1976; Murakami 1977)*. The canonical space-time structures of a typical boreal summer ISO event have been well represented by *Chen and Murakami (1988), Goswami et al (1998), Annamalai et al (1999), Annamalai and Slingo (2001), Lawrence and Webster (2002)* and *Hsu et al (2004)*.

In addition to the nominal time scale of 30-60 days, there also exists considerable intraseasonal variability at higher frequencies, at time scales around 10-20 days. Identification of these higher frequency fluctuations came from early studies on cloudiness and conventional synoptic observations *(Krishnamurti and Bhalme 1976; Murakami 1976; Yasunari 1979; Krishnamurti and Ardanuy 1980)*. 10-20 day mode accounted for about a quarter of the sub-seasonal monsoon variability while 30-60 day accounted for about two third *(Annamalai and Slingo 2001)*. In contrast to the low frequency ISO, variability of this mode is focused almost entirely over East Asia and the northwest Pacific region. Also 30-60 days mode originate in equatorial Indian Ocean and propagate northward/northeastward *(Kripalani et al 1999; Singh and Kripalani 1985, 1986, 1990; Kripalani et al 1991)* but 10-20 days mode originates in the equatorial western Pacific and propagates westward/northwestward in the form of Rossby waves at about 5 ms^{-1}. Another noteworthy feature of 10-20 days mode is that it possesses a relatively strong seasonal variation, in particular during the first half of the summer monsoon period (May-July). The 30-60 day variability prevails near the equator in particular over India, as compared to ISV of 10-20 days.

1.1.2 Interannual variability

Seasonal mean prediction and predictability experiments with General Circulation Models (GCM's) indicate that a significant fraction of observed interannual variability (approximately 50% or more) of the Indian summer monsoon may be due to internal low frequency variability *(Goswami 1998)*. The internal low frequency variability acts as a background of unpredictable noise mixed with the predictable externally forced signal. Improvement in seasonal mean prediction would require successful extraction the signal from the background of noise of comparable magnitude. *Goswami and Xavier (2005)* carried out a numerical study using only annual cycle of solar external forcing and annual cycle of SST as boundary forcing. It is shown by their study that model simulates interannual variability of the Indian monsoon comparable in amplitude to the observed interannual variability. Any interannual variability of the simulated Indian summer monsoon (or any other climate system for that matter) is, therefore, of internal origin.

Observational studies have shown that there may be two time scales in the interannual variability of the monsoon-ocean-atmospheric system i.e. a quasi-biennial system with the tropical biennial oscillation (TBO) and a 4–6 year cycle associated with the El Nino Southern Oscillation (ENSO). These two scales are observed in a range of parameters like rainfall, surface pressure, wind and SST *(Meehl 1987; Lau and Shen 1988; Rasmusson et al 1990; Barnett 1991; Meehl 1993). Meehl (1994)* has proposed that the variability of the Asian monsoon is closely tied to the warm and cold phases of the TBO. *Shen and Lau (1995)* have suggested that the Asian monsoon as a whole may be more tightly coupled to the tropical ocean atmosphere on the time scales of TBO rather than ENSO. Long term climate simulations by most of the general circulation models suggest that approximately 30-40% of the variability in the Indian

12

summer monsoon precipitation is attributable to SST /Sea Ice variations, *(Folland and Rowell 1995)*. In other words, a large part (60-70%) of the interannual variability of the Indian summer monsoon may be due to internal dynamics. While seasonal predictions of the mean rainfall in other parts of the tropics is not sensitive to small changes in the initial condition, simulation of seasonal mean Indian monsoon rainfall has been found to be sensitive to small changes *(Palmer and Anderson 1994)*.

1.1.3 Long-range forecast of Indian Monsoon

Due to the intrinsic complexity, the predictability of day-to-day weather patterns in the tropics is restricted to 2–3 days. But the seasonal mean monsoon circulation in the tropics is potentially more predictable. This is due to the fact that the low-frequency component of the tropical variability is primarily forced by slowly varying boundary forcing such as sea surface temperature (SST), land surface temperature, soil moisture, snow cover which evolves on a slower time scale than that of the weather systems themselves. Observational studies have established that the Indian Summer Monsoon Rainfall is linked with several surface boundary conditions like east Pacific SST, Indian Ocean SST, Eurasian and Himalayan snow cover and land surface temperature. However data analysis and numerical modeling studies have suggested that an unyielding component indicating that the mean monsoon is also affected by internal dynamics.

1.2 Total column moisture

Moisture is critically important to life on Earth. It also plays an important role in the heat balance of Earth especially through the greenhouse effect of water vapour and, at the same time, by moderating surface temperature changes due to the removal of latent heat of evaporation. Reasons for the scanty

13

knowledge of moisture in the atmosphere and precipitation stem from the lack of observations (especially over the oceans) and their spatial as well as temporal variability. Rainfall and clouds usually occur on quite small temporal and spatial scales, so that an observation of moisture or precipitation event may not be representative of more than an area with dimensions of a few kilometers across or more than a small fraction of a day. Total precipitable water (TPW), which is defined as the total water vapor obtained by integrating the mass weighted specific humidity vertically from the surface to the top of an atmospheric column, varies essentially with hemispheric insolation changes. The spatiotemporal pattern of TPW over the Indian Ocean and nearby regions is closely associated with the variability of the Asian monsoon *(Singh et al 2000)*. An increase in the Southern Hemispheric insolation results in an increase of TPW over the southern Indian Ocean. When the Southern Hemispheric insolation is enhanced from December to April, the largest increase in TPW occurs in the southern Indian Ocean in March-May. The patterns of TPW change are consistent with those of the SST change. Therefore, the increased SST is responsible, in large part, for the increase of TPW in the southern Indian Ocean *(Liu et al 2006)*.

Theoretical studies on the moisture budget of the tropics suggest that the water vapour temperature relation in the tropics is height dependent. The observed interannual variation of water vapour and temperature give an opportunity to assess the water vapour temperature relation in the tropical troposphere. The interannual variability in the tropics is affected by the El Nino phenomenon.

1.3   Solar activity and Earth's weather

Solar variability, which originates from the solar interior, has time scales from hours to billions of years. One aspect of solar variability is linked to solar

evolution driven by nuclear conditions in the core. This is a relatively slow process with changes on time-scales of the order of several million years and above for parameters such as mass, radius and luminosity. Many forms of solar activity, such as flares, solar radiation bursts and solar wind can cause radiation enhancement and plasma movement. All these affect global climatological changes directly or indirectly *(Herman and Goldberg 1978)*. Another aspect of solar variability is related to solar magnetic fields generated below the convective zone in the interior. The evolution of magnetic fields results in many manifestations, on time-scales in the range of hours to several hundred even thousand years, such as the well-known sunspot cycle and its longer-period modulations, solar wind structures, and coronal mass ejections. Spectral studies of solar activity unveil certain periods and frequencies. However, wavelet analyses have showed that the periods and frequencies change with time. A much more complex picture therefore appears, than variability on only the 11-year sunspot cycle. A third aspect of solar variability deals with periodicities due to orbital conditions such as solar rotation, changes in Earths orbit, or inclination of rotation axis with respect to the ecliptic plane.

Many of these processes are also the mechanisms by which the Sun can influence Earth and the climate. The influences from the variation of the electromagnetic radiation are most often considered. However, a changing solar wind and energetic particles can also influence Earth either directly or indirectly through modulating the cosmic ray flux. In this scenario many research works have been done on Sun Climate relations and they have detected solar signals in climate records.

Many previous studies have shown that there is a regional to global factor caused by ENSO signal with periodicity about 3-6 years and a signal with 11

years periodicity indicating the solar influence on cloud cover over Indonesia, which is typically an equatorial region. This solar signal does not appear on all regions with different climate patterns or seasonal time ranges. The stronger solar signal appears over regions with monsoon activity and during dry seasons, when local or regional effects are the least. Though there are empirical evidences about solar effects on climate in many regions of the world, actually the physical mechanism behind this is not yet well understood. Cosmic rays mechanism plays a vital role. The cosmic rays interact in the upper atmosphere and produce secondary particles neutrons and muons. When these particles interact with the air molecules or water molecules, they get polarised and act as condensation nuclei for the formation of clouds. During the sunspot minimum, the intensity of the cosmic ray becomes maximum which in turn increases the coverage of clouds. This implies that solar radiation reaching Earth will be minimized. Conversely, during sunspot maximum, the intensity of cosmic ray reaching lower levels of the atmosphere reduces and the cloud cover decreases. Many studies have shown that monsoon could be sensitive to relatively small changes in forcing (0.25% change in solar output) *(Overpeck et al 1996; Neff et al 2001; Fleitmann et al 2003)*

While greenhouse gas forcing is more spatially uniform, solar forcing is more spatially heterogeneous (i.e., acting more strongly in areas where sunlight reaches the surface). Consequently, solar forcing induces feedbacks involving temperature gradient–driven circulation regimes that can alter clouds. Over relatively cloud-free oceanic regions of low-level moisture divergence in the subtropics, the enhanced solar forcing produces greater evaporation. Moisture then converges into the precipitation zones, intensifying the regional monsoon and Hadley/ Walker circulations. This produces greater subsidence and less cloud over the subtropical ocean regions and this process get reinforced.

The solar signal in tropospheric zonally averaged winds has also been studied by many researchers *(Gleisner and Thejll 2003, Haigh et al 2004, 2005, Crooks and Gray 2005)*. They show that the subtropical jets are weaker and further poleward at solar maximum than at solar minimum. The magnitudes of these signals are relatively small compared with the variations associated with the North Atlantic Oscillation and volcanic signals. *Gleisner and Thejll (2003)*, also examined the solar signal in zonally averaged vertical velocities and the longitudinal distribution of the solar signal in vertical velocities at the equator, and found a stronger subsidence at mid-latitudes and a poleward movement of the peak subsidence. They found evidence for a latitudinal broadening of the equatorial upwelling region, in good accord with the results of *Haigh (2003) and Crooks and Gray (2005)* though they did not find a significant solar signal in the strength of the ascending branch of the Hadley circulation. The solar signal in tropospheric zonal averaged temperatures and circulation was studied using the NCEP reanalysis by *Labitzke (2002), Haigh (2003), Gleisner and Thejll (2003)* and in the ERA-40 reanalysis by *Crooks and Gray (2005)*. The results are fairly complimenting each other. A positive solar response is seen in the tropical lower stratosphere i.e. warmer tropospheric temperatures in solar maximum than in solar minimum. This signal extends in vertical bands throughout the troposphere in both hemispheres at latitudes 20^0-60^0 with maximum amplitude of 0.5 K around 40^0-50^0N where there are strong gradients. Hence substantial local changes can be produced by modest North-South shifts.

1.4 Role of Indian Ocean on monsoon activity over India

Air sea interaction over the Arabian Sea and the Bay of Bengal are found to influence precipitation variability associated with summer monsoon over India. The Arabian Sea is a cardinal source of moisture fluxes across the west

coast of India resulting in more orographically forced rainfall over Western Ghats *(Saha and Bavadekar 1977; Rakhecha and Pisharoty 1996). Vecchi and Harrison (2004)* examined the role of SST anomalies in the northern Indian Ocean onto the interannual variability of precipitation in the Western Ghats region where summer monsoon rainfall shows local maximum in the seasonal mean and its interannual variability. For the Western Ghats region, they found a strong positive correlation with Sea Surface Temperature (SST) anomalies in the Arabian Sea at the onset of summer monsoon. The mean SST for winter and summer for Indian Ocean is given in Fig. 1.3. The active-break cycle of the Indian summer monsoon is associated with the northward propagation of clouds and convection bands from the equatorial region to around 30°N over the South Asian monsoon region, at a phase speed of about 1° latitude per day *(Yasunari 1979; Sikka and Gadgil 1980; Yasunari 1980; Gadgil and Asha 1992; Goswami 2005)*. Many studies have attempted to develop a theoretical basis of atmospheric dynamics in the northward propagation of the cloud bands on this time scale *(Murakami et al 1984; Jiang et al 2004; Yokoi and Satomura 2006)*.

Kemball-Cook and Wang (2001) examined the influence of latent heat flux on the northward migration of outgoing long wave radiation (OLR) anomalies over Indian Ocean. They suggest that the moisture flux from the Indian Ocean do favour convection by building up moist static energy. However, since their study is based on convective maximum over the equatorial Indian Ocean, the resultant composite signals get weaken towards higher latitudes and hence may not be effective in explaining the processes involving the regional precipitation over the Indian subcontinent. In addition, there is a meridional variation of the mean winds from the equator to the north Indian Ocean. *Vecchi and Harrison (2002)* examined the intraseasonal variability of OLR with respect to SST anomalies over the Bay of Bengal. They pointed out that positive (negative) SST anomalies on the intraseasonal scale in the Bay of Bengal

exhibit a strong statistical relation with the active (break) periods. The southern part of India lies between two seas; the intraseasonal precipitation variability may have regional characteristics between the east and west coast. Another feature of the Arabian Sea during the monsoon season, which influences the Indian subcontinent, is the Somali Jet. *Halpern and Woiceshyn (1999)* suggested that the Somali Jet in the Arabian Sea and the rainfall of west coast of India is connected because of simultaneous increases in surface wind convergence and integrated cloud liquid water in the eastern Arabian Sea.

1.4.1 Role of Sea Surface Temperature

Sahai et al (2003) have shown that despite the weakening relationship of ENSO-Indian Summer Monsoon in recent years, the relationship between SST in some regions of the global oceans and the ISMR is consistent for more than a century and any small variation in this relationship is part of natural oscillations. In different decades, about 55–85% of the variance associated with the ISMR is explained by SST alone and only 15–45% is explained by other boundary forcings and internal dynamics.
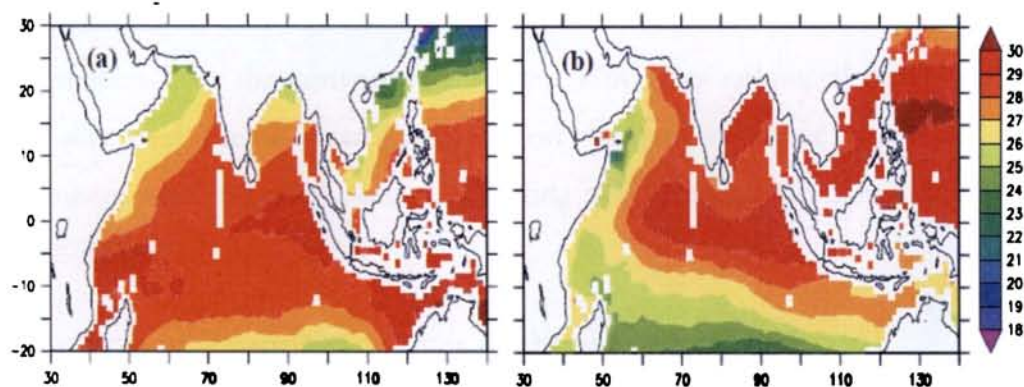
Figure 1.3. Climatological mean SST (°C) during (a) boreal winter (DJF) and (b) summer (JJA), for a period 1998–2002. SST data is taken from TRMM.

19

Change in SST is important in the energy balance and the inter-hemispheric heat exchange over the Asian continent and Indian Ocean in a coupled ocean–atmosphere system *(Wang et al 2003; Clemens and Oglesby 1992)*. Tropical observations show convective activity increasing sharply above SSTs of around 26°C and then decreasing as the SST exceeds 30°C and a maximum is observed when SST is about 32°C. Although some aspects of this relationship are reasonably well understood even though no theory has fully explained the decrease in convective activity above 30°C.

Active (break) phases of precipitation occur by the northward propagation of positive (negative) precipitation anomalies over the Arabian Sea and the Bay of Bengal. Over the windward side of the Western Ghats region during the active phase, the positive SST anomalies over the Arabian Sea formed by suppressed surface latent heat flux and increased downward shortwave radiation flux lead the positive precipitation anomalies. Surface air temperature anomalies follow the SST anomalies and then destabilize the lower atmosphere between 1000hPa and 700hPa. These results indicate that, in the northward propagating dynamical surface convergence, underlying SST anomalies tend to form a favorable condition for convective activity and may sustain enhanced precipitation over the convergence region. This gives enhanced precipitation anomalies over the Western Ghats region that move further northeastward and merge with the northward propagating precipitation anomalies from the Bay of Bengal.

1.4.2 Role of Evaporation over Arabian Sea on Monsoon

The role of oceanic divergence in determining the seasonal cycle in evaporation rate is very important in the viewpoint that the amount of rainfall over India during the southwest monsoon is a function of the amount of water evaporated over the pathways of monsoon as well as orographically

induced convective activity. *Wajsowicz and Schopf (2001)* in their analysis of Comprehensive Ocean–Atmosphere Dataset (COADS) shows that nearly 90% of the water vapour available to precipitate over India during the southwest monsoon results from the annual mean evaporation field. The seasonal change in direction of airflow, which opens up a pathway from the southern Indian Ocean to the Arabian Sea, rather than the change in evaporation rate is key to explaining the climatological cycle, though the change in latent heating due to seasonal variations is similar to that needed to account for observed interannual to interdecadal variability in monsoon rainfall.

1.4.3 Regional climate modeling of Indian summer monsoon

It has been demonstrated that for the study of the weather or climate features in greater detail, regional models are more suitable than the global models. Computationally it is affordable to increase the resolution of regional models so as to resolve regional climatic features reasonably well. Simulation of the Indian summer monsoon circulation features and the associated rainfall by a numerical model have been the most challenging problems so far. There have been some attempts to simulate monsoon features and extreme weather events over India by regional models. *Bhaskaran et al (1996)* simulated the Indian summer monsoon using a RCM with a horizontal resolution of 50 km nested with global atmospheric GCM. Their study showed that regional model derived precipitation exceeds 20% than GCM.

The regional climate modeling technique consists of using initial conditions, time-dependent lateral meteorological conditions and surface boundary conditions to drive high-resolution Regional Climate Models (RCMs). The input data is derived from GCMs (or analyses of observations) and can include greenhouse gas and aerosol forcing. Another method of this technique is to

force the large-scale component of the RCM solution throughout the entire domain *(Kida et al 1991; Cocke and LaRow 2000; von Storch et al 2000).* Till now, this technique has been used only in one-way mode, i.e., with no feedback from the RCM simulation to the driving GCM. The basic strategy is, thus, to use the global model to simulate the response of the global circulation to large-scale forcings and the RCM to (a) account for sub-GCM grid scale forcings (e.g., complex topographical features and land cover inhomogeneity) in a physically-based way; and (b) enhance the simulation of atmospheric circulations and climatic variables at fine spatial scales. The nested regional modelling technique essentially originated from numerical weather prediction and the use of RCMs for climate application was pioneered by *Dickinson et al (1989) and Giorgi (1990).* They can provide high resolution (up to 10 to 20 km or less) and multi-decadal simulations and are capable of describing climate feedback mechanisms acting at the regional scale. A number of widely used limited area modelling systems have been adapted and developed for, climate applications. More recently, RCMs have begun to couple atmospheric models with other climate process models, such as hydrology, ocean, sea-ice, chemistry/aerosol and land-biosphere models. Two main theoretical limitations of this technique are the effects of systematic errors in the driving fields provided by global models, and the lack of two-way interactions between regional and global climate. Practically, for a given application, consideration needs to be given to the choice of physics parameterizations, model domain size resolution, technique for assimilation of large-scale meteorological conditions, and internal variability due to non-linear dynamics not associated with the boundary forcing *(Giorgi and Mearns 1999; Ji and Vernekar 1997).* Depending on the domain size and resolution, RCM simulations can be computationally demanding, which has limited the length of many experiments. GCM fields are not available at high temporal frequency (6-hourly or higher), as required for RCM boundary conditions, and thus

careful co-ordination between global and regional modelers is needed in order to perform better RCM experiments.

In this study, based on these background information, an attempt has been made to study the spatial and temporal characteristics of the weather and climate of peninsular India having influenced by external factors such as solar forcing, northern Indian ocean SST and moisture, air temperature and zonal wind. A regression model has been developed using parameters like SST, air temperature and zonal components of wind. A regional climate model RegCM3 has been validated and interpreted to study the influence of SST and moisture over this region. Detailed description and methods are discussed in respective chapters.

CHAPTER 2

Variability in the Vertically Integrated Moisture over Peninsular India on Various Time Scales

2.1 INTRODUCTION

Atmospheric water vapour provides the single largest greenhouse effect on the Earth's climate (*Hansen et al 1984*). When more heat energy is added to the climate system, part of the increase is used to enhance the evaporation of water and the associated phase change keeps the temperature constant. However, these mechanisms involve a change in the atmospheric water vapour concentration, which is sensitive to the surface temperature. This in turn is affected by the greenhouse effect and the contribution from the atmospheric water vapour.

In order to outline the relation between temperature and humidity, we need to consider the *Clausius-Clapeyron* equation, describing how the saturation vapour pressure e_s (a measure of the water content of air) varies with temperature 'T'.

$$\frac{de_s}{dT} = \frac{L}{T(\alpha_v - \alpha_l)} \qquad \qquad ...(2.1)$$

The parameters α_v and α_l represent the specific volume of gas phase and liquid phase of fluid respectively and L is the latent heat. Humidity, vapour pressure and temperature are related as

$$\frac{dq^*}{dq} = \frac{de_s}{e_s} = \left[\frac{L}{R_v T}\right]\frac{dT}{T} \approx 20\frac{dT}{T} \qquad \qquad ...(2.2)$$

A change of 1% in the temperature produces a 20% change in the humidity at saturation q^*. The relative humidity R_H is assumed to be constant.

$$R_H = \frac{q}{q^*} \approx const. \qquad \qquad \qquad \ldots(2.3)$$

This means that an increase in the surface temperature reinforces the increase in the atmospheric water vapour concentration and consequently the greenhouse effect is enhanced. This mechanism may therefore act to amplify the effect of variations in the total solar irradiance associated with the solar cycle assuming everything else is constant.

Solar activity has profound influences on geodynamical processes and living environments on the Earth. Sunspots are an important factor for describing solar variations and a solar cycle of about 11 years corresponds to increasing and decreasing sunspot numbers. Even a minor variation in Total Solar Irradiance (TSI) (0.1 - 0.3%) can bring about major changes in monsoonal precipitation via various positive feedback processes such as moisture availability and changes in atmospheric circulations.

The solar signal in tropospheric zonal averaged temperature and circulation was studied using the NCEP reanalysis data by many researchers like *Labitzke (2002)*, *Haigh (2003)*, *Gleisner and Thejll (2003)* and ERA-40 reanalysis data by *Crooks and Gray (2005)*. The results are generally in good agreement with each other. A solar signal in the lower stratospheric temperature and circulation is likely to influence the troposphere below. A number of mechanisms were discussed in those studies, not only in the context of solar influence but in the wider context of examining to what extent stratospheric processes might influence tropospheric weather and climate. A general overview of stratosphere troposphere coupling has been provided by *Shepherd (2002)* and *Mohanakumar (2008)*.

The troposphere at high latitudes receives less solar radiation in the northern winter during intense sunspot activity because of the solar induced changes in the

25

stratospheric ozone. *Haigh (1999)* conducted a series of model studies with solar induced changes in the stratospheric ozone and found that the Hadley cell is weakened and broadened in January during solar maximum and that this broadening is accompanied by a poleward shift of the subtropical jet stream. These shifts in the circulation pattern result in bands of warming and cooling. This variation in the stratospheric ozone is believed to be one of the mechanisms, which may amplify the total solar irradiance.

Shindell et al (1999) have suggested that changes in the ultraviolet (UV) radiation may influence the stratospheric chemistry and hence changes in the upper tropospheric ozone concentration (1-2% change for a solar cycle). Changes in the ozone affect the UV absorption and induce temperature changes and hence modulate circulation. As ozone absorbs UV light it traps energy, which is converted into heat. Differences in the absorption rates at various locations results in spatial temperature gradients, which in turn affect the mean circulation according to the thermal wind equation. As a consequence the westerlies are enhanced and the flow is diverted towards the poles by the surface friction, leading to a cell of rising air in the polar region and a descent between 40°N and 50°N. *Shindell et al (2001b)* tried to estimate the global temperature difference between the present and the Maunder minimum according to UV–ozone mechanism and estimated this to be ~0.3-0.4° C. Regional changes in temperature are quite large.

The quasi-biennial oscillation (QBO) in the equatorial stratospheric zonal wind is believed to be driven by wave forcing, originating from the troposphere. *Balachandran et al (1999)* assumed that solar UV with wavelengths shorter than 300 nm changes by 5% (either increase or decrease) over a solar cycle and studied the relation of solar variance on the lower stratosphere. They proposed that the solar activity influences the stratosphere by altering the vertical temperature and zonal

wind profiles. The stratospheric response further more affects the planetary wave propagation and perturbs the Eliassen-Palm flux divergence and hence the lower stratospheric and tropospheric structure.

Lean and Rind (1998) observed that changes in the refractive properties associated with the zonal winds, caused by solar activity, might result in induced warm and cool regions in the stratosphere, which subsequently alter the vertical stability of the stratosphere and troposphere. The QBO also alters the meridional gradient in the zonal wind in the lower stratosphere whereas UV variations alter the vertical gradient of zonal wind. The refractive index of the planetary waves is affected by gradients in both the zonal and vertical directions.

Analyses of the global surface temperature record since 1860 lend some support for this interpretation by identifying climate cycles in the range 2–8 year and 11–12 year with confidence limits in excess of 90% *(Mann and Park 1994)*. Although decadal and multi decadal periods are common in climate time series, their physical origins are difficult to specify, partly because of the paucity of global coverage by long-term climate records with ample temporal resolution. Since sunspot numbers exhibit a pronounced 11-year cycle, periods near 11 and 22 years are tentatively connected with solar variability, often for lack of another plausible mechanism. But the transitory nature of this periodicity and its absence in some climate records lead *Pittock (1979)* to dismiss the implied sun–climate connection as unconvincing. Recognition that the solar radiative output varies, does imply a potential mechanism for excitation of these periods by solar forcing. Alternative mechanisms are also postulated for the decadal periodicities, in particular an internal oscillation of the climate system that is present in some climate model simulations in the absence of external forcing *(James and James 1989; Mehta and Delworth 1995)*.

Tropospheric temperatures during the past few decades appear to be about 0.58 to 1.58°C warmer during times of solar maxima, notably in the midlatitude Western Hemisphere (*Labitzke and van Loon 1993a,b*). A 0.158°C increase in land-surface temperatures from 1986 to 1990 has been attributed to increasing solar irradiance from 22-year solar cycle minimum to maximum activity (*Ardanuy et al 1992*). Sea surface temperatures band passed to isolate the decadal component of their variability exhibit changes of the order of 0.18°C that are highly correlated (r=0.9) with the Sun's 11-year activity cycle in the past four decades (*White et al 1997*). Furthermore, solar related Sea Surface Temperature (SST) changes may initiate regional precipitation fluctuations (*Perry 1994*). Neither climate nor solar variability are sufficiently well defined, either spatially or temporally, nor their causes adequately understood, to verify that the correlations really arise from climate forcing by changing solar radiation rather than from statistical coincidence (*Baldwin and Dunkerton 1989, Salby and Shea 1991*).

Experiments with a simplified GCM provide some indication as to how these responses arise (*Haigh et al 2005*). In these experiments idealized heating perturbations were applied only in the stratosphere but effects were shown throughout the troposphere with vertically banded temperature anomalies and changes in circulation.

2.2 OBJECTIVES OF THE STUDY

The main objectives of the study are to identify any possible relationship between the eleven-year solar forcing and its influence on the mass weighted columnar moisture over the peninsular Indian region. In this work, an attempt is made to identify any possible connection between the 11-year solar cycle related to the interactions in the Sun and climate variability over the Indian peninsular region. The intraseasonal variability of the Vertically Integrated Moisture (VIM) for the

three recent contrasting monsoon years 1996, 1997 and 2002 over the peninsula also forms a part of the objective.

2.3   Climatology of Seasonal Total Precipitable Water

The climatology of VIM over the Indian monsoon region is shown in Fig 2.1. VIM is computed by integrating the specific humidity from 1000 to 300 hPa and taking averages for respective seasons. For the pre-monsoon season March, April and May (MAM), the maximum value of VIM is observed over tropical region with intrusion into china and Indian peninsula. During monsoon season June, July, and August (JJA), the moisture abundance is over China and adjoining Indo-China peninsula. For post-monsoon season September, October and November, (SON) also the surplus moisture is over Indo-China peninsula and Bay of Bengal. The seasonal mean moisture for winter December, January and February (DJF) over Indian peninsula is having very less moisture than any other season.
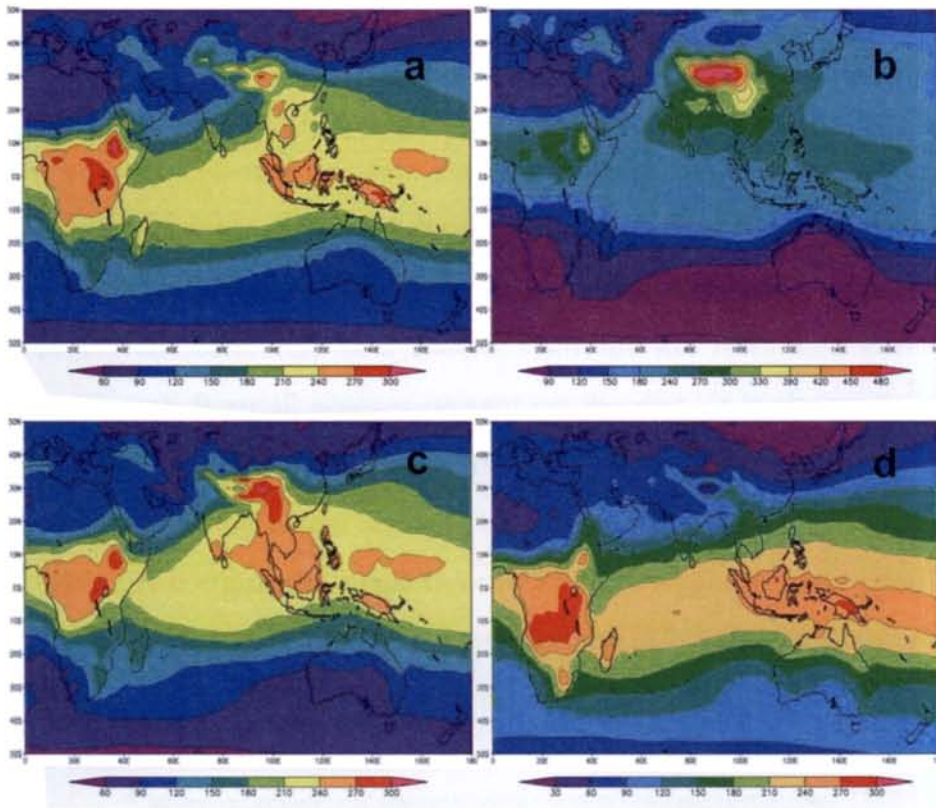
Fig. 2.1. Climatology of seasonal means of total precipitable water from surface to 300 hPa for (a) March-May, (b) June-August, (c) September-November and (d) December-February respectively.

2.4 DATA

The interannual and intraseasonal variability of VIM was studied using the monthly and daily Specific humidity data obtained from Climate Diagnosis Center website *(http://www.cdc.noaa.gov/cdc/reanalysis/ reanalysis.shtml)*. This has a spatial resolution of 2.5^0 x 2.5^0 latitude and longitude at 17 vertical levels and a temporal coverage from 1950 to 2004. The monthly air temperature data used is having the same spatial, temporal and vertical resolution. A comparison between the NCEP and ERA40 VIM are presented in Fig. 2.2. The data used as the proxy for solar activity is the 10.7 cm solar radio flux obtained from the website of Solar Radio Monitoring Program *(http://www.spaceweather.ca/ spw_data_e.php)*. The Solar Radio Monitoring Programme is operated jointly by the National Research Council and

the Canadian Space Agency. It is a routinely observed radio wave emitted by the Sun, which is highly correlated with the sunspot number but is a more objective measure of solar variability. The various manifestations of solar activity are driven by the total amount of magnetic flux emerging through the photosphere into the chromosphere and corona, and its temporal and spatial distribution. For reasons not clearly understood, solar activity ebbs and flows over a cycle of about 11 years. The 10.7cm solar flux is a measurement of the integrated emission at 10.7cm wavelength from all sources present on the disc. It is almost completely thermal in origin, and directly related to the total amount of plasma trapped in the magnetic fields overlying active regions. This in turn is related to the amount of magnetic flux. A comparison made over more than a solar activity cycle shows that there is indeed a linear correlation between the 10.7cm solar flux and the total photospheric magnetic flux in active regions.
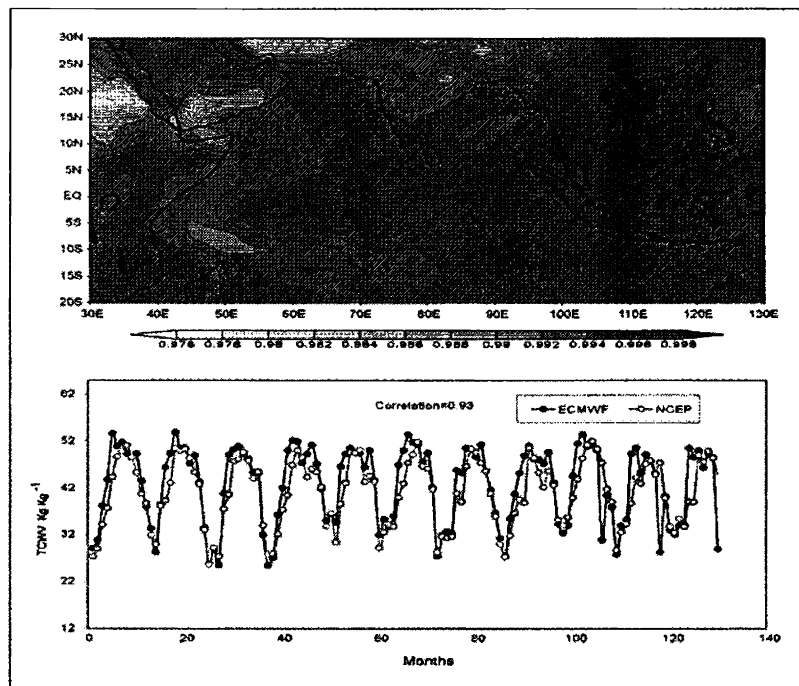

Fig. 2.2 (a) The spatial correlations between NCEP and ERA40 vertically integrated moisture and (b) their monthly time series

The 10.7cm solar flux, i.e., the solar flux density at 10.7cm wavelength is measured using two fully automated radio telescopes called Flux Monitors, located at the Dominion Radio Astrophysical Observatory. The observed value is the number measured by the solar radio telescope. This is modulated by two quantities, such as the level of solar activity and the changing distance between the Earth and Sun. Since it is a measure of the emissions due to solar activity hitting the Earth, this can be used when terrestrial phenomena are being studied. In this study the observed solar radio flux is used.

2.5 METHODOLOGY

The specific humidity is used to compute the Vertically Integrated Moisture (VIM) using the formula

$$W = \frac{1}{g} \int_{p1}^{p2} q.dp \qquad \qquad ...(2.4)$$

where q is the specific humidity and g, the acceleration due to gravity. The integration is done between the pressure levels p1 and p2. This integration was carried out between different levels, viz., 1000-300 hPa, 1000-500 hPa, 1000-700 hPa, and 1000-850 hPa and between the standard atmospheric levels in which the data are available. The moisture thus computed was averaged seasonally for different seasons viz., winter (December-February), summer (June-August) and post-monsoon (September-November). The VIM is averaged spatially for a geographic region 74-78⁰ E and 7-14⁰ N and wavelet analysis is carried out. The method follows *Torrence and Compo (1998)*.

The time-averaged wavelet also is done for each wavelet analysis. The time averaged wavelet spectrum over a certain period is given by

$$\overline{W}_n^2(S) = \frac{1}{n_a} \sum_{n=n_1}^{n_2} \left| W_n(S) \right|^2 \qquad \ldots (2.5)$$

where the index a is arbitrarily assigned to the mid point of n_1 and n_2, and $n_a = (n_2 - n_1 + 1)$ is the number of points averaged together. When n_a is the total number of time in the spectra it is the global wavelet spectrum, given by

$$\overline{W}^2(S) = \frac{1}{N} \sum_{n=0}^{N-1} \left| W_n(S) \right|^2 \qquad \ldots (2.6)$$

The smoothed Fourier spectrum (which is another method used in this study) is analogous to the global wavelet spectrum. A comparison of Fourier spectra and wavelet spectra can be found in *Hudgins et al (1993)*, while a theoretical discussion is given in *Perrier et al (1995)*. *Percival (1995)* showed that the global wavelet spectrum provides an unbiased and consistent estimation of the true power spectrum of a time series.

The mother wavelet used was Morlet given by

$$\psi_0(\eta) = \pi^{-1/4} e^{i\omega_0 \eta} e^{-\eta^2/2} \qquad \ldots (2.7)$$

To study the spatial coherence of the periodicity, spatial FFT analysis is done for the area 0-160°E and 20°S-50°N. The period in the FFT analysis corresponds to scales in wavelet analysis using Morlet as mother wavelet. The method used is non-orthogonal wavelet analysis since the time series in climate studies are not discrete. After identifying the spatial patterns of the significant modes of variability, cross spectral analysis was done for MAM, JJA, SON and DJF seasons, in order to study the relation between VIM and solar radio flux.

Linear correlation was done between monthly values of solar radio flux and VIM for a spatial perspective of linear association between these parameters. Similarly correlation was done between monthly solar radio flux and air temperature in the

vertical through 80⁰E and 10⁰N. Statistical significance was done for the correlation analysis.

$$\left(r_{xy}\right)_k \approx \frac{\sum_{i=1}^{n-k}\left[\left(x_i - \overline{x}\right)\left(y_{i+k} - \overline{y}\right)\right]}{\left[\sum_{i=1}^{n-k}\left(x_i - \overline{x}\right)^2 \sum_{i=k+1}^{n-k}\left(y_i - \overline{y}\right)^2\right]^{1/2}} \qquad \dots(2.8)$$

To study the intraseasonal variability of the VIM, Empirical Orthogonal Function (EOF) analysis is employed for three seasons having 128 days (three months and few days before first month and after last month, for facilitating the wavelet analysis). The corresponding PCs are subjected to wavelet analysis. This reveals the variability in order of priority and specifies the period of oscillations.

2.6   RESULTS

2.6.1 Interannual variability in Moisture

Wavelet analysis of the VIM for a geographical area bounded by 7-14⁰N and 74-78⁰E carried out for different seasons show variability at a scale of 10-12 years for monsoon and post-monsoon season. The wavelet power spectra of VIM for the SON season at all integration levels show spectral power significant at 95% confidence (Fig. 2.3a-2.3d).
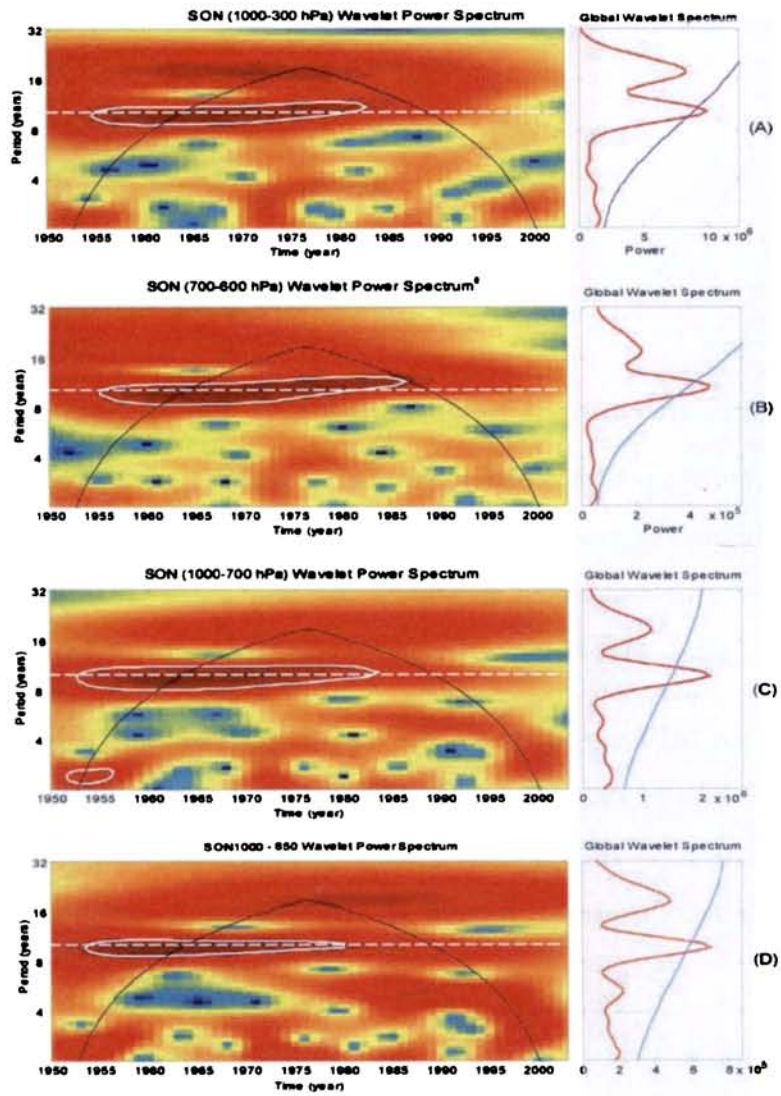
Fig. 2.3. Wavelet power spectrum of VIM for SON for integration from (a) surface to 300 hPa (b) 700 to 600 hPa (c) surface to 700 hPa and (d) surface to 850 hPa

The significant variability seizes at about mid seventies. The significant spectrum shows a tilt towards higher periodicities as time increases. The spectra at 90% confidence level show persistence for a longer period after 1975 (Figure not shown). For the analysis during summer season (JJA), the variability is limited to lower levels (Fig. 2.4).

35
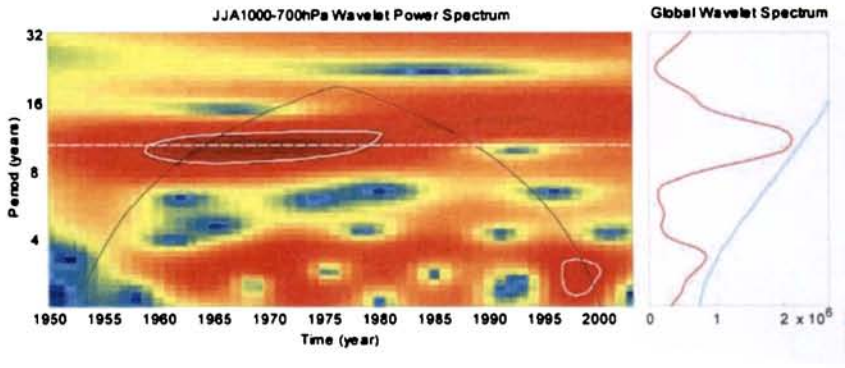
Fig. 2.4. Wavelet power spectrum of VIM for JJA for integration from surface to 700 hPa

Results for summer season indicate that the global wavelet spectrum, which is the time averaged representation of the wavelet spectral power, is significant up to the integration level of 600 hPa. This could be due to the fact that the majority of moisture is limited to lower levels in the mean monsoon flow during this season.

Further study that applied Fast Fourier Transform of the VIM for SON season revealed that the Fourier power spectra corresponding to 11 and 12 years show high values over peninsular Indian region (see Fig. 2.5a & 2.5b). The spectral power has a significant magnitude over the central Indian region and southeastern Asia.

For the monsoon season, spectra corresponding to both 11 and 12 years show high power over the peninsular India (see Fig. 2.6a & 2.6b). This extends over to the Bay of Bengal to the Indo-China peninsula and Indonesia. High spectral power could also be seen over the African and Australian continents. For the summer season the maxima of the spectral power are elsewhere other than peninsular India. The cross-spectral estimates of seasonal VIM for (a) Mar-May (b) Jun-Aug (c) Sep-Nov and (d) Dec-Feb are shown in Fig 2.7. The higher amplitudes are obtained for the seasons JJA and SON, whereas the least is observed for DJF.

36
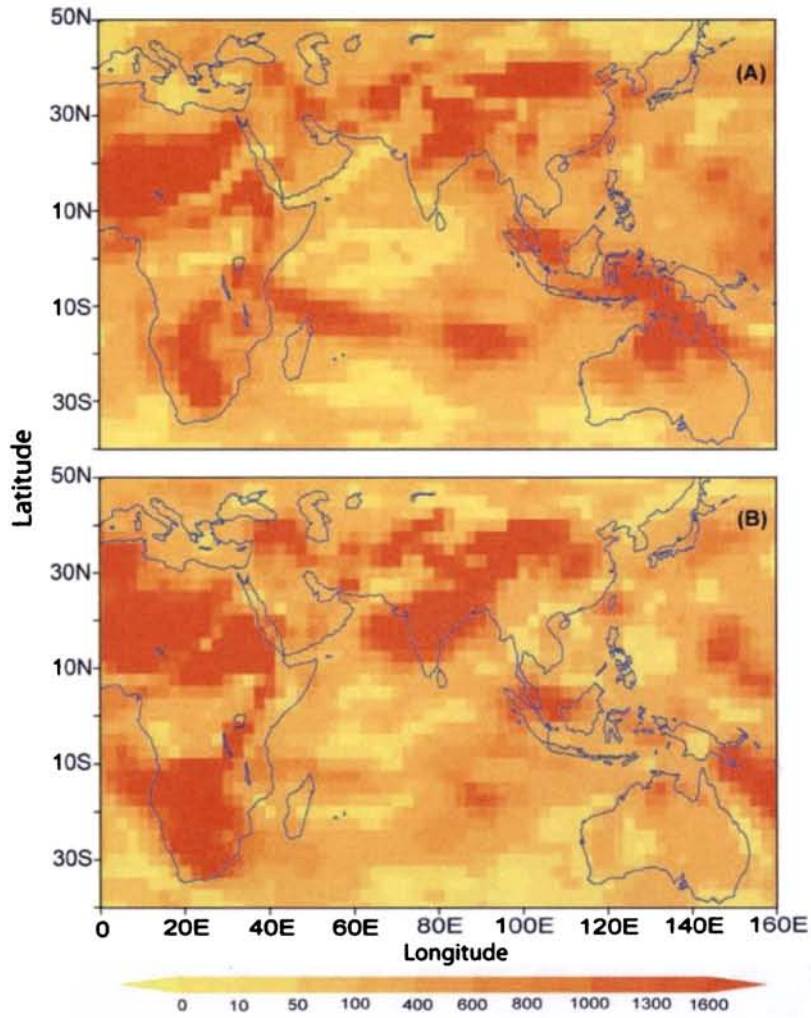
Fig. 2.5. Spatial distribution of Fast Fourier Transform of Vertically Integrated Moisture during post monsoon (SON). Maximum Spectral power at each grid points is shown for (a) 11 and (b) 12 years. Values are multiplied by a factor 10^{-3}
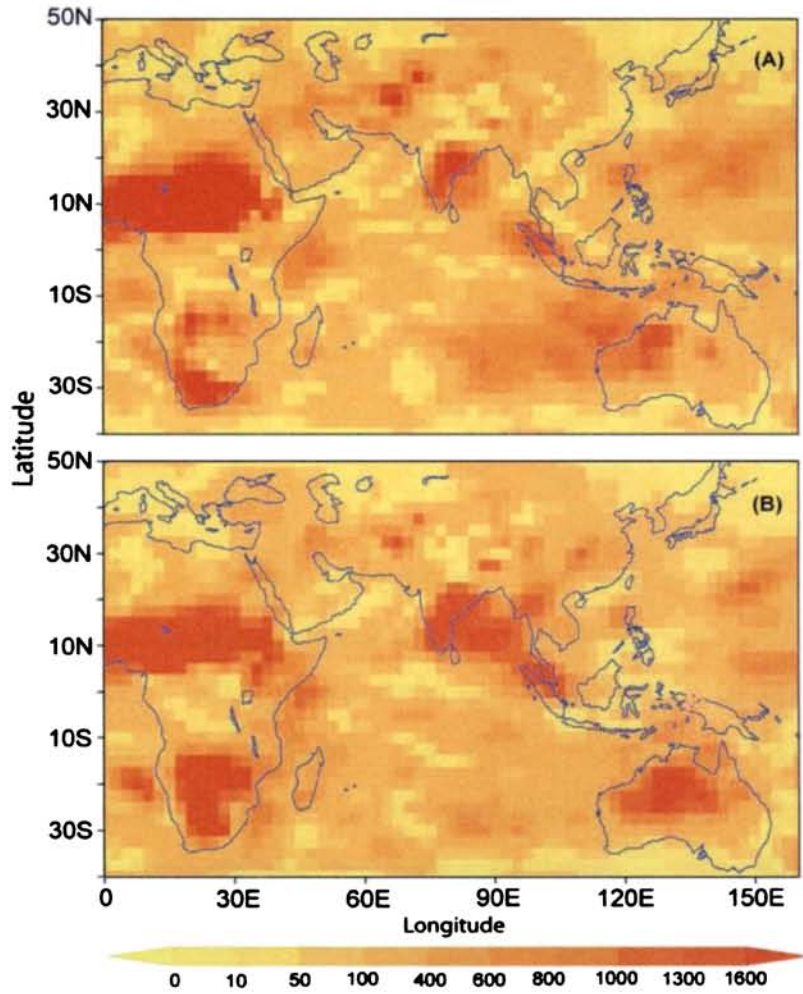
Fig. 2.6. Spatial distribution of Fast Fourier Transform of Vertically Integrated Moisture during monsoon (JJA). Maximum Spectral power at each grid points is shown for a) 11 and a) 12 years. Values are multiplied by a factor 10^{-3}
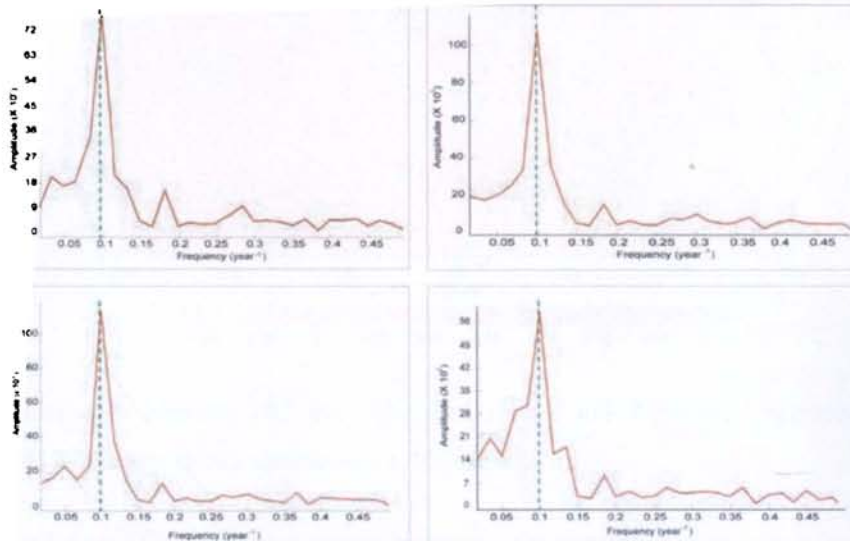
Fig. 2.7 The cross spectral estimates of seasonal VIM for (a) Mar-May (b) Jun-Aug (c) Sep-Nov and (d) Dec-Feb

To understand the plausible relation of this type of 11-year mode of variability in the moisture and its spatial extend, correlation coefficients between 10.7 cm solar radio flux and the VIM were found out spatially to get a qualitative idea (Fig. 2.8). It is seen that the tropical Indian and Pacific Oceans are having highest correlation. The analysis is done on monthly values of both the data sets.
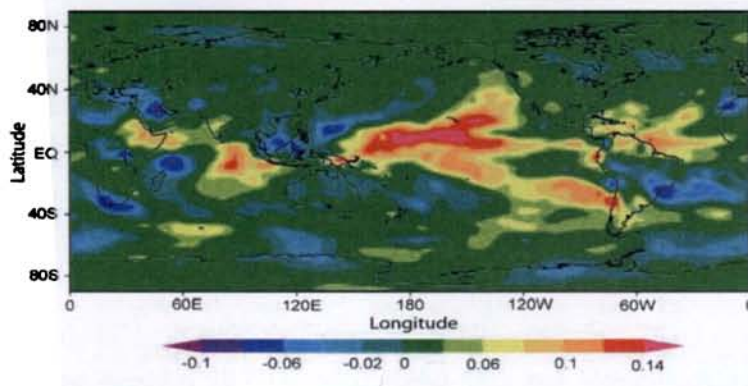
Fig. 2.8. Correlation between Vertically Integrated moisture and 10.7 cm Solar Radio Flux.

39
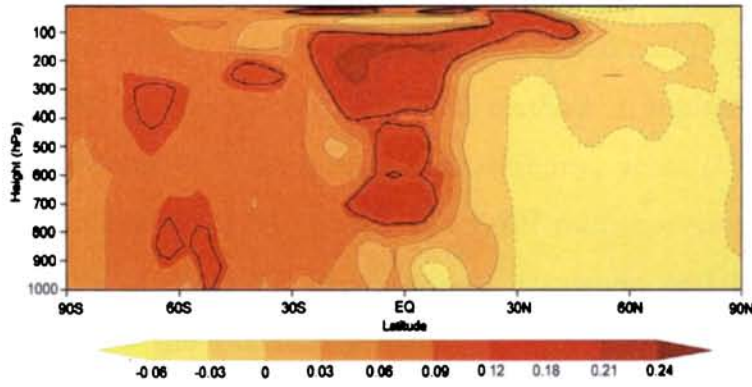
Fig. 2.9. Correlation between 10.7 cm Solar Radio Flux and Vertically Integrated Moisture through 80⁰E. Thick line shows significance at 99% level.

Vertical sections of correlation maps between tropospheric temperature and 10.7 cm solar flux (Fig. 2.9 & 2.10) show the possibility of the connection of solar activity with the moisture through tropospheric temperature variability. It is evident from Fig. 2.9 that over Indian region correlation exists between solar radio flux and tropospheric temperature over the tropical region. Similarly, Fig. 2.10 shows a correlation over the Pacific and less strong correlations over Indian longitude.
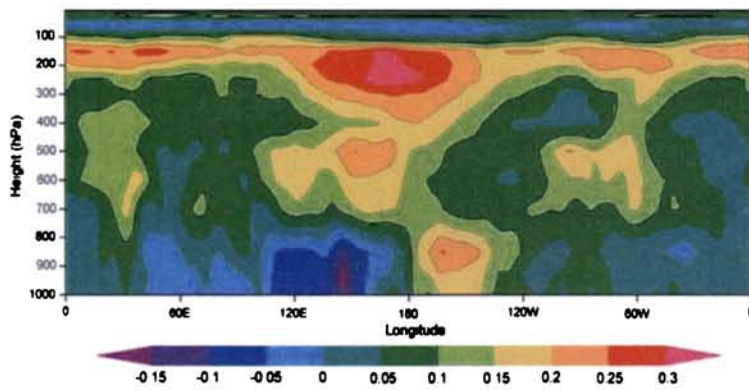
Fig. 2.10. Correlation between 10.7 cm Solar Radio Flux and Vertically Integrated Moisture through 10⁰N.

2.6.2   Intraseasonal variability in Seasonal Moisture

The EOF analysis is used to identify the dominant spatial and temporal patterns present in the VIM. In this section the EOF method is applied to study the intraseasonal variabilities of VIM during three different years (1996, 1997 and 2002) characterized by WET, NORMAL and DRY monsoon respectively. The leading three EOFs of VIM for pre-monsoon, monsoon and post-monsoon seasons are illustrated in the following session.

The first EOFs of all the seasons during 1996 does not show any centers of loading over the study area but have negative loading over the entire region, with EOFs for MAM, JJA and SON explaining 56.3, 39.8 and 63.3 % of the total VIM variability of the respective seasons (Fig. 2.11a, 2.11d and 2.11g). The second EOF of MAM VIM explain 7.6% and positive loading is over the northern Arabian Sea and adjoining Indian subcontinent and negative loading over Bay of Bengal (Fig. 2.11b). The second EOF of JJA VIM explains 10.2% of the total variability and the Arabian Sea is loaded with negative pattern while for SON season (Fig 11.h), the percentage variability is only 5.3%. Arabian Sea and peninsular India are loaded positive while Bay of Bengal is loaded negative (Fig. 2.11e). The third EOF of all the seasons have positive loading over peninsular India and southern Arabian Sea with 5, 8.7 and 4.5% for MAM, JJA and SON seasons respectively (Fig. 2.11c, 2.11f and 2.11i).

As in the case of 1996 for the year 1997 also, the first EOFs for all the seasons show that the primary loadings are not centered over the peninsular India or Arabian Sea except that the core of monsoon EOF pattern has a spread over the central India (Fig. 2.12a, 2.12d and 2.12g). The first EOFs of MAM and JJA moisture are loaded negatively over Arabian Sea and Indian Continent while for SON season it is positive, with respective percentage variabilities 53.5, 40.9 and 63.6. The second EOFs explain 6.5, 11.8 and 4.1% with the pre-monsoon positive

loading centered over Bay of Bengal (Fig. 2.12b). The third EOFs have negative loading centered over Bay of Bengal (5.2%) for MAM, over northern Arabian Sea for JJA (7.4%) and Bay of Bengal and southern Arabian Sea (4%) for SON monsoon season (Fig. 2.12c, 2.12f and 2.12i).

The first EOFs of 2002 VIM show similar spatial pattern but positive loading over the study region for MAM season explaining 53.1% of the total pre-monsoon moisture variability. The JJA and SON variabilities have negative loading over the region with 35.1 and 63.3% variability for each season respectively (Fig 2.13d and 2.13g).

The second EOF of spring VIM shows 5.8% variability and has positive loading over Arabian Sea and negative loading over peninsular India and southern part of the oceanic region. The EOFs of summer and autumn VIM show negative loading over similar areas (northern Arabian Sea) and explain 13.4 and 5.3% variability (Fig. 2.13e and 2.13h).

The third EOFs show spatially organized variability over the study region for all seasons. For MAM, negative loading is centered over Peninsular India with positive loading over Arabian Sea (4.2%) (Fig. 2.13c), for summer entire Arabian Sea having negative loading (7%) and for SON season, peninsular India is positively loaded with 4.5% of the total variability (Fig. 2.13i).

In order to find the time scales of these principal modes of variability, the first three PCs are subjected to wavelet analysis. The figures are presented (see Fig. 2.14-2.16).
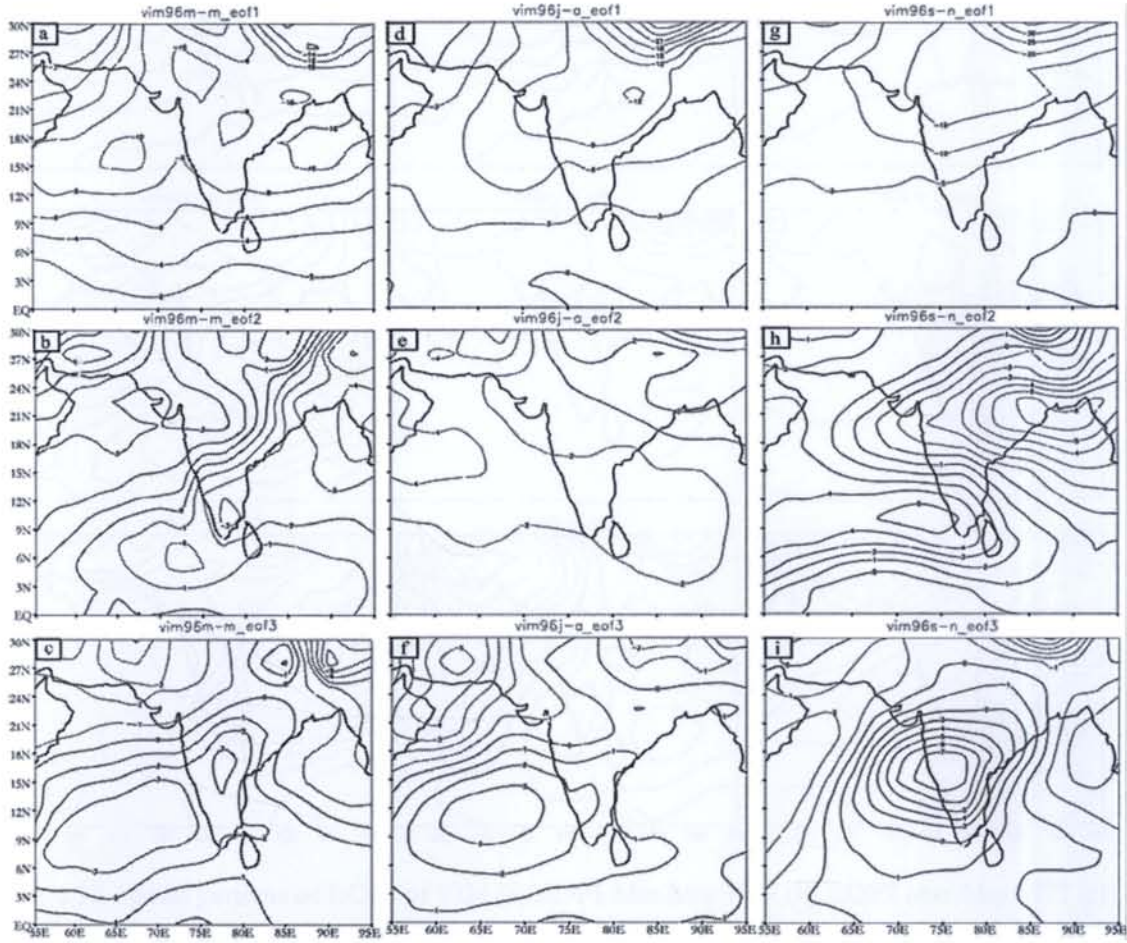
Fig. 2.11. Spatial patterns of EOFs of VIM (a) EOF1 Mar-May 1996 (b) EOF2 Mar-May 1996 (c) EOF3 Mar-May 1996 (d) EOF1 Jun-Aug 1996 (e) EOF2 Jun-Aug 1996 (f) EOF3 Jun-Aug 1996 (g) EOF1 Sep-Nov 1996 (h) EOF2 Sep-Nov 1996 (i) EOF3 Sep-Nov 1996

Fig. 2.12. Spatial patterns of EOFs of VIM (a) EOF1 Mar-May 1997 (b) EOF2 Mar-May 1997 (c) EOF3 Mar-May 1997 (d) EOF1 Jun-Aug 1997 (e) EOF2 Jun-Aug 1997 (f) EOF3 Jun-Aug 1997 (g) EOF1 Sep-Nov 1997 (h) EOF2 Sep-Nov 1997 (i) EOF3 Sep-Nov 1997
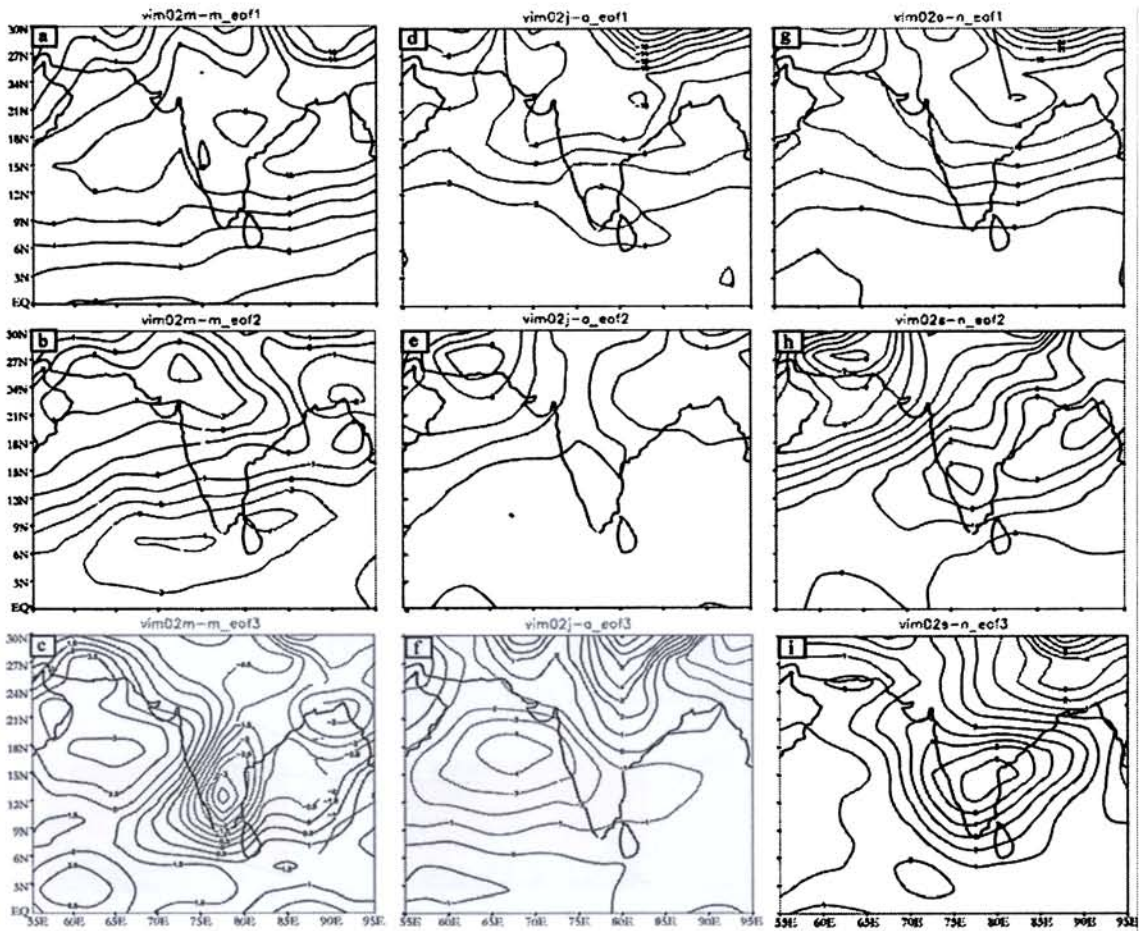
Fig. 2.13. Spatial patterns of EOFs of VIM (a) EOF1 Mar-May 2002 (b) EOF2 Mar-May 2002 (c) EOF3 Mar-May 2002 (d) EOF1 Jun-Aug 2002 (e) EOF2 Jun-Aug 2002 (f) EOF3 Jun-Aug 2002 (g) EOF1 Sep-Nov 2002 (h) EOF2 Sep-Nov 2002 (i) EOF3 Sep-Nov 2002
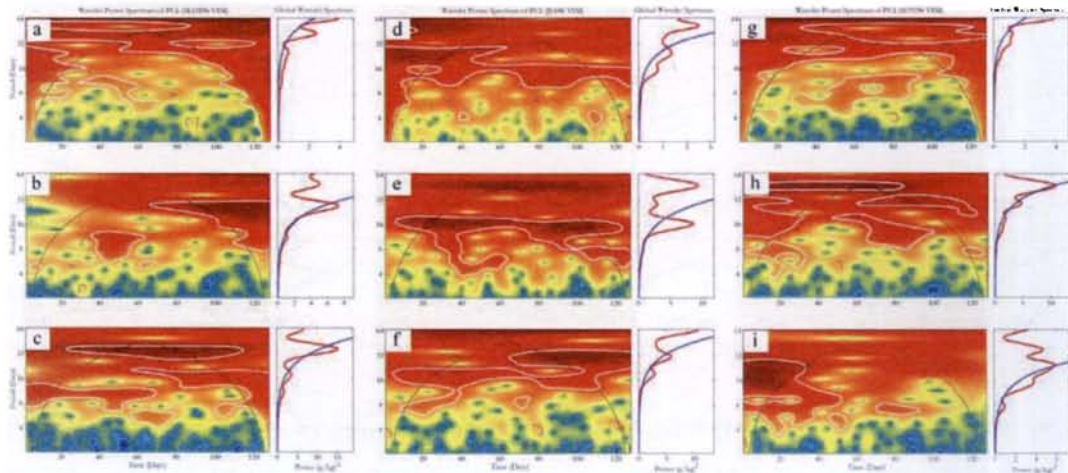
Fig. 2.14. Wavelet power spectrum of vertically integrated moisture for (a) PC1 Mar-May 1996 (b) PC2 Mar-May 1996 (c) PC3 Mar-May 1996 (d) PC1 Jun-Aug 1996 (e) PC2 Jun-Aug 1996 (f) PC3 Jun-Aug 1996 (g) PC1 Sep-Nov 1996 (h) PC2 Sep-Nov 1996 (i) PC3 Sep-Nov 1996

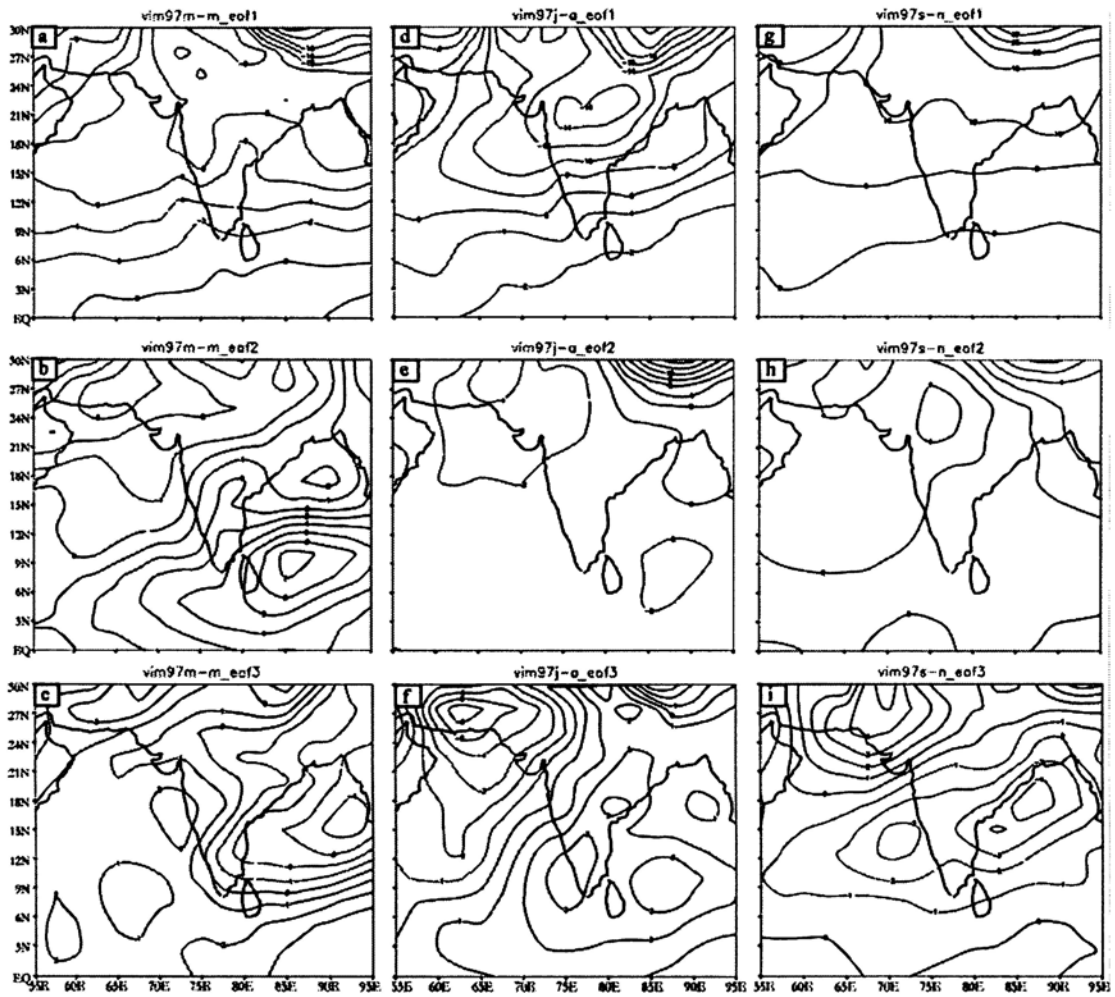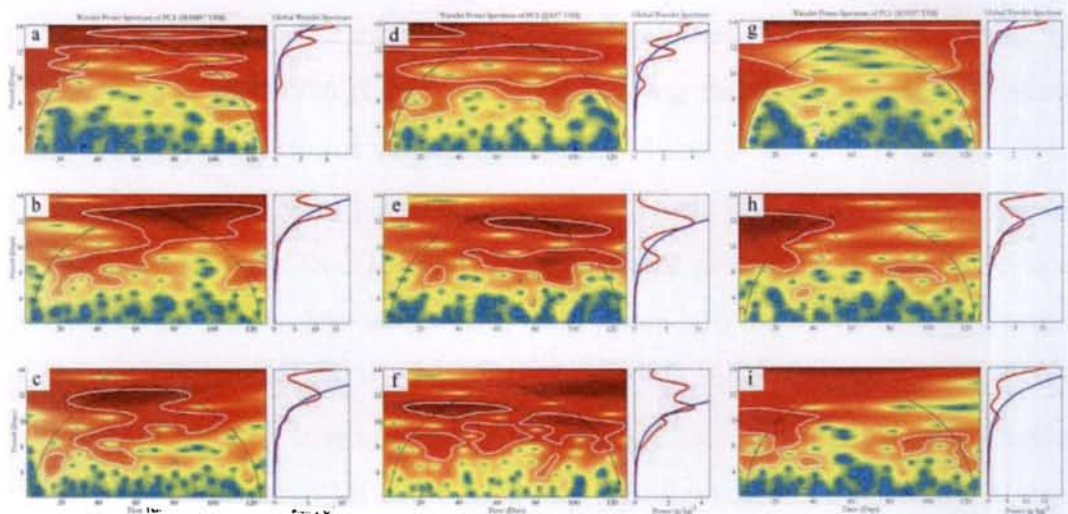Fig. 2.15. Wavelet power spectrum of (a) PC1 Mar-May 1997 (b) PC2 Mar-May 1997 (c) PC3 Mar-May 1997 (d) PC1 Jun-Aug 1997 (e) PC2 Jun-Aug 1997 (f) PC3 Jun-Aug 1997 (g) PC1 Sep-Nov 1997 (h) PC2 Sep-Nov 1997 (i) PC3 Sep-Nov 1997 of Vertically Integrated Moisture
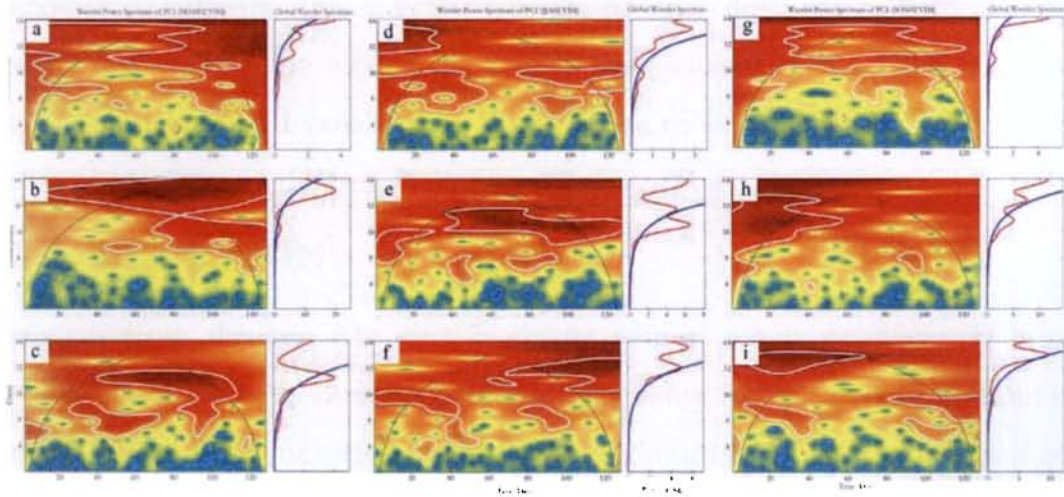
Fig. 2.16. Wavelet power spectrum of (a) PC1 Mar-May 2002 (b) PC2 Mar-May 2002 (c) PC3 Mar-May 2002 (d) PC1 Jun-Aug 2002 (e) PC2 Jun-Aug 2002 (f) PC3 Jun-Aug 2002 (g) PC1 Sep-Nov 2002 (h) PC2 Sep-Nov 2002 (i) PC3 Sep-Nov 2002 of Vertically Integrated Moisture.

From the wavelet spectrum of first three PCs of MAM VIM, it is seen that the main significant period of variability is 24 days significant at 95% confidence, for the NORMAL year 1996 (Fig. 2.14a.). VIM during the JJA season for the same year 1996 shows significant variability at scales 16 and 24 days. This extends from 10 days to 32 days, with peculiar variability to each PCs. (Fig. 2.14b). Wavelet power spectrum of SON VIM for 1996 shows that principal variability is around 30 days, second around 16 and 30 and third around 16 days (Fig. 2.14c). Wavelet power spectrum of MAM VIM for WET year 1997 there is not much significant variability except one at around 10- 16 days (Fig. 2.15a). For the third PC, wavelet spectrum of Monsoon VIM shows clear and significant periods at 12 and 30 days (Fig. 2.15c). First and third PC shows variability over 16-day window and second PC shows 30-day oscillation also (Fig. 2.15c). MAM VIM for the DRY year 2002 shows 30-day mode for first and third EOF (Fig. 2.16a). The second PC shows highly significant wavelet power at around 24 days (Fig. 2.16b). VIM for SON season of 2002 shows periodicities around 20 days (Fig. 2.16c)

47

In all the years that were analysed, the first EOFs for all seasons show zonally homogenous patterns. This indicates that the primary variability in VIM over the study region follows the meridional temperature gradient. The second and third modes of intraseasonal variability in the VIM are more localized and follows the land sea contrast over the peninsular region.

2.7 DISCUSSION

Radiation from the sun (the earth's energy source) varies continuously at all wavelengths and on all observed timescales. A change in total radiative output of about 0.1% has been measured between the maximum and minimum of the sun's recent 11-year solar activity cycle. Accompanying changes occur throughout the solar spectrum, with larger cycle amplitudes in radiation at UV wavelengths than in the visible emissions. Although not measured directly, total radiative output changes of a few tenths percent are postulated to occur over centennial timescales, based on evidence from cosmogenic isotope proxies of solar activity and activity levels in sun-like stars, both of which exhibit a larger range of variability than yet evident in the present day sun.

Inferences from sun–climate correlation studies can depend critically on the type and length of the climate and solar variability records chosen for the study. Although in the past 130 year the *Hoyt and Schatten (1993)* irradiance reconstruction correlates well with NH surface temperatures (r=0.8), from 1700 to 1990 its correlation with the *Bradley and Jones (1993)* NH temperature data drops to 0.5 (*Crowley and Kim, 1995*). When annual sunspot numbers (SSN) (which lack the long-term component evident in cosmogenic isotopes and the irradiance reconstructions) are used as a proxy for solar activity the influence of SSN on global temperatures is found to be negligible (*Visser and Molenaar, 1995*). *Crowley and Kim (1995)* attribute 30% to 55% of climate variability on decadal–centennial timescales to solar variability.

In the recent past, correlations between solar variability and surface temperatures rival those between surface temperatures and greenhouse gases, and there exists evidence of the 11-yr solar activity cycle in a variety of climate data. Neither the amplitude of the climate response to the changing solar radiation, nor its temporal or geographic character has yet been established with the certainty needed to either validate or dismiss these observed sun–climate associations. In this background, this study proposes a possible association of the solar activity over the tropical Indian region. Here the variability in the VIM over the peninsular Indian region during the SON and JJA season has been proposed to be associated with solar activity based on some empirical evidence. The cross spectrum between seasonal VIM and solar radio flux also shows spectral power having peaks at 11 year period for monsoon and post-monsoon seasons (for other seasons the power is less).

In the case of intraseasonal variability, for all the years the first principal mode of variability describes zonally homogenous patterns implying that VIM variability over peninsular India is coherent with VIM variability over the Arabian Sea. For a normal year 1996, the intraseasonal variability of the vertically integrated moisture over peninsular India is prominent in the 12-32 day scale. For wet year 1997 also, multiple significant modes are present with the scales having a shift to the greater scales. For the dry year 2002, the scales are even greater. For all the three years pre-monsoon and post-monsoon VIM variability scales are almost in same band but for monsoon season VIM is unique for three years.

2.8   CONCLUSION

The total precipitable water or Vertically Integrated Moisture (VIM) from surface to various levels over the peninsular India for different seasons were studied using NCEP/ NCAR monthly specific humidity datasets. The wavelet spectrum of VIM over the peninsular India during the summer monsoon (June-August) and post monsoon (September-November) showed decadal mode of variability for the

study period of 1950-2004. The spatial extend of this mode of variability for different seasons were studied using Fast Fourier Transform (FFT) of the VIM for the region 20°S-50°N and 0-160°E. The spatial patterns of spectral power corresponding to 11 years for the JJA season shows high values over the Peninsular India and extending over Bay of Bengal to Indo-China peninsula. This also has a southeastward spread towards Indonesian region. Similar analyses for post monsoon season SON show high spectral power for 11-year period over Peninsular India. The spectrum for JJA season show highest spectral powers concentrated over regions other than peninsular India.

To suggest a possible association with moisture and air temperature in connection with solar activity, the correlation of monthly solar flux and tropospheric air temperature was studied along vertical sections of 80°E and 10°N. The meridional cross-section shows that in the northern hemisphere the correlation extends down to about 850 hPa up to 25°N. The zonal cross section shows that the correlations are significant up to 800hPa in the eastern hemisphere. Thus it seems that the small influence of solar flux on the tropospheric temperature may be amplified (as described by Eq. 2.2) and reflected on moisture as the described mode of variability.

The wavelet analysis of PCs of VIM for various seasons and various years shows that the intraseasonal variability in the integrated moisture over the Arabian Sea and Peninsular India is of around 16-24 days. The EOF patterns show that the third greatest variability over the Indian domain regarding the VIM is over the Arabian Sea and Peninsular India, though the variabilities account for a small percentage. Spectral analysis of seasonal VIM shows intraseasonal variability of 12-32 days with significant variation in the scale band and the principal modes of variability in the EOF analysis show zonal coherence over peninsular India and adjoining Seas.

50

CHAPTER 3

Solar Activity and Low Frequency Variability in the Rainfall of Peninsular India

3.1 INTRODUCTION

India's economy depends largely on agriculture, which in turn depends mainly on rainfall. Nearly a quarter of the total domestic production towards the country's economy is agriculture, which depends mainly upon the monsoon rainfall. Recently for many years, the Indian subcontinent has suffered severe drought due to the failure of southwest monsoon. Causes for the abnormal conditions in rainfall over India, such as occurrence of floods and droughts are not yet completely understood. It is believed that major cause is the localized anthropogenic influences over the environment, *viz.*, deforestation, and excessive discharge of fossil fuel residuals. Another reason that is clearly discernible in most of the recent findings is the solar radiative forcing over the global climate and the Earth's environment. *Hiremath and Mandi (2004)* indicate that the solar cycle and related phenomena have a good correlation with the Earth's global climate and temperature. Their study indicated the influence of low frequency (> 20 yrs) variability of the solar activity on the Indian monsoon rainfall.

Since 1850, industrially produced concentrations of greenhouse gases (CO_2, CH_4, N_2O, chloroflurocarbons (CFCs)) and of tropospheric sulfate aerosols, have increased significantly *(Houghton et al 1995)*. The overall activity level of the Sun has risen, too. Earth's surface is warmed both by increased greenhouse gas concentrations and the enhanced solar radiation speculated to accompany the

Sun's increased activity, since both input additional energy in the climate system. In contrast, increasing atmospheric aerosol concentrations are expected to cool the Earth's surface by reflecting more of the Sun's radiant energy back to space. Whereas surface cooling is expected from tropospheric industrial aerosols, which have increased in the past century *(Penner et al 1995)*, the amount of aerosols injected into the stratosphere by volcanoes decreased for much of the twentieth century *(Robock and Free 1995)*, contributing to surface warming by allowing sunlight to warm the Earth's surface, unobstructed by atmospheric aerosol scattering, reflection, or absorption.

Climate responds differently to individual forcings—greenhouse gases, aerosols, ozone, solar variability etc. —because the forcings have distinct regional and altitude distributions and different temporal histories. Understanding solar influences on climate requires improved specification of both the amplitudes and timescales of solar radiative output changes on climatological timescales and the climate sensitivity to small insolation changes. Space-based solar monitoring has documented unambiguously the existence of an 11-yr cycle in the primary energy provided from the Sun to the Earth (its total radiative output). The possibility of larger amplitude changes over longer timescales that might physically account for significant climate change cannot be dismissed. Knowledge of climate response to the sun's changing solar radiation is rudimentary, encompassed in simple processes that fail to explain climate change observed on timescales from the past century to the 100 000-yr Milankovitch forcing *(Rind et al 1989)*. Present inability to quantify climate forcing by changing solar radiation, whether negligible or significant, is a source of uncertainty that impacts policy making regarding global climate change *(Houghton et al 1995)*.

3.1.1 Solar Radiative Output Variability

The Sun, whose surface temperature is near 6000 K, provides electromagnetic particle and plasma energy to the Earth at levels summarized in Table 3.1. Electromagnetic radiation is by far the largest solar energy source for the Earth and the most important for its climate. When the solar spectrum is integrated over all wavelengths, the total radiative out put from the sun at the Earth is 1366 W m^2 (with a measurement uncertainty of 63 W m^2).

Similarities among various climate and solar activity records (Fig. 3.1) suggest that climate variability in the recent Holocene may be partly attributable to the variable Sun. Some climate records have periodicities at 11 and 22 yr that are common also in solar activity proxies. Other climate records appear to correlate well with long-term solar activity on decadal to centennial timescales. Some of these relationships are summarized below. That not all climate time series exhibit this anecdotal evidence for solar forcing is usually interpreted as evidence to reject the hypothesis of a sun– climate connection, leading to present ambiguity about the physical reality of the effect. Resolving this ambiguity requires proper identification of physical mechanisms to explain the cycles and correlations.

Tropospheric temperatures during the past few decades appear to be about 0.58 to 1.58°C warmer during times of solar cycle maxima, notably in the mid-latitude Western Hemisphere *(Labitzke and van Loon 1993a,b)*. A 0.158°C increase in land-surface temperatures from 1986 to 1990 has been attributed to increasing solar irradiance from cycle 22 minimum to maximum activity *(Ardanuy et al 1992)*. Sea surface temperature (SST) band-passed to isolate the decadal component of their variability exhibit changes of the order of 0.18C that are highly correlated (correlation .0.9) with the Sun's 11-year activity cycle in the past four decades *(White et al 1997)*. Coral records of $\delta^{18}O$ infer that the relationship between the

Sun's 11- year cycle and SST extends over the past 400 yr *(Dunbar et al 1994).* Furthermore, solar related SST changes may initiate regional precipitation fluctuations *(Perry 1994).* High resolution ice core records provide further evidence for apparent correlations of climate parameters with the sun's 11-year cycle both at mid-latitude high-altitude sites, and in the high-latitude Greenland *(Grootes and Stuivers 1997)* ice core. Furthermore, correlations of climate parameters with the 11-year cycle may be enhanced significantly when the climate data are sorted according to the phase of the Quasi Biennial Oscillation (QBO) *(Barnett 1989; Labitzke and van Loon 1990).*

Forcing factor	Generic mechanism
Total solar irradiance (variations due to orbital variations or to solar emission).	Radiative forcing of climate. Direct impact on sea surface temperatures and hydrological cycle.
Solar UV irradiance.	Heating the upper and middle atmosphere, dynamical coupling down to troposphere. Middle and lower atmosphere chemistry and composition; impacts temperature structure and radiative forcing.
Solar energetic particles.	Ionisation of upper and middle atmosphere; impact on composition and temperatures. Magnetosphere – ionosphere – thermosphere coupling.
Galactic cosmic rays	Ionisation of lower atmosphere; impact on electric field. Impact on condensation nuclei.

Table 3.1: Summary of routes through which solar variability may influence the climate of the lower atmosphere

According to *Hiremath (2006),* for a particular solar cycle period, there appears to be an overall trend that irrespective of signs of the correlation coefficients, the monsoon rainfall variability is strongly correlated during the weak sunspot activity and weakly correlated during the strong sunspot activity. That means during the 11-year solar cycle, a weak sunspot activity leads to strong Indian rainfall variability and vice versa.

Spectral analysis and visual matching of the high-resolution isotopic data from a region best suited to study South West Monsoon precipitation with Total Solar Irradiance (TSI) reconstruction, indicates a possible solar control over South West Monsoon on centennial timescales. Variations in TSI (~ 0.2%) seem to be too small to perturb the South West Monsoon, unless assisted by some internal amplification mechanism with positive feedback. Two such mechanisms have been proposed. The first involves heating of the Earth's stratosphere by increased absorption of solar ultraviolet (UV) radiation by ozone during periods of enhanced solar activity. It is known that the magnitude of variation in UV is higher than that in TSI. The positive feedback is that more the UV, more the ozone production and heating. This heating is transferred to the troposphere as shown by theoretical models. Enhanced heating results in increased thermal contrast between the Asian land mass and the Indian Ocean, and also increases evaporation from the oceans, thus enhancing the monsoon winds and precipitation. This involves another possible feedback: release of latent heat to the troposphere by monsoon precipitation, which in turn strengthens the monsoon winds. The second mechanism is that during periods of higher solar activity, the flux of galactic cosmic rays to the Earth is reduced, providing less cloud condensation nuclei, resulting in less cloudiness. This extra heating of the troposphere increases the evaporation from the oceans. With a maximum entropy spectrum estimate, *Mitra and Dutta (1992)* analyzed the ISMR series from 1871 to 1985 and observed 11- and 18.6-year periodic oscillations in the rainfall variations.
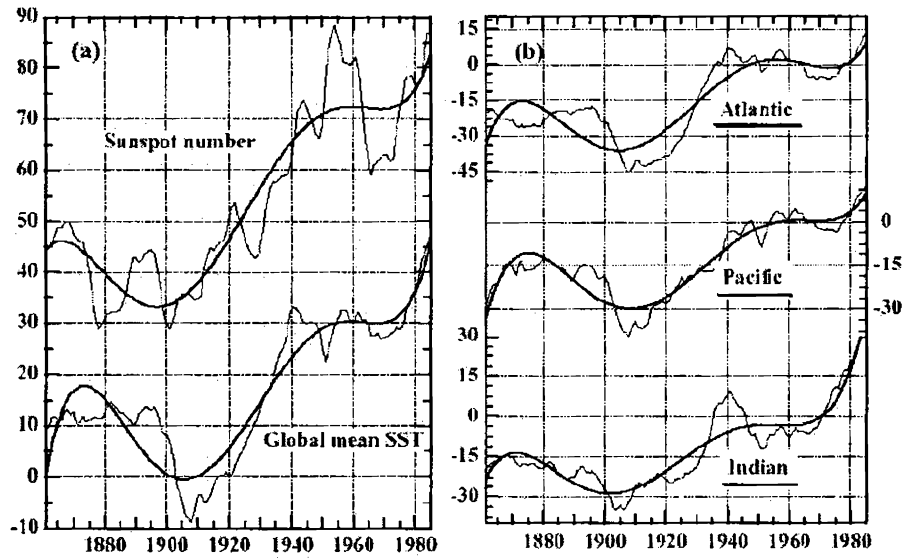
Fig. 3.1 Sea Surface Temperature anomalies in 0.01K (lower left is global average and right panel basin averages) compared to sunspot number (upper left). To emphasise the long term similarity 7th degree polynomial have been fitted to the curves. Adapted from Reid (2000).

Ma et al. (2007) studied the periodicity of Indian Summer Monsoon Rainfall (ISMR) changes between 1871 and 2004 using Scargle periodogram and wavelet transform methods, and reviewed the possible influence of solar activity on the rainfall. They noticed some periodic oscillations at about 2, 5, 7, 10, 13, 17, and 80 years in the ISMR series. The 2.3 to 2.8 year fluctuation peaks maybe due to the Quasi-biennial Oscillation (QBO) in the atmospheric stratosphere *(Parthasarathy and Mooley, 1978)*. *Mitra and Dutta (1992)* hypothesized that the 10 to 11 year rainfall cycle might be effected by the 10 to 11 year solar cycle. There are no stable periodic oscillations in the rainfall variations and almost all periodic fluctuations have significant variations over time. *Pant and Rupa (1997)* mentioned this point during analysis of the ISMR. All these studies suggest invariably an association between ISMR and solar activity. More studies on the detailed physical mechanisms need to be made in future.

In the present study we investigate the effect of the solar activity for a decadal (~11 years) scale and the influence of the solar activity on the rainfall over India. There exist many studies on the connection between solar activity and Indian rainfall, but a high resolution all India daily rainfall dataset provides a better tool for studying the spatial variability of this connection in a region small in spatial scale.

3.2 DATA

The high-resolution daily gridded rainfall data (1^0x1^0) obtained from India Meteorological Department (IMD) for the Indian region has been used for this study. A detailed description of the data is given in *Rajeevan et al (2005)*. The data used as proxy for the Solar activity is the 10.7 cm solar radio flux obtained from the website of the Canadian Space Agency. The three dimensional wind data has been taken from the National Centre for Environmental Prediction (NCEP) website.

3.3 METHODOLOGY

Wavelet analysis was carried out for high frequency removed Kerala Summer monsoon Rainfall (KSMR) to analyse the low frequency signals. To avoid the annual and biennial variabilities inherent in climate data, 4-year running mean was calculated for KSMR. To effectively find out the periodicity of the low frequency variability in the KSMR it was subjected to wavelet analysis using morlet as the mother wavelet. A cross-spectral analysis has been carried out between individual subdivisional summer rainfall and observed 10.7cm solar radio flux (F10.7). In order to analyse the spatial perspective of the low frequency variability on an 11-year period spatial correlation was done for the 4-year mean 1^0x1^0 seasonal rainfall data with adjusted, observed and absolute Solar Radio Flux for lag3, lag2, lag1 and

concurrent time. The daily gridded rainfall from the India Meteorological Department was used to compute seasonal mean rainfall for doing a spatial analysis.

To suggest a pathway for the relation between solar activity and the low frequency variability in the seasonal rainfall the following method was adopted. To find the modulation of convection over the monsoon region by the solar activity, the F10.7 and vertical velocity at 500 hPa ($\omega500$) has been correlated. The zonal wind fields at 850 hPa were regressed with F10.7 and the resultant vectors were overlayed on the spatial maps of correlation between vertical $\omega500$ and F10.7. This was carried out for June, July, August and September independently. The same analysis was carried out for seasonally averaged values of $\omega500$ and wind field at 850 hPa for two time sections before and after 1976 to find any departure between them.

3.3.1 Cross Spectrum Analysis

Cross-spectral analysis allows one to determine the relationship between two time series as a function of frequency. Normally, one supposes that statistically significant peaks at the same frequency have been shown in two time series and that we wish to see if these periodicities are related with each other and, if so, what is the phase relationship is between them. If we have two time series whose power spectra both are indistinguishable from red noise and still there be some coherent modes at particular frequencies, we can test this by looking at the coherency spectrum. Suppose we have two time series x (t) and y (t) and we want to look for relationships between them in particular frequency bands. First consider harmonic analysis in terms of line spectra:

$$x = \bar{x} + \sum_{k=1}^{n/2-1}\left(A_{xk}\cos\left(\frac{2\pi kt}{T}\right) + B_{xk}\sin\left(\frac{2\pi kt}{T}\right)\right) + A_{xN/2}\cos\left(\frac{\pi Nt}{T}\right) \quad \ldots(3.1)$$

$$y = \bar{y} + \sum_{k=1}^{n/2-1}\left(A_{yk}\cos\left(\frac{2\pi kt}{T}\right) + B_{yk}\sin\left(\frac{2\pi kt}{T}\right)\right) + A_{yN/2}\cos\left(\frac{\pi Nt}{T}\right) \quad \ldots(3.2)$$

Because of the orthogonality of the functions for evenly spaced data we can write the covariance between them as a sum of contributions from particular frequencies.

$$\overline{x'y'} = \frac{1}{2}\sum_{k=1}^{\frac{N}{2}-1}\left(A_{xk}A_{yk} + B_{xk}B_{yk}\right) + A_{x\frac{N}{2}}A_{y\frac{N}{2}} \quad \ldots(3.3)$$

$$\sum_{k=1}^{\frac{N}{2}} CO(k) = \text{the cospectrum of } x \text{ and } y$$

3.4 RESULTS

The time series of 4-year mean KSMR and F10.7 reveal a close covariability for a period of 50 years from 1948 to 1998 (Fig. 3.2). Both the series have peaks at an interval of 10-12 year period. The maximum value of KSMR during this fifty-year period is obtained in the year 1958 whereas the maximum of solar radio flux of this series is observed in 1959. The correlation coefficient of these two time series is significantly high, with a value of 0.567. This points out that the solar radio flux is having a positive relationship with the 4-year mean KSMR.
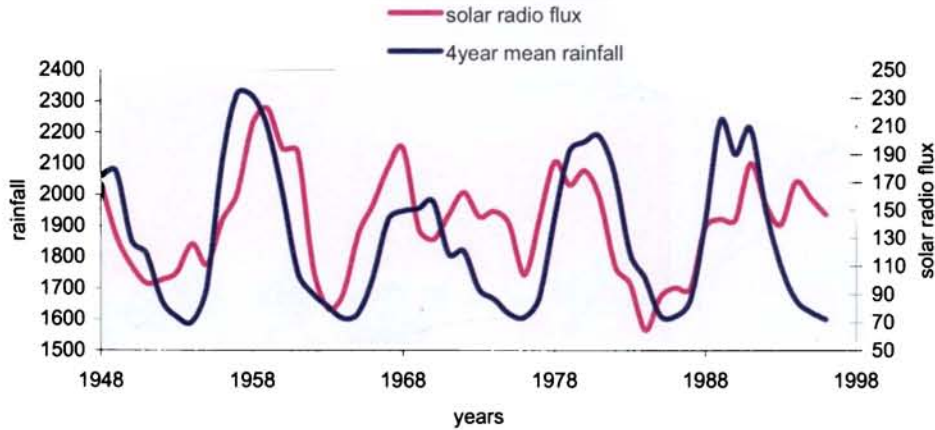
Fig. 3.2 time series of 10.7 cm solar radio flux (adjusted) and four year running mean of Kerala Summer Monsoon Rainfall from 1948 to 1998.

In order to quantify the periodicity of this covariability, wavelet analysis of the 4-year mean KSMR for the period 1901-2000 was carried out, which gives a significant power spectrum in the 6-14 year band (Fig 3.3). From 1901-1970, the power is dominant and significant in the 6-9 year frequency band, even though power in the low frequency band (10-14 year) is also significant in the period 1940-1970. The spectrum shown is significant at 95% level. Up to 1930, the power is also found to be significant in the 16-18 year band. This band is not well defined after 1930. A shift from high frequency to the low frequency band is noted after 1970's. Therefore, during the recent years a change in the frequency has been noted in the 4 year mean KSMR towards the low frequency band (11-12 year). The time average plot also shows that the power is significant and maximum power obtained in the 11-12 year band. The 11-12 year band is strong from 1940-1990 and this band alone persists in the recent years.
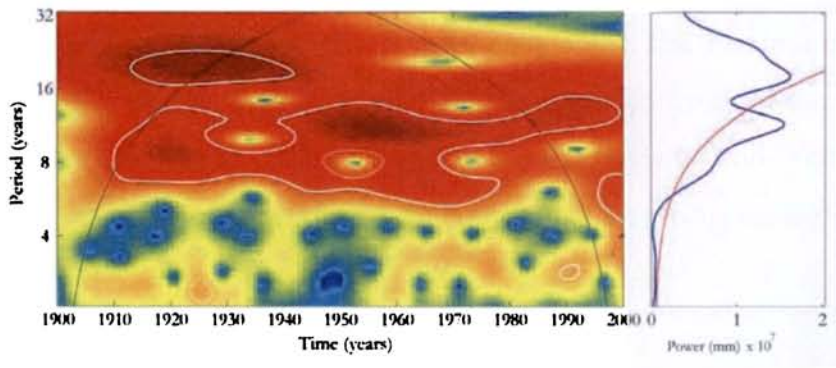
Fig. 3.3. Wavelet power spectrum of high frequency removed Kerala Summer monsoon rainfall. Right panel shows the time averaged power (blue line) and 95% significance background spectrum (red line)

The scatter plot of F10.7 and KSMR (Fig. 3.4) shows a clear indication of the association between the two series. The red line shows the regression fit to the data. From the figure it can be seen that there are not many outliers.
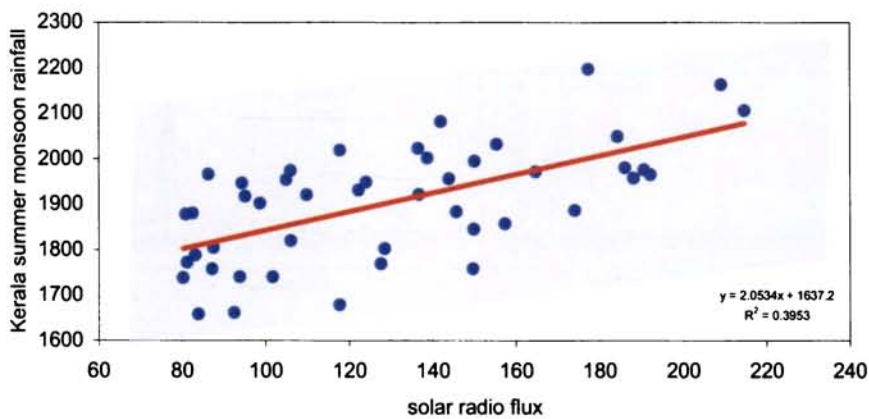
Fig. 3.4. Kerala subdivisional summer rainfall regressed as function of F10.7

The cross-spectral estimates of 10.7 cm solar radio flux and rainfall of eight subdivisions over Peninsular India region is shown in Fig 3.5. The spectral peaks obtained for all the eight subdivisions correspond to the decadal frequency. The maximum power is observed for Kerala followed by coastal Karnataka, both lying on the windward side of Western Ghats. The least values are for Rayalaseema and South Interior Karnataka. The power obtained for each subdivisions are given in Table 3.2.
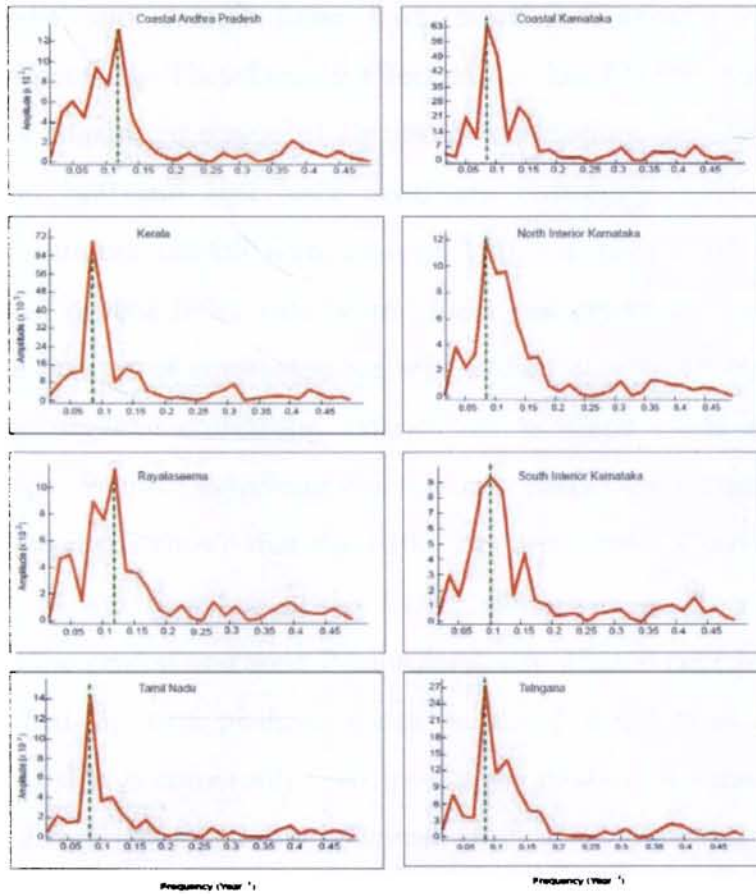
Fig. 3.5 The cross spectral power as a function of frequency between 10.7 cm solar radio flux and seasonal rainfall of eight subdivisions over the homogenous region peninsular India

The observed F10.7 and summer rainfall shows very low spatial correlation over India (Fig 3.6). The correlation maps are shown for lag3, lag2, lag1 and lag0. The

contours show the correlation is significant at 95% level. For the lag3, significant correlation is obtained over a small region where the monsoon trough exists. When the correlation between the 4-year mean rainfall and observed F10.7 is calculated, significant correlations were obtained over central India and south peninsular region. For the correlation of summer rainfall (actual and 4 year mean) with absolute F10.7, a similar pattern is observed (Fig 3.7). The lag2 correlation shows high values over central India and central peninsular India. The central peninsular India and central India have significant negative and positive correlations respectively. Therefore the effect of absolute F 10.7 is opposite in the nearby regions. Maximum region of significant correlations is obtained for lag1 correlation and lag0 and lag2 have significant correlation over Kerala. The correlation of summer rainfall with adjusted F10.7 is significantly related over some regions of central India, east central India and peninsular India (Fig 3.8). The maximum regions of correlation are seen in lag1 correlation maps. For lag0 correlation the negative correlation extends up to Tamil Nadu from Central Peninsular region. Positive significant correlation is also observed over Kerala. All these correlation maps shows that the F10.7 has a positive influence on rainfall over the central and west peninsular India, whereas a negative influence is observed over the central and west Peninsular India. Thus a negative correlation zone sandwiched by two positive zones is noted throughout the analysis. Observed F10.7 data is commonly used for climate studies. Not much difference is noted for the correlation pattern of summer rainfall with observed, absolute and adjusted F10.7.

Subdivision	Amplitude (10^3)
Coastal Andhra Pradesh	13
Coastal Karnataka	63
Kerala	70
North Interior Karnataka	12
Rayalaseema	11
South Interior Karnataka	10
Tamil Nadu	14
Telangana	27

Table 3.2. The peak value of spectral power corresponding to the decadal mode obtained for each subdivision in Peninsular India

The regression and correlation coefficient maps (Fig 3.9) show that for the month of June (Fig 3.9a), the low level cross equatorial monsoon flow over the oceanic region is enhanced and a convergent zone develops over Northern Arabian Sea. When the monsoon gets established over the Indian region, during June, however the influence of F10.7 on convective activity over peninsular India is negative. In the northern Arabian Sea convection is enhanced, while over Southern Arabian Sea it is hindered. Almost all region above Bay of Bengal also convection is inhibited. Over entire peninsular India there is a strong weakening of convective activity. However the monsoonal flow gets reinforced.
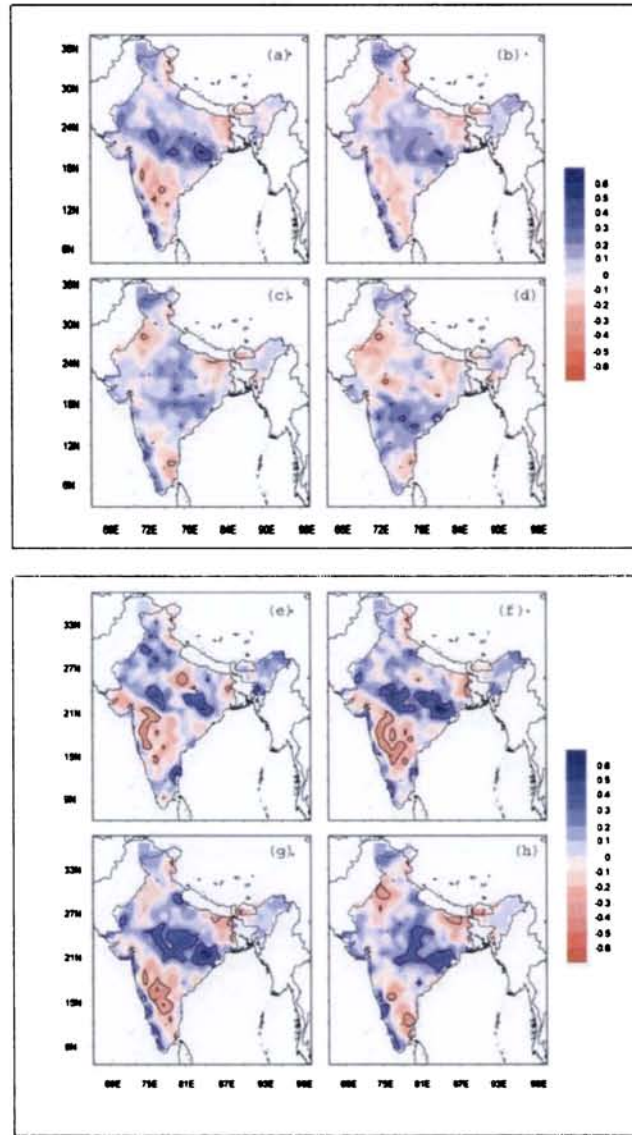
Fig 3.6 Spatial correlation maps of observed F10.7 and seasonal rainfall over India (upper panel for the actual rainfall and lower panel 4-year averaged rainfall) for (a) and (e) lag3, (b) and (f) lag2, (c) and (g) lag1 and (d) and (h) for concurrent time steps.
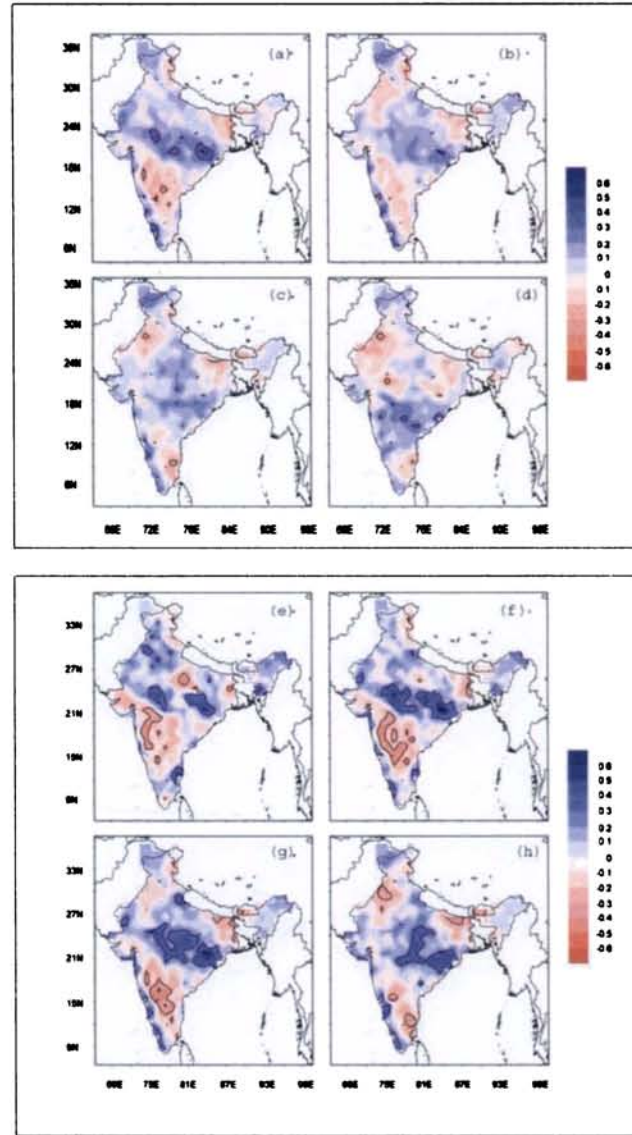
Fig. 3.7 Spatial correlation maps of absolute F10.7 and seasonal rainfall over India (upper panel for the actual rainfall and lower panel 4-year averaged rainfall) for (a) and (e) lag3, (b) and (f) lag2, (c) and (g) lag1 and (d) and (h) for concurrent time steps.

66
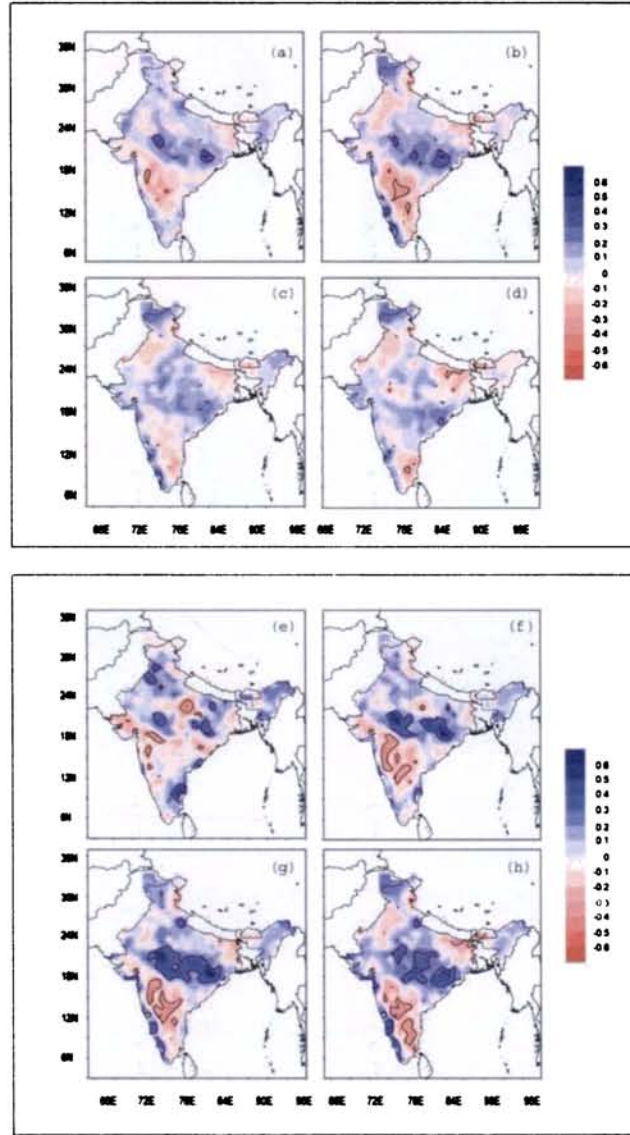
Fig. 3.8 Spatial correlation maps of adjusted F10.7 and seasonal rainfall over India (upper panel for the actual rainfall and lower panel 4-year averaged rainfall) for (a) and (e) lag3, (b) and (f) lag2, (c) and (g) lag1 and (d) and (h) for concurrent time steps.
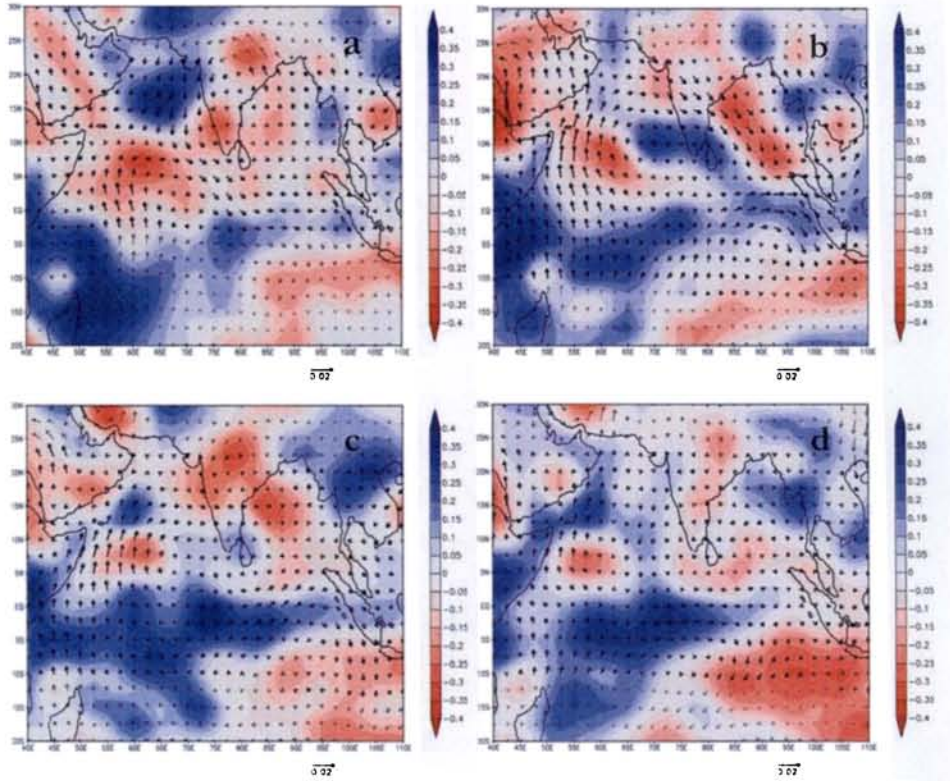
Fig. 3.9 Distribution of monthly regression coefficients of 850 hPa wind (vectors) and correlation coefficients of 500 hPa vertical velocity versus F10.7 (shading) for (a) June, (b) July, (c) August and (d) September.

During July (Fig. 3.9b), the monsoon currents get even stronger and there exists a very strong convergent zone over peninsular India and adjoining Arabian Sea. The descending limb over the Bay of Bengal gets very stronger and convergent zone over northern Arabian Sea gets weakened. For August (Fig. 3.9c) also the cross equatorial flow gets intensified as a function of F10.7 and entirely a strong equatorial belt of convergence exists over the oceanic region with its descending limb at around 20^0 N. Still over peninsular India convection is enhanced. For September (Fig. 3.9d), the response of the wind field is not as strong as that for the months of July and August. Here also a major part over the Arabian Sea is convective.
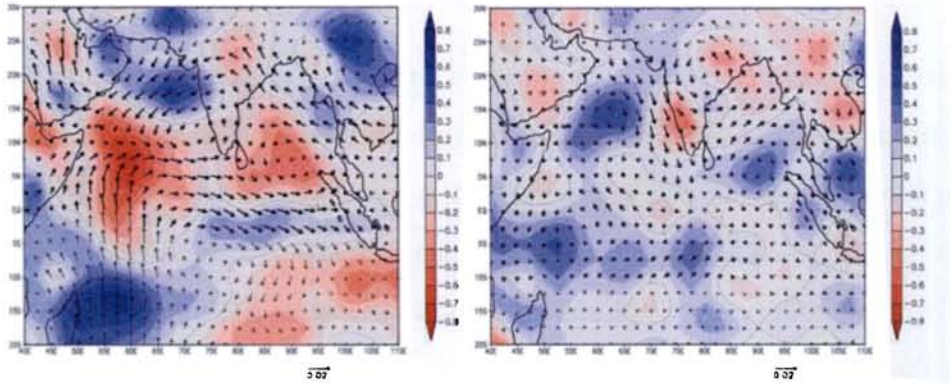
Fig. 3.10 Distribution of monthly regression coefficients of 850 hPa wind (vectors) and correlation coefficients (shading) of 500 hPa vertical velocity versus F10.7 (June-September averaged) for periods before (left panel) and after (right panel) 1976

From the earlier analysis it is clear that the variability of rainfall influenced by solar radio flux is physically meaning full as the zones of significant correlation between 500 hPa vertical velocity and solar radio flux supports the regression vectors of solar radio flux with low level monsoon flow. To check if any changes have happened in the relationship during the period of analysis, the same analysis was carried out for seasonal values of vertical and horizontal wind fields before and after 1976. From Fig. 3.10 it is clear that the activity of F10.7 on the monsoon current convection is significantly changed after 1976. The influence of solar activity on the intensification of average cross equatorial monsoon current (average wind for Jun-Sep) is weakened after the decade. A strong zonal suppression belt of convection over the southern Arabian Sea has vanished almost entirely. Still the significant effect over the northern Arabian Sea remains almost the same. After 1976 a strong descending limb is observed over the peninsular Indian region.

3.5   CONCLUSION

The wavelet analysis of high frequency removed KSMR showed a significant mode of decadal variability corresponding to 11-12 year period. The cross-spectral analysis of subdivisional rainfall over peninsular India also showed spectral peaks at a decadal frequency scale. The correlation maps of 4-year running mean Indian summer monsoon rainfall shows significant values for concurrent time and lag1 and lag2. While the western coastal region shows a positive relation between them the entire leeside of the Western Ghats shows negative relation. Almost entire peninsular India except the windward side of Western Ghats shows negative correlation with F10.7.

The regressed vectors between F10.7 and zonal wind indicate that the monsoon flow in the months of July and August is influenced by solar flux and the convection also is very much influenced by solar flux. Though there have been significant changes in the regions and intensity in these relations after 1976.

CHAPTER 4

Peninsular Indian Rainfall and its Association with Meteorological and Oceanic Parameters over Adjoining Oceanic Region

4.1 INTRODUCTION

The Indian summer monsoon exhibits large interannual and intraseasonal and spatial variability. Many observational and modeling studies have pointed out that the slowly varying surface boundary conditions, particularly in the winter and pre-monsoon seasons, contribute a major forcing on the interannual variability of the monsoon. Global and regional parameters representing these conditions provide the handle for seasonal prediction. Empirical modeling strategies include the identification of reliable precursors and an optimal utilization of the information contained in the data on precursors. The reasonable success achieved by the empirical approach has motivated further work on global/regional teleconnections of the Indian summer monsoon season. This resulted in a large number of predictors as well as a variety of statistical techniques. Despite the fact that atmospheric general circulation models have made quick and appreciable advances in the recent past with vastly improved representations of the Asian summer monsoon, empirical approaches still continue to have an important place in operational seasonal forecasting. In spite of the strong physical basis inherent in the empirical formulations, the relationships considered are by no means consistent in space and time, with consequent implications to their predictive skills. The notable failure of empirical models in predicting the deficient summer monsoon of 2002 is a case in point. Modeling methodologies do not appear to substantially improve

forecast skill for a given set of predictors. Further, several studies have shown that decadal variability plays a major role in the secular variation of predictand-predictor relationships. Predictability of intraseasonal variability also is a limiting factor that is proving to be a daunting task. In order to provide seasonal monsoon predictions of practical value, predictands based on sub-regional and sub-seasonal monsoon rainfall need to be given more emphasis in empirical forecasting research. While a few attempts have been made in this direction, sufficient number of predictors is not available specific to such predictands. Therefore, predictor identification needs to be pursued in a comprehensive manner using modern data sets (like reanalysis), to identify new predictors with possibly non-linear teleconnections. There have been some methodological innovations recently to handle secular variations in the teleconnections and optimize the predictive information.

There is sufficient empirical and theoretical evidence to believe that sea surface temperatures exert significant control over the atmosphere. The works of *Singh (1983), Joseph and Pillai (1984), Rao and Goswami (1988), Vinayachandran and Shetye (1991), Sadhuram et al (1991)* have shown the significance of SST over Arabian Sea as an input parameter for the Indian monsoon rainfall. The rainfall is also related to the sea-surface temperatures (SSTs) of the Indian Ocean, Arabian Sea, and Bay of Bengal. *Shukla (1975)* used a numerical model and found that cold SSTs in the Arabian Sea would reduce evaporation, increase surface pressure downstream, and therefore reduce monsoon rainfall over India. *Washington et al (1977)* attempted to reproduce the simulations of Shukla and reported the effect of local SSTs on monsoon rainfall.

Weare (1979) used an empirical approach involving principal component analysis (PCA) and found that SSTs in the Arabian Sea and Indian Ocean over the

period 1949–1972 were negatively, but weakly, related to monsoon precipitation throughout India. *Rao and Goswami (1988)* examined ship records from 1900–1979 and found that warmer SSTs in the southern portion of the Arabian Sea tended to generally increase monsoon rainfall; similar findings were reported by *Kumar and Sastry (1990)* and *Hastenrath and Greishar (1993)*. SSTs in the Arabian Sea, Indian Ocean, and Bay of Bengal were positively related to rainfall in southern India and weakly related to the rainfall in other regions of the subcontinent. Many others *(Shukla and Mishra 1977)* have found similar results about the significant role of the SST anomalies over the Indian Ocean, the Arabian Sea and the Bay of Bengal. These studies point out the importance of the moisture budget and the amount of evaporation taking place in these seas as a determinant of the amount of precipitation taking place in different parts of the country.

Indian Ocean is different from other Oceans in many aspects. The northern boundary of Indian Ocean does not extend beyond 25° N. It is not bounded by a solid coastal eastern boundary, as that of the Atlantic and Pacific Oceans. The Indian Ocean is split into two basins - the Arabian Sea and the Bay of Bengal. Thus the Indian Ocean doesn't have the currents to transport and discharge heat to higher latitudes, as the Gulf Stream and Kuroshio do in the Atlantic and Pacific, respectively. It is relatively well connected to the western part of the Pacific Ocean characterized with its Warm Pool. The two-basin split of the ocean is a recipe for winds pattern unlike any other over the rest of the oceans where more stable trade winds patterns are observed
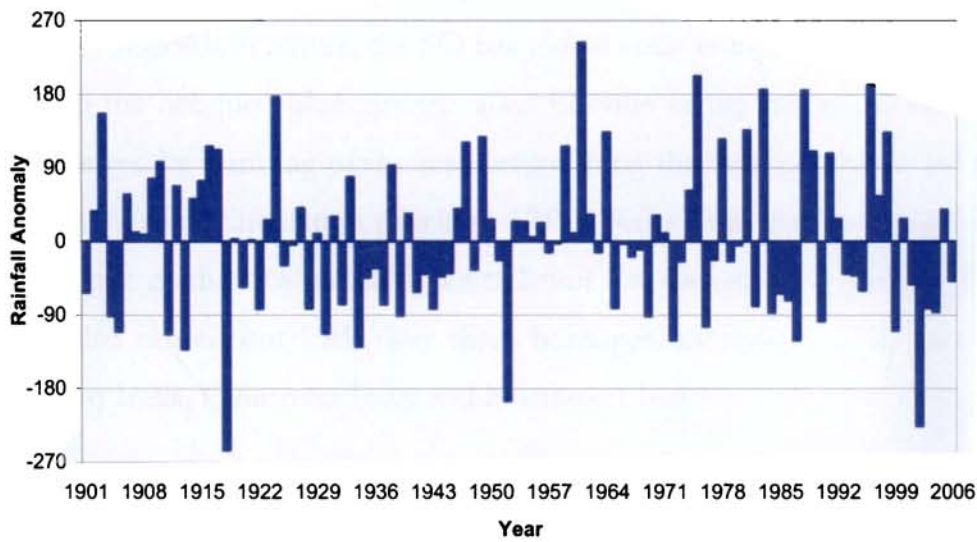
Fig 4.1. Rainfall anomaly for the period 1901-2005 over peninsular India. The mean rainfall for the period is 661 mm with a standard deviation of 94 mm.

The forecast of monsoon rainfall was first made by Blanford, based on his hypothesis that varying extent and thickness of the Himalayan snows exercise a great and prolonged influence on the climate conditions and weather of the plains of northwest India *(Blanford, 1884)*. His success in Long Range Forecast (LRF) of monsoon led to start operational LRF. Sir John Elliot, who succeeded Blanford gave forecasts based on (i) Himalayan snow cover, October to May, (ii) local peculiarities of pre-monsoon weather in India and (iii) local peculiarities over Indian Ocean and Australia *(Thapliyal 1987)*. Expanding on the works *Lockyer and Lockyer (1904), Walker (1908, 1918, 1923)* initiated extensive studies of worldwide variation of weather elements such as pressure, temperature, rainfall etc., with the main aim to develop an objective method for LRF of monsoon rainfall over India. These studies led him to identify three large-scale pressure seesaw patterns; two in the Northern Hemisphere (North Atlantic

Oscillation, NAO and North Pacific Oscillation, NPO) and one in the Southern Hemisphere (Southern Oscillation, SO). While the NAO and NPO are essentially regional in nature, the SO has global-scale influences, which was later linked to the oceanic phenomenon called El Niño in the east-equatorial Pacific characterized by warming of the sea surface along the Peru coast; this led to the theory of Walker Circulation *(Bjerknes, 1969)*. Walker was the first to introduce an objective method by including Correlation Coefficient (CC) analysis. *Walker (1924)* also carried out LRF over three homogenous regions of India namely Northeast India, Peninsular India and Northwest India.

Most of the studies on LRF of Indian monsoon rainfall are based on empirical or statistical techniques. These statistical techniques range from simple correlation analysis to advanced procedures such as canonical correlation analysis and artificial neural networking. But the commonly used statistical technique for LRF of monsoon rainfall is the linear regression analysis. A large number of regression models have been proposed so far *(Hastenrath, 1991)*. The predictors for the model are chosen either subjectively or by applying objective criteria. The limitation of the subjective selection is that it may not optimize the variance explained whereas the objective selection is highly sensitive to the data window and overfit the data sample *(Thapliyal 1987; Parthasarathy and Sontakke 1988; Hastenrath and Greischa, 1993)*. The reliability of regression models needs to be assessed by testing on as large and independent data sets, as they are sample-specific in nature.

Gowariker et al (1989) developed parametric and multiple power regression (MPR) models with 15 predictors for LRF of AISMR, which were modified *(Gowariker et al., 1991)* to include 16 predictor parameters. The model indicates the likelihood of the monsoon rainfall to be excess or deficient, depending upon

75

the proportion of favourable/unfavorable parameters out of the total of 16 parameters. This method is highly sensitive to the nature of the predictor data set. The power regression model, successful in operational LRF during the period 1988-97, claims to account for possible non-linear interactions of different climatic forcings with the Indian monsoon system. But the predictors were identified based on their linear correlation with AISMR. The model requires rigorous statistical testing using longer and homogeneous data sets and independent verification as it failed in 1994 and 1997 as other models.

The dynamic stochastic transfer (DST) model developed for the prediction of AISMR as well as the monsoon rainfall over peninsular and northwestern India has only one predictor *(Thapliyal, 1987)*. But the model performs with high accuracy than multiple-regression, MPR, ARIMA *(Thapliyal, 1990)*. *Shukla (1987) and Gregory (1989)* suggested grouping the subdivisional rainfall, to define area averages for large homogeneous regions due to the large spatial variability of monsoon rainfall. They yielded better formulae for forecasting rainfall over homogeneous regions than when India was treated as one unit. *Kumar (1994)* attempted LRF of monsoon rainfall over the 29 meteorological sub-divisions in India using canonical correlation analysis (CCA) technique and found that the spatial extent and the magnitudes of skill scores are much larger than those obtained with multiple regression analysis *(Prasad and Singh, 1992)*. The problems in LRF is also addressed *(Rajeevan, 2001)*

The studies on the seasonal prediction of monsoon rainfall using general circulation models (GCMs) are very few. This may be partly attributed to the lack of skill in the simulation of monsoon rainfall over the Indian subcontinent *(Gadgil et al, 1992)*. Also, different GCM simulation gives marked differences in the simulated monsoon precipitation *(WCRP, 1992)*. The simulation of the

Indian summer monsoon rainfall is very sensitive to the initial conditions *(Palmer et al, 1992)* also adds up problem to the present situation. However, strong and weak monsoon circulations based on the SST distributions over tropical Pacific and Indian Oceans could be simulated *(Ju and Slingo, 1995* and *Soman and Slingo, 1997)*. Thus, the sensitivity of the model in simulating the interannual variability in tropical circulation seems to be closer to the observed characteristics of the monsoon, while a realistic simulation of monsoon rainfall is yet to be achieved by most GCMs.

Reliable predictors for LRF are identified by analysing the relationships between Rainfall and regional/global fields of several surface/upper-air parameters. Correlation coefficients are used to identify the various forcings on the monsoon. They also exhibit notable sensitivity to the data window considered both in terms of the position and length of the window in the time domain. This leads to variations in their magnitude as well as sign, imposing some limitations on the reliability of the predictors.

4.1.1 Interrelationships among the predictors

Large numbers of predictors identified so far are highly interrelated and they fall into one of the categories like regional conditions, ENSO indicator, cross equatorial flow etc. The presence of such high multicollinearity among the predictors imposes the problem of redundancy and unnecessary loss of degrees of freedom when they are used in large numbers in regression-based forecast schemes *(Kumar et al 1995)*.

Though the predictors can be classified into four different groups based on their known physical linkage with the monsoon, the forcings represented by them are not entirely exclusive to their respective groups. The forcings represented by the

various predictors can be objectively delineated and the common variance among them pooled into a set of independent principal components. However, not much work has so far been done using this approach. The results of a work by *Kumar et al (1997)* indicate that a single component accounts for about half of the total variance in the predictors. This component apparently represents ENSO type variability in the predictors and is highly and significantly correlated with AISMR. This clearly shows that the ENSO has a ubiquitous influence on the monsoon circulation, playing a dominant role in the LRF.

In a macro regional scale, peninsular India has got very low degrees of relation to the AISMR *(Nayagam et al, 2007)*. A great amount of attention is given for work on regional scale forecast models for regions such as Peninsular India, northwest India and other homogenous regions *(Rajeevan et al, 2000)*. Fig 4.1 shows the rainfall anomaly obtained over the Peninsular Indian region during the summer monsoon season for the period 1901-2005. The mean rainfall for the period is 661 mm with a standard deviation of 94 mm. The rainfall expressed in anomaly shows that the rainfall anomaly has a positive increase after 1975. Of the nineteen WET years during the period, 9 occur after 1970's. The WET years are defined as years with rainfall greater than one standard deviation. This necessitates a study in the recent years. The correlation between the AISMR and subdivisional rainfall is given in Table 4.1. It is noteworthy that all the subdivisions bear low correlation values with AISMR, which points out the requirement of a new model for the peninsular region separately. Therefore, despite attempting to have a predictive formula for India as a whole, it would be sensible to have identified some parameters, which uniquely explain the Peninsular Indian Rainfall (PIR). This work is an attempt to derive some meteorological and oceanic parameters over the adjoining oceanic region of peninsular India and to regress them into a linear model. The study is

concentrated on the recent 32 years from 1975-2006 and the region over which the rainfall is predicted is shown in Fig 4.2.

Subdivisions	Correlation with AISMR
Coastal Karnataka	0.03
South interior Karnataka	0.13
North interior Karnataka	0.3
Kerala	0.09
Tamil Nadu	0.15
Coastal Andhra Pradesh	0.55

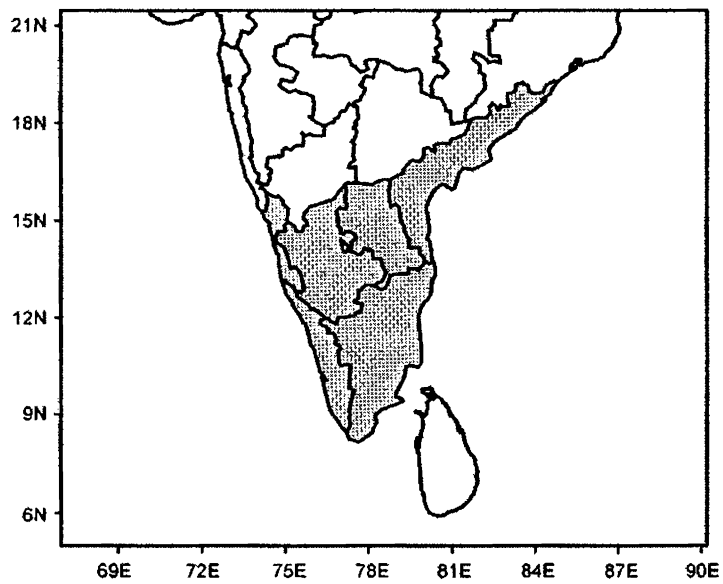Table 4.1. The correlation of AISMR with the subdivisional seasonal rainfall over peninsular India

Fig 4.2. Geographical map of peninsular India. Shaded area constitute the macro region, of which the rainfall data has been taken as peninsular Indian Rainfall (PIR)

4.2   DATA

Sea Surface Temperature used is, NOAA Optimum Interpolation (OI) SST V2 having 1×1^0 resolution in latitude and longitude. Air temperature, Zonal and

Meridional wind for 1975-2006 used for this study has been taken from NCEP. NCEP Reanalysis Derived data provided by the NOAA/OAR/ESRL PSD, Boulder, Colorado, USA, from their Web site at http://www.cdc.noaa.gov/. The spatial resolution of the data is 2.5×2.5^0 latitude and longitude. This has 17 vertical levels. A more detailed description can be seen in *Kalnay et al (1996)*.

Another data set used is the monthly rainfall of peninsular India obtained from the Indian Institute of Tropical Meteorology website (IITM-IMR). The primary datasets are from India Meteorological Department. The network selected for the study consists of 306 uniformly distributed stations for which rainfall data are available from 1871. The selection of the network of rain-gauge stations were based on the criteria that the network would provide one representative station per district having a reliable record for the longest possible period. The monthly (January - December) area weighted rainfall series for each of the 30 meteorological subdivisions have been prepared by assigning the district area as the weight for each rain-gauge station in that subdivision. Similarly assigning the subdivision area as the weight to each of the subdivisions in the region, area weighted monthly rainfall series are prepared for homogeneous regions of India as well as for all India, as a whole.

4.3 METHODS

4.3.1 Derivation of predictors and selection of best predictor sets

Linear regression model is a popular statistical method for meteorological prediction on various timescales like inter-annual, intra-seasonal, monthly, weekly etc. The main task of the development of the regression model includes the selection of predictors based on empirical relations between various parameters and rainfall, their careful and optimum selection in a stepwise

regression analysis, formulation of the regression equation and verification on independent samples.

The PIR was taken for the period 1975–1997, which we refer to as training period. Spatial correlation coefficient (CC) was calculated between PIR and the set of parameters under consideration for the period. The areas that bear CC's at 1% level of significance were identified and selected for calculating indices by taking area averages of the parameter over the respective significant area. The CC of these indices with PIR were checked for consistency for the entire period of analysis by doing 15-year sliding window correlation *(Bell, 1977)* Indices that have a significant CC at 5% level in all the 15- year sliding windows were retained. Thus, a total of 14 predictors were selected as the input to the stepwise regression analysis and are listed in Table 4.2. The sliding correlation for these predictors is shown in Fig 4.3.
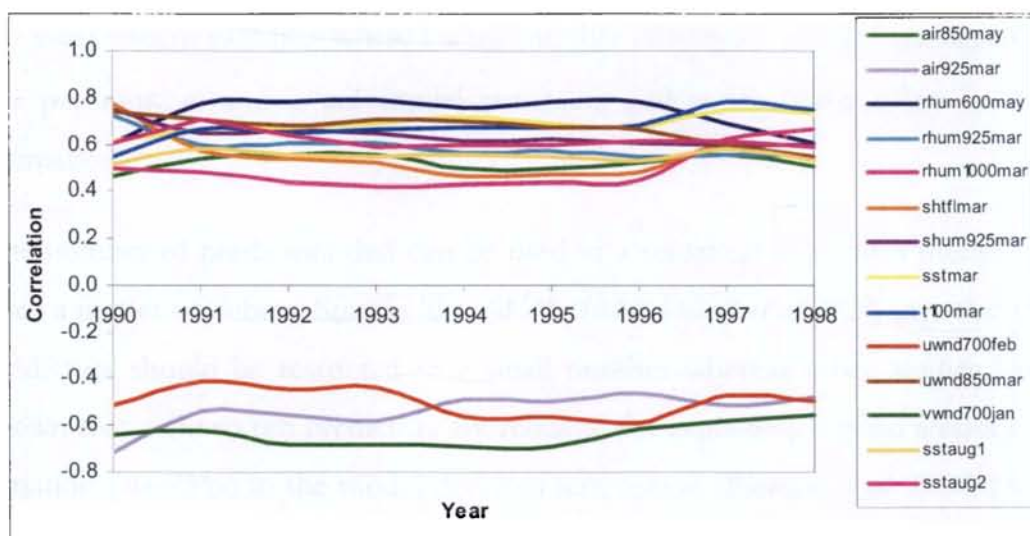

Fig. 4.3. Fifteen years moving C.C. between ISMR and selected 14 predictors for the period 1975–1998. The horizontal dotted lines represent the C.C. significant at 90% level. The central year is shown in the x-axis. The details of the predictors are given in Table 4.2.

Stepwise regression analysis was employed to reduce the dimensionality of these indices *(Draper and Smith, 1981)*. Thus, the extensive basic predictor set is reduced to a candidate set by eliminating those with less influence in the variance of rainfall. The predictors thus identified are also listed in Table 4.2. The correlation maps of the selected variables with the KSMR are shown (Figure 4.4 a-d). The CC's which are significant at 1% are contoured, and the selected areas are marked (rectangles in Figure 4.4 a-d).

Formulation of regression equation from among the refined candidate predictors, various regression models were formulated with the following general form using different iteration schemes.

$$R_j = a_0 + \sum_{i=1}^{n} a_i(X_{ij}) + \varepsilon_j \qquad\qquad ...(4.1)$$

Where, R_j is the dependent variable (rainfall) for j=1 to m time steps and X_{ij} are the independent variables where i is the number of predictors and j analogous to the previous. a_0 and a_i are model constants and ε_j the error value in that estimation.

The number of predictors that can be used in a statistical regression model has been a matter of debate. Studies like *(Wilks 1995, Delsole et al 2002)* says that the predictors should be restricted to a small number whereas other studies have shown that eight to ten predictors are required for explaining a good amount of variation (70–75%) in the model development period *(Rajeevan et al, 2004.* Here the stepwise regression has restricted the number of predictors to four.

Parameter	Predictors	Level	Month	C.C. (1975-1997)	Area
Air Temperature	Air850may	850 hPa	May	0.492	75-85E, 10-20N
Air Temperature	Air925mar	925 hPa	March	-0.468	50-75E, 10-20N
Relative Humidity	Rhum1000mar	1000 hPa	March	0.512	60-75E, 0-8N
Relative Humidity	Rhum925mar	925 hPa	March	0.479	50-75E, 10-20N
Relative Humidity	Rhum600may	600 hPa	May	0.560	75-85E, 0-5N
Sensible Heat Flux	Shtflmar	Surface	March	0.514	55-65E, 10-20N
Specific Humidity	Shum925mar	925 hPa	March	0.534	55-65E, 10-18N
Sea Surface Temperature	SSTaug1	Surface	August	0.494	55-65E, 5S-10N
Sea Surface Temperature	SSTaug2	Surface	August	0.549	85-95E, 10-20N
Sea Surface Temperature	SSTmar	Surface	March	0.559	70-80E, 10-20S
T1000	T1000	1000 hPa	March	0.534	70-110E, 5-13S
Zonal Wind	Uwnd700feb	700 hPa	February	-0.459	60-85E, 3-10N
Zonal Wind	Uwnd850mar	850 hPa	March	0.555	55-70E, 10-15N
Meridional wind	Vwnd700jan	700 hPa	January	-0.579	65-75E, 10-20N

Table 4.2. List of parameters, their geographical and temporal location and correlation coefficients with PIR

The dynamics of the predictors used in this study are detailed here. The intensive NH summer insolation induces more Precipitable Water (PW) in the northern Tropics from North Africa to South and East Asia. Similarly, enhanced SH insolation in boreal winter and spring gives rise to increased PW over the

Arabian Sea, India, and the southern tropical Indian Ocean in boreal summer. Air temperature at 850 hPa (May) having positive correlation co-efficient in the analysis imply the possible connection to rainfall as follows. When air temperature increases, the Planetary Boundary Layer (PBL) becomes more turbulent and the winds will accelerate. This will increase the transport of moisture in to the atmosphere. The gradient of air temperature can affect the winds through thermal wind relation, which in turn affect the rainfall.

Sea Surface Temperature (March) bears a significant positive correlation co-efficient with PIR. SST anomalies will lead to more evaporative and sensible heat flux anomalies, which in turn affect the winds. The gradient of SST is directly influencing the winds at upper levels through thermal wind relation.

Zonal and meridional wind at 700 hPa during February and March respectively bear a negative correlation coefficient with PIR. When the winter winds are strong (correspondingly the subtropical westerly jet is stronger) the ensuing rainfall will be less.
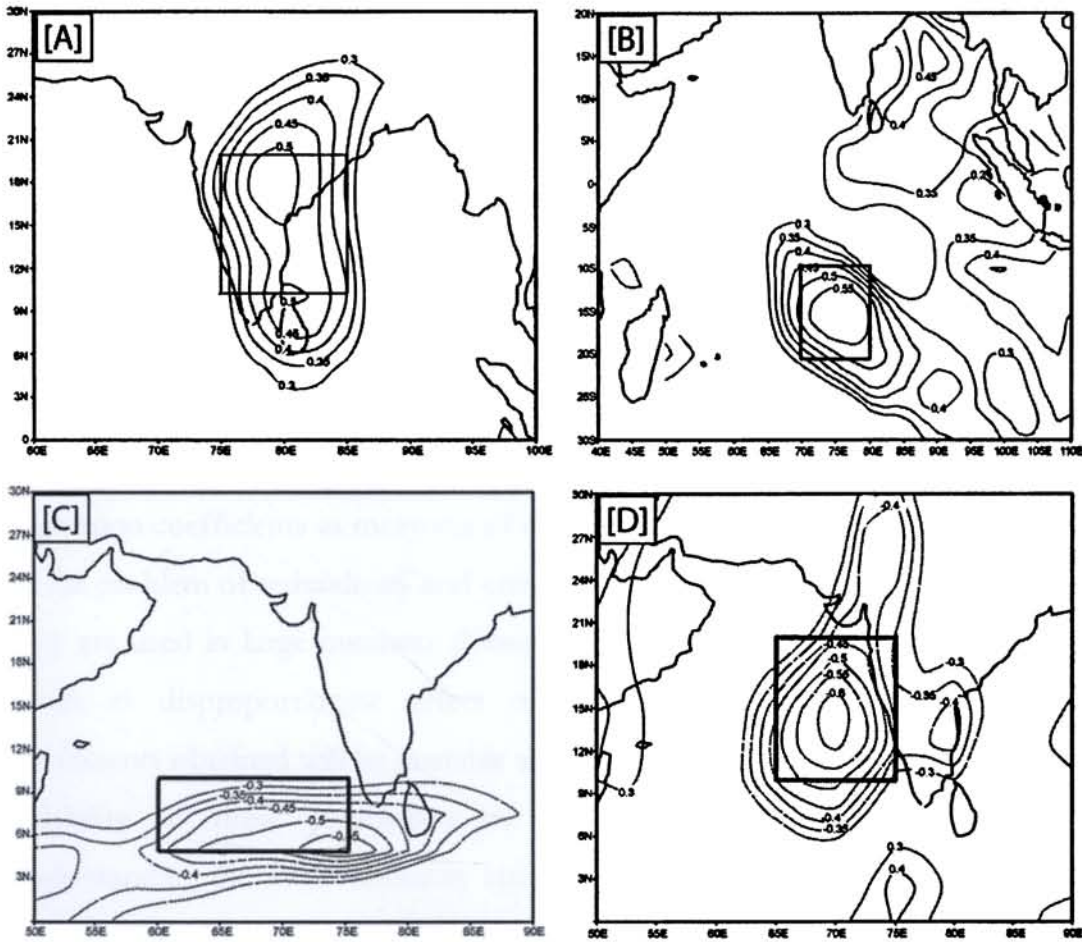
Fig 4.4 Correlation maps of the potential predictors of PIR a) Air Temperature b) Sea Surface Temperature c) Zonal Wind and d) Meridional wind, with PIR

4.4. RESULTS

The selected indices over the Arabian Sea and adjacent seas were subjected to stepwise regression and four potential predictors for PIR were identified. The final form of the regression model is

$$Y = -4364.514 - 33.354(x_1) + 48.035(x_2) + 135.717(x_3) - 15.876(x_4) \qquad \ldots(4.2)$$

where X values are the predictors (Table 1) and Y the predicted rainfall. The regression coefficients in the model show disproportionate values because the predictors were not expressed in standardised form. The regression coefficients do not imply relative importance, as the input parameters into the regression model are not standardized.

Multicollinearity is a measure of non-orthogonality of the predictors, i.e. there exists inter-correlation between the predictors. Thus, a multiple linear regression model lacks in its accuracy and may lead to unclear interpretation of the regression coefficients as measures of original effects *(Mc Cuen, 1985)*. This leads to the problem of redundancy and unnecessary loss of degrees of freedom when they are used in large numbers *(Kumar et al, 1995)*. Small data revisions would result in disproportionate effect on the calculated coefficients, i.e. the coefficients obtained will be unstable and this in turn affects the prediction. The reliability of these parameters in the prediction could be ensured by understanding the multicolinearity statistics. Variance inflation factor (VIF) is a common method used to study the multi-co-linearity (Fox, 1991). It is defined as:

$$\text{VIF }(a_i) = \frac{1}{1-R_i^2} \qquad \qquad ...(3)$$

where R_i^2 is the unadjusted R^2 when X_i is regressed against all the other explanatory variables in the model. The VIF measures how much the variance of the estimated regression coefficients are inflated compared to situations when the independent variables are uncorrelated. Values in excess of 10.0 could significantly affect the stability of the regression coefficients (Neter *et al.*, 1990). So, the candidates having a smaller VIF only are considered so that the

parameters inhibiting interdependence is avoided to increase the credibility of the regression output

The VIF analysis of all the parameters that is retained in the stepwise regression have values around 1.2 indicating an insignificant level of multicollinearity (Table 4.3).

Variables	Sig. of t-test	VIF
Air Temperature	0.015	1.134
Sea Surface Temperature	0.001	1.078
Zonal Wind	0.020	1.253
Meridional Wind	0.011	1.187

Table 4.3. The t-test results and variance inflation factor corresponding to the variables.

Scatter matrix plot shows the relationship between each pair of variables (Fig. 4.5). Each column shows the relationship between the parameter listed in that column with the other four parameters named in the respective rows. The variable on the vertical axis is the variable named in that row and the variable on the horizontal axis is the variable contained in that column. The correlation coefficients between the dependent variable and four independent variables are listed atop the columns. From the figure it can be seen that the PIR is positively related to air temperature and Sea Surface temperature, but negatively correlated to zonal and meridional wind at 700mb. The independent parameters do not show much relation among themselves though feeble relations exist. Therefore the predictors are independent and do not have any significant patterns. So the interdependencies among the predictors, if any, are well below the potential to affect the forecast.

When the *t*-test is conducted, the P values indicate that the coefficients of all the predictors in regression are highly significant, with maximum significance for SST (Table 4.3). The model has a coefficient of determination (which is the proportion of variation in the dependant variable explained by the regression model) of 77.7% and a multiple correlation coefficient (correlation between the observed and predicted rainfall) of 0.88. The F statistic, which tests the significance of regression model, gives F=15.64 and the P value in the *ANOVA* test (Analysis of Variance) is very small. This strongly suggests that the included predictors collectively account for a significant part of the variance in the PIR.

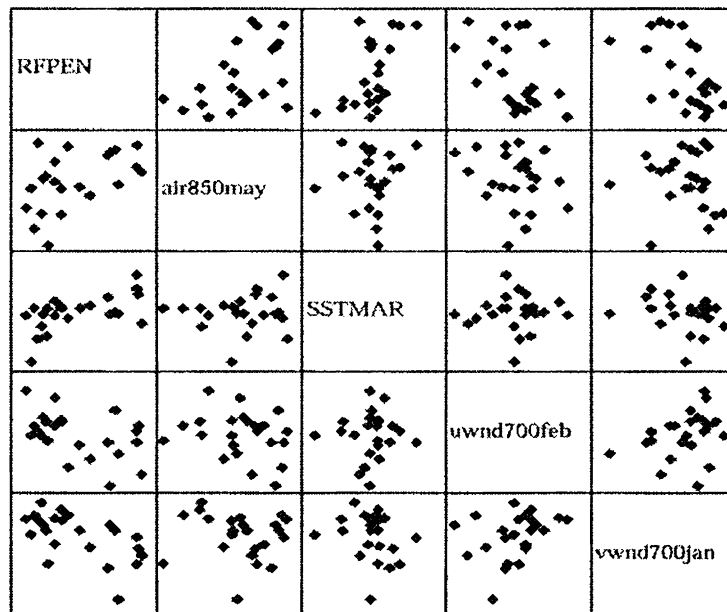Fig. 4.5. Scatter Matrix Plot of the inter relations between the dependant and independent parameters and among predictors. The predictors are Air temperature at 850 hPa for the month of May (air850may), Sea Surface Temperature for the month of March (SSTmar), Zonal wind at 700 hPa for the month of February (uwnd700feb) and Meridional wind at 700 hPa for the month of January (vwnd700jan). RFPEN is the Peninsular Indian rainfall.

The standardized departure of PIR and its forecast is shown in Fig 4.6. PIR has a standard deviation of 110.1mm, which is 16.6% of the mean rainfall (662.9 mm). The forecast of the model presented here, picks a standard deviation of 14.8% (101.1mm) of the mean rainfall. Thus both the mean (684.2mm, 662.9 mm) and the standard deviations (101.1mm, 110.1mm) of the forecast are comparable with the observed. This statistics shows that the interannual variability of PIR is well represented by this model.
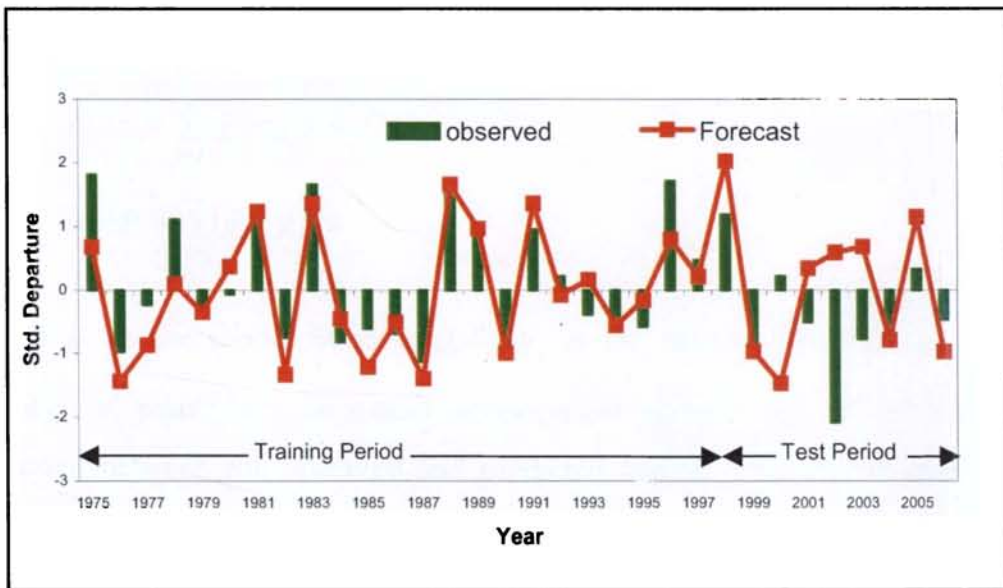
Fig 4.6. The standardized departures of PIR and its forecast. The model could capture the sign of the anomaly of extremes (± 1standard deviation), except 2002. The WET (DRY) years are classified as years with rainfall greater (less) than 1 standard deviation.

During the test period the standardized departures of the actual and model fitted rainfall shows four years (2000,2001,2002 and 2003) with opposite sign of anomaly (Fig.4.6). Except 2002, in all these years the observed values are very close to the mean, so that a small deviation of the forecast from the observed rainfall may end up with a departure opposite to that of the observed. But, none

89

of these years were extreme, except 2002, and they lie within the range of one standard deviation of normal monsoon. The model showed the maximum departure for the year 2002, in which other models also failed.

The model performance was assessed by calculating CC, Root mean square Error (RMSE), Absolute Error (ABSE) and the bias (BIAS) for the (1) training period, and (2) test period. Equations used to calculate these measures are given below *(Nicholls, 1984; Hastenrath, 1987)*.

$$\text{RMSE} = [\sum_{y=1}^{n}(\hat{R}_y - R_y)^2 / n \ ]^{1/2} \qquad \qquad ...(4)$$

$$\text{BIAS} = \sum_{y=1}^{n}(\hat{R}_y - R_y)/n \qquad \qquad ...(5)$$

$$\text{ABSE} = \sum_{y=1}^{n}\left|\hat{R}_y - R_y\right|/n \qquad \qquad ...(6)$$

Where $\hat{R}_y$ is the model fitted rainfall, R_y is the observed rainfall and n, the number of years. For the model development period high C.C of 0.88 was obtained between the observed and predicted rainfall. The RMSE was 7.6 % (50.48 mm) of observed mean rainfall, BIAS was 0 mm and ABSE was 40.2mm. The CC has dropped to 0.67 (significant at 1% level) for the period 1975-2006. The RMSE for the test period (1998-2006) has increased to 21.5% (142.79 mm) of mean rainfall. BIAS and ABSE for the predicted rainfall are 75.59 mm and 119.18 mm respectively. Climatological predictions are also made and the RMSE, BIAS and ABSE were also computed. The values obtained for RMSE, BIAS and ABSE are 117.61mm, -67 mm and 96.73mm respectively.

Scatter plots of residuals with the predictors and fitted values (not shown), helps us to visualize the patterns in the residuals. Any organized pattern present in it reveals the existence of the relation between fitted and residuals. If any pattern

could be identified then the model can be further improved by extracting the relationship. No such relation is identified and therefore no relationship is found. The Durbin Watson statistic is also used to check the relationship in the residuals. It checks whether the residuals for successive observations are uncorrelated. If any significant lag one autocorrelation exists, then the residuals are not independent and the model can be further improved *(Makridakis et al, 1998)*. It is defined as

$$DW = \frac{\sum_{t=2}^{n}\left(e_t - e_{t-1}\right)^2}{\sum_{t=1}^{n}e_t^{\,2}} \qquad \qquad ...(7)$$

where e_t is the residual at the time t and e_{t-1} that at time t-1. Its value ranges from 0 to 4. Values above two means there is some negative autocorrelation and values below 2 has a positive correlation. A value of 1.854 is obtained which suggests that the lag-1 autocorrelation is negligibly small in the residuals.

4.5   SUMMARY AND CONCLUSION

In this study a linear regression model was developed and tested for the seasonal rainfall prediction of Peninsular India using immediate regional parameters such as (i) lower tropospheric temperature during the month of May over the Peninsular India and adjoining Bay of Bengal (ii) Sea Surface Temperature during the month of March over the mid-Indian Basin over the Indian Ocean (iii) Zonal wind at 700 hPa during February and (iv) meridional wind at 700 hPa during January. The period of analysis was from 1975-2006 of which last nine years were tested against the observed rainfall. These parameters were arrived from a larger set of candidates, which had statistically significant relation with PIR. Our results show that the empirical model could explain 77.7% of the total variance in the PIR for the model development period. The model showed an RMS error of 7.6%, BIAS of 0 mm and an absolute error of 40.2 mm. The model could capture the extreme years reasonably but for the years 2001, 2002 and

2003 the model over predicted the rainfall. It is noteworthy that in 2002, a prolonged 30-day break in summer rains had lead to an extremely dry monsoon season whereas IMD models in use at the time had predicted normal rains in 2002.

CHAPTER 5

Effects of Arabian Sea Surface Temperature on the Summer Monsoon over Peninsular Indian Region

5.1   INTRODUCTION

The southwest summer monsoon, occurring every year from June–September, is one of the most well known seasonal phenomena for the Indian subcontinent, which is also a dominant feature of the general circulation of the atmosphere. The extended range forecasting (ERF) of monsoon is done with the help of statistical models by the India Meteorological Department (IMD) ever since *Walker (1923)* presented their mathematical foundation in his pioneering work. However, the prospect of seasonal forecasting of the Indian summer monsoon must also be investigated with numerical models because they are fairly complete and sufficiently sophisticated to reproduce the weather and climate features. In this regard, *Charney and Shukla (1981)* stressed the relative importance of sea surface temperature (SST) and land-surface conditions as sources of anomalous forcing for the large scale atmospheric flow.

The interannual variability in monsoon activity depends on air-sea interactions, during the course of travel of the monsoon current across the Ocean. One of the important surface boundary conditions which influence the Indian summer monsoon rainfall (ISMR) is sea-surface temperature (SST). Several investigators have done extensive work on the sensitivity of SST on the monsoonal circulation and associated rainfall patterns. *Chandrasekar and Kitoh (1998)* carried out an

experiment with a GCM to examine the sensitivity of the monsoon circulation and ISMR to SST anomalies over the Indian Ocean. They found that an increase (decrease) in rainfall over the Indian Ocean is associated with a warm (cold) SST anomaly. The Indian Ocean plays a very important role in the ISMR interannual variability due to its proximity and the importance of both the land-sea meridional thermal contrast and the SST-convection relationship for the strength of ISMR.

Tropical atmospheric convection is highly sensitive to the sea surface temperature (SST) of the underlying ocean. Deep atmospheric convection in the tropics is found to increase sharply when SST exceeds a threshold of about 27.5°C. The convection is also sensitive to fluctuation in SST above 28°C. Although SST above 28°C is not sufficient to produce organized deep convection in the tropical atmosphere, it is a necessary condition. Therefore, oceanic regions with SST above 28°C, known commonly as _warm pools_, occupy a significant place in tropical climate.

Shukla (1975) tested the hypothesis that colder SST anomalies over the west Arabian Sea may significantly influence the ISMR by a numerical experiment with the GFDL general circulation model. His experiment shows that the imposition of a persistent 1-3°C colder SST anomaly over the Somalia coast and the Arabian Sea lead to an increase of surface pressure and a significant reduction of cross equatorial moisture flux, which in turn is associated with a decrease in evaporation. The interesting result of this experiment is the reduction in the rainfall rate by 40-50% over India and the adjoining seas. The reduction in rainfall is remarkable at and near the colder SST anomaly regions and over the remaining parts of India it is less. _Washington et al (1977)_ examined the impact of different types of idealized SST anomalies over the tropical Indian Ocean to ISMR. They found an increase in rainfall and vertical velocity over the warm SST anomalies in

their experiments. However, the statistical relationship between model-simulated rainfall and wind anomalies obtained in his experiment was insignificant.

Some of the previous observational studies have shown that the Indian Ocean has no significant influence on ISMR interannual variability. This was due to lack of significant statistical relationships between various ISMR indices and Indian Ocean SST *(Shukla 1987; Webster et al 1998)*. Recent modeling studies have shown that the SST anomalies over the Indian Ocean in certain areas and under certain conditions can have a significant effect on ISMR variability *(Meehl and Arblaster 2002)*. Most of the past studies on the SST-monsoon relationships are based mainly on the GCM simulations. Though GCMs capture the large scale features of the monsoon circulation reasonably well, their performance in representing the regional climate details are very poor *(Rind et al 1989; Mearns et al 1990)*. Previous investigators *(Giorgi et al 1994; Jones et al 1995)* have shown that rainfall distribution simulated by a regional climate model (RCM) contain a strong orographically related component on scales not resolved by the GCMs. Considering the complex nature of the ISMR and its spatial variability due to complex orography, it is essential to study its characteristics in detail using Regional Climate Models. Although the Regional Climate Model (RegCM) has been used widely for various mesoscale studies *(Qian and Giorgi 1999; Pal et al 2000; Giorgi et al 2003)*, it has not been tested to study the characteristics of circulation features and associated rainfall over India. Only a few studies, mainly by *Shekhar and Dash (2005)* and *Dash et al (2006)*, have used the National Center for Atmospheric Research (NCAR) RCM (version-II) in the study of ISMR. *Singh and Jai (2007)* also has studied the effect of SST on ISMR with an SST increment of 0.6^0 C

It has been demonstrated that for examining the weather/climate features in greater detail, regional models are more suitable than the global models.

Computationally it is affordable to increase the resolution of regional models so as to resolve regional climatic features reasonably well. Various regional models have been used for a wide variety of applications including operational weather forecasting, studies of the present-day climate and possible future climates over a number of regions throughout the world _(Mesinger 1984; Dickinson et al 1989; Giorgi 1990; Dudhia 1993; Walsh and McGregor 1995; Bhaskaran et al 1996; Ji and Vernekar 1997)_.

Simulation of the Indian summer monsoon circulation features and the associated rainfall by a numerical model have been the most challenging problems due to its large variability. _Bhaskaran et al. (1996)_ simulated the Indian summer monsoon using a regional climate model with a horizontal resolution of 50 km nested with global atmospheric GCM. Their study showed that regional model derived precipitation is larger by 20% than GCM.

In this study, a recent version of the NCAR regional climate model (RegCM3) is used to simulate the monsoon over peninsular India for the years 1996, 1997 and 2002, which are considered as WET, NORMAL and DRY years respectively. The monsoon of 2002 has been regarded as the driest and peculiar of the recent drought years. Thus the characteristics of the circulation and the moisture during the year have been studied by many researchers _(Valsala and Ikeda 2005)_. It is evident that the 2002 mean rainfall was less than normal and an anomalous month-long drought existed in July. Unlike usual drought years, the extreme drought years deserve special attention in their processes. Since the moisture for Indian monsoon rainfall is being carried over and supplemented by the Arabian Sea _(Mohanty et al 1983, 1994)_, sea surface temperature which influences the circulation and precipitation pattern of monsoon is to be studied in detail. Although the RegCM modeling system has been widely used for different regional

climate studies *(Giorgi and Mearns 1999)*, it has not been extensively tested over the South Asia region, particularly concerning the simulation of Indian summer monsoon. The suitability of RegCM3 model in simulating ISMR has been examined by *Dash et al (2006)*. In the present study an attempt has been made to understand the possible effect of the Indian Ocean SST on the summer monsoon circulation and precipitation over the peninsular region in specific, since the orography and spatial distribution of monsoon over this region are very complex.

5.2   MODEL DESCRIPTIONS

The modified version of RegCM used in the present study is originally developed by *Giorgi et al (1993a, b)* and then augmented and described by *Giorgi and Mearns (1999) and Pal et al (2000)*. The dynamical core of the RegCM3 is similar to the hydrostatic version of the NCAR/Pennsylvania State University mesoscale model MM5 *(Grell et al 1994)*. The model includes cumulus parameterization schemes, large scale precipitation scheme, planetary boundary layer (PBL) parameterization, state-of-the-art surface vegetation and soil hydrology package, the Biosphere-Atmosphere Transfer Scheme (BATS), Ocean flux parameterization, pressure gradient scheme, explicit moisture scheme, the radiative transfer scheme and the ocean-atmosphere flux scheme.

Surface processes are represented via the Biosphere-Atmosphere Transfer Scheme (BATS) *(Dickinson et al 1989)*. BATS is a state-of–the art surface package designed to represent the role of vegetation and interactive soil moisture in modifying the surface atmosphere exchanges of momentum, energy and water vapor. Boundary-layer physics is following the nonlocal vertical diffusion scheme of *Holtslag et al (1990)*. Different schemes are available for the generation of precipitation in RegCM3. Nonconvective precipitation can be represented by an implicit scheme

(Xie et al 1984). Convective precipitation can be described using a simplified Kuo-type scheme *(Anthes 1977),* Grell scheme *(Grell 1993)* and Massachusetts Institute of Technology (MIT). The newest cumulus convection option to the Regional Climate Model version 3 (RegCM3) is the MIT scheme. More detailed descriptions can be found in *Emanuel (1991).* In addition to a more physical representation of convection, the MIT-Emanuel scheme offers several advantages compared to the other RegCM3 convection options. For instance, it includes a formulation of the auto-conversion of cloud water into precipitation inside cumulus clouds, and ice processes are accounted for by allowing the autoconversion threshold water content to be temperature dependent. Additionally, the precipitation is added to a single, hydrostatic, unsaturated downdraft that transports heat and water. Under this scheme, fundamental entities are sub-cloud scale draft rather than cloud themselves. The MIT has recently been implemented within RegCM3, and therefore its performance has not been tested extensively to date. This scheme assumes that the mixing in clouds is highly episodic and inhomogeneous and considers convective fluxes based on an idealized model of sub-cloud-scale updrafts and downdrafts. Convection is triggered when the level of neutral buoyancy is greater than the cloud-base level. Between these two levels, air is lifted and a fraction of the condensed moisture forms precipitation while the remaining fraction forms a cloud. The cloud is assumed to mix with air from the environment according to a uniform spectrum of mixtures that ascend or descend to their respective levels of neutral buoyancy. The mixing entrainment and detrainment rates are determined by the vertical gradients of buoyancy in the clouds. The fraction of the total cloud base mass flux that mixes with its environment at each level is proportional to the rate of change in the undiluted buoyancy with altitude. In other words, the mass flux at the cloud base is a function of buoyancy, and the air parcel can lose its buoyancy during

ascent due to the entrainment of dry air from the environment. The Grell scheme is widely used within both the MM5 and RegCM modeling framework. This is a mass flux scheme that includes the moistening and heating effects of penetrative updrafts and corresponding downdrafts. The scheme can use two closure assumptions, the so-called *Arakawa-Schubert* and *Fritsch-Chappel* type closures. After a few initial test experiments, we selected the Grell scheme, which yielded generally better results for our domain. In the RegCM3 modelling framework, precipitation is derived by the combined process of resolved (gridscale) precipitation as well as unresolved (sub-grid-scale) precipitation. The resolvable grid-scale precipitation is described using the sub-grid explicit moisture scheme of *Pal et al (2000)*, which accounts for the sub-grid variability in the clouds by linking the average relative humidity of a grid cell to the cloud fraction and cloud water.

Resolvable scale precipitation is represented via the scheme of *Pal et al (2000)*, which includes a prognostic equation for cloud water and allows for fractional grid box cloudiness, accretion and re-evaporation of falling precipitation. Cloud radiation is computed in terms of cloud fractional cover and cloud water content, and a fraction of cloud ice is diagnosed by the scheme as a function of temperature. The RegCM3 has 18 vertical levels and a 60 km horizontal resolution.

5.3   DATA AND METHODOLOGY

In this study, RegCM3 has been integrated for simulating the Indian summer monsoon circulation and associated rainfall for the years 1996, 1997 and 2002. The lateral boundary conditions for wind, temperature, surface pressure and water vapor are interpolated from 6 hourly ECMWF reanalysis. The terrain height and land-use data for the given domain are generated from the United States

Geographical Survey (USGS) global 5 min resolution terrain and land-use data. The original weekly averaged optimum interpolated Sea Surface Temperature (OISST) available from the National Oceanic and Atmospheric Administration (NOAA) for the whole year is horizontally interpolated into the specified domain and also in each time step for the model integration. Three typical rain years 1996, 1997 and 2002 are selected for the study. The model domain covers the area approximately 50 °E to 110 °E and 5°S to 40°N with a horizontal grid distance of 60 km. The grid is defined on a Normal Mercator Projection. The control runs are integrated from May 1 to September 30, for every year using the original SST. The initial condition SST input into the model is incremented by steps of 0.1° C in the sensitivity experiments. The experiments are repeated for increment up to 1° C. The difference in wind vectors and precipitation for the CONTROL Run and the Experiments (SST-CTL) are analyzed to get a spatial perspective of the results. In this study, a control simulation is made over the domain and topography as shown in Fig. 5.1. The land-use data used in the model is described in Fig. 5.2.
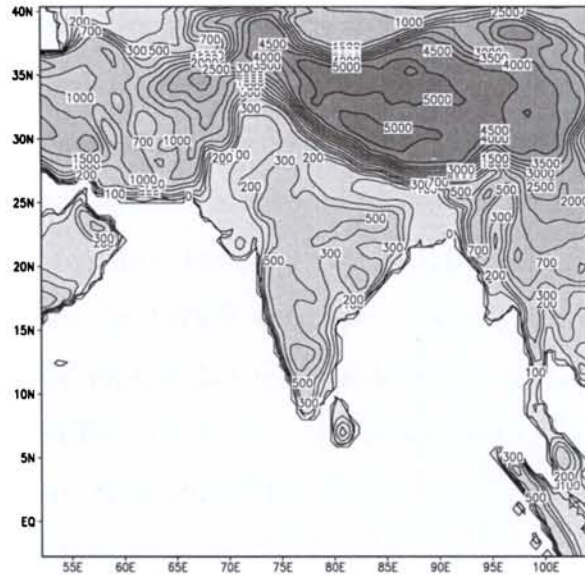
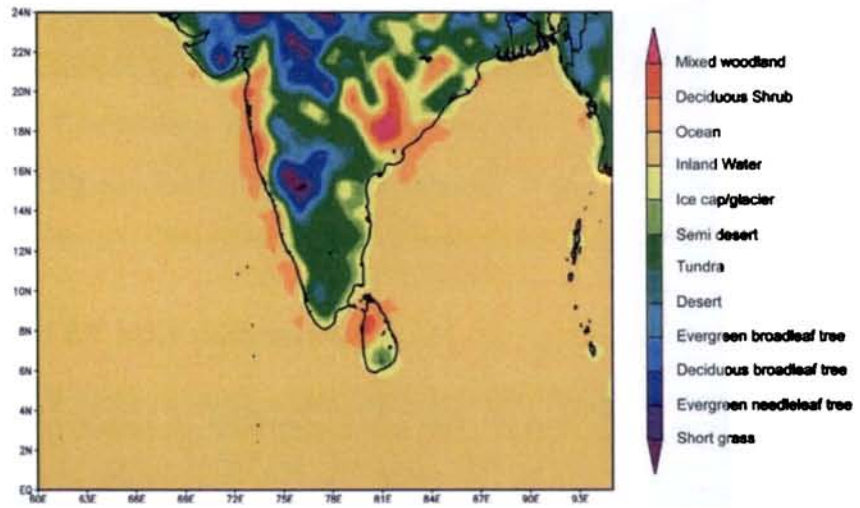Fig. 5.1 Model domain and topography used in the model. Contour heights are in meters.

Fig. 5.2. Land-use data used in the model

5.3.1 CONTROL EXPERIMENT

The model was integrated for five months from May to September for the years 1996, 1997. For the year 2002, the model integrations were made from May to August, due to the unavailability of September data from ERA 40. The lateral boundary conditions are updated and supplied every 6 hours into the model and the time step of the integration has been kept at 150 seconds. Compared with the total precipitation from the GPCP data, the model is found to be capable of simulating the monsoon rainfall to a reasonable degree in both spatial distribution and quantity, particularly the large-scale precipitation zones owing to the southwesterly monsoon flow along the southwest to northeast diagonal of the domain and the equatorial region in the whole season.

To facilitate the interpretation of the results of the sensitivity experiments, the total precipitation and horizontal wind fields simulated in CTRL are shown in Figs. 5.3 and 5.4 respectively. Compared with the observational data from the Global Precipitation Climatology Project (GPCP) in 2002 (Fig. 5.3a) the RegCM3 is capable of simulating the basic precipitation pattern over Indian region (CTRL Fig. 5.3b).

5.3.2 SENSITIVITY EXPERIMENT

The interannual variability in the monthly mean SSTs is typically around 0.5-0.6° C over the Indian Ocean *(Meehl and Arblaster 2002)*. To test the influence of warm Indian Ocean SST's on ISMR, they increased the SST by 0.75° C north of 15° S in their sensitivity (warm SST) experiments. Here we design the sensitivity experiments such that the initial condition Sea surface temperature incremented by 0.1° C to a maximum increment of 1.0° C (hereafter referred to as SST0.1 to

SST1.0 respectively) and the model was run for whole the season for each of these experiments.

The model is integrated from May to September for the year 2002. The first month is taken as the spin up time for the model. The rest four months averaged to get the seasonal averaged values of vertically integrated moisture, wind and precipitation.

5.4 RESULTS

Overall evaluation of the model performance is provided within this section. A comparison of control simulation with observation over the study region is provided. Results of control run simulations with sensitivity experiments are discussed, based on seasonal averages of moisture, precipitation and zonal and meridional wind.

The RegCM3 integration shows that the model simulates the Indian summer monsoon circulation fairly well, even though precipitation is overestimated. The results from the control experiments are compared with observations (Fig 5.3 and Fig 5.4). The discussions in this section are based on seasonally averaged values, i.e. the differences between the seasonally averaged results of a sensitivity experiment and the corresponding results of the control experiment. The seasonal monsoon circulation and precipitation are well represented. For the year 1996, the increment of SST has a negative influence over the peninsular Indian region. Vertically Integrated Moisture, north of 15^0N for SST0.1 and SST0.2 increments (Fig 5.5). For SST0.5 and SST0.6, almost entire peninsular India has abundance in moisture except in some pockets of negative anomaly. As SST increased further to 0.9, the northern parts of the study region gets negative anomaly in moisture.

In almost all the experiments, the region south of 15°N shows generally positive anomalies in moisture, though there are spatial inhomogeneity in the distribution of moisture (Fig. 5.5). The sensitivity experiments show that the increase in the total precipitation rate occur for the experiment SST0.3, SST0.4, SST0.5 and SST0.6 over the southern peninsular India (Fig. 5.6). This positive anomaly in precipitation decreases after SST0.7. In all the experiments adjoining Bay of Bengal region also gets benefited from the SST increment. The maximum anomaly in the SST- CTL experiments are to the south of 15° N. The increase in the precipitation are as much as 8-10mm/day for SST0.4 to SST0.6. Theses results are given in Fig. 5.6.

Results for zonal wind show that the wind anomaly to the north of 15° N over the study region is positive (0.7 m/s) for the experiments SST0.1 and negative anomaly exists over the southern part and adjoining oceanic region. In the successive experiments, the positive anomaly decreases to the north and the negative anomaly to the south begin to increase (Fig. 5.7). The spatial extend of the positive anomaly diminishes and the negative anomaly spreads over the southern peninsula and southeastern coastal region. The maximum negative anomaly covers entire peninsula for SST0.5 and after reaching maximum negative anomaly for SST0.7, the initial pattern reappears gradually and reaches maximum positive value for SST1.0. SST0.9 shows similar pattern for wind anomaly as of SST0.1. For Meridional wind the peninsular India shows negative anomaly for SST0.9 and the maximum value is for SST1.0 (Fig. 5.8). The vector winds show convergence over the peninsular India, which is in agreement with the anomalous precipitation pattern (Fig. 5.9).
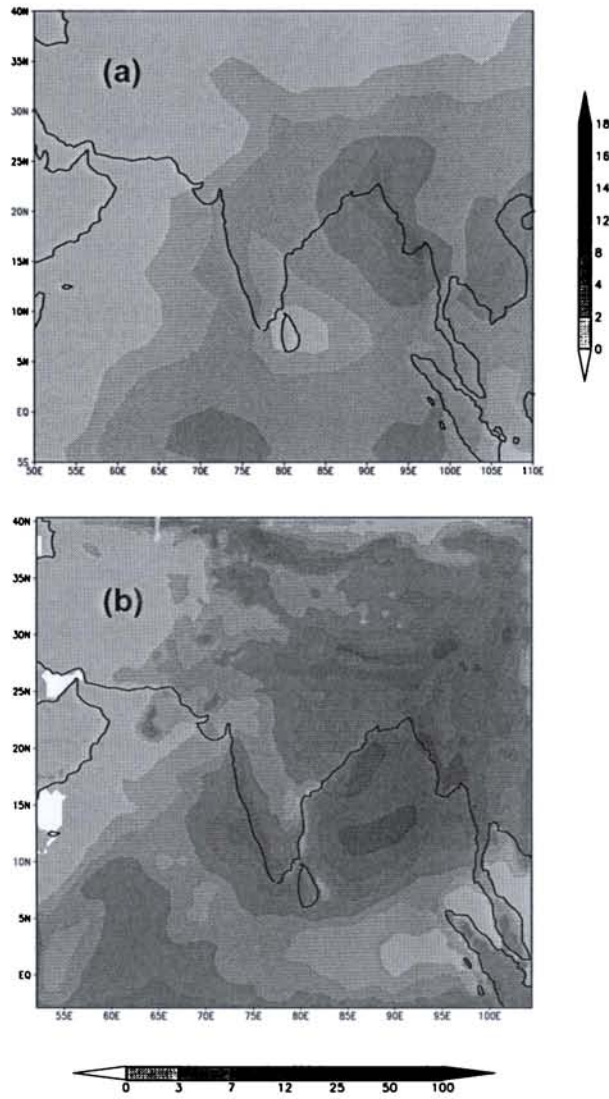
Fig. 5.3. Seasonal precipitation from a) GPCP and b) RegCM3 for summer 2002

For the year 1997, the simulated anomaly pattern shows that the increase in SST causes a negative moisture anomaly from SST0.3 to SST0.9 (Fig. 5.10). The maximum spatial coverage for negative anomaly is for SST0.5 and 0.9. In the case of precipitation (Fig. 5.11), for the normal year 1997 there is not much influence of SST over the land area. However, over eastern coastal region and adjoining

105

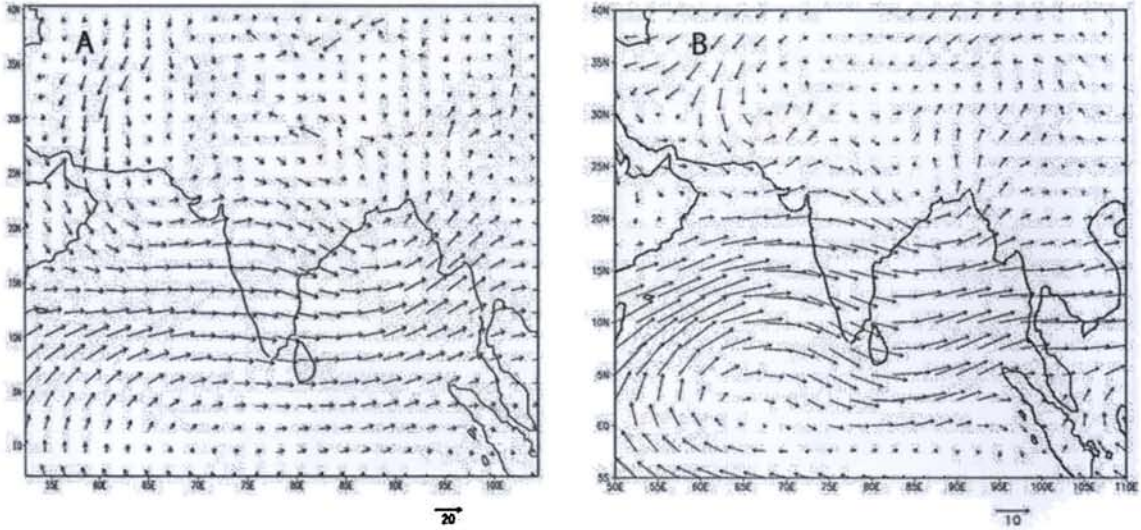oceanic region, there is a feeble increase of 3-5mm/day. The maximum Increase is for SST0.7.

Fig. 5.4. Seasonal wind vectors for summer A) RegCM3 and B) NCEP

For zonal wind, positive anomaly exists over peninsular India north of about 15^0 N. This decreases gradually and a negative anomaly establishes over peninsular India by SST0.4 (Fig. 5.12). This zonal wind increases again for SST0.5 to 0.8 reaching a maximum value of 0.7 and a great spatial spread over the entire peninsular India. Again the wind anomaly becomes negative hereafter. Meridional wind for 1997 has a positive anomaly over peninsular India for SST0.1 (Fig. 5.13). For subsequent experiments negative anomaly gets established till SST0.4. Positive anomaly over western peninsular India revives and the negative anomaly gets strengthened. The vector wind (Fig. 5.14) shows convergence over the Bay of Bengal and peninsular India in accordance with the precipitation anomaly pattern.
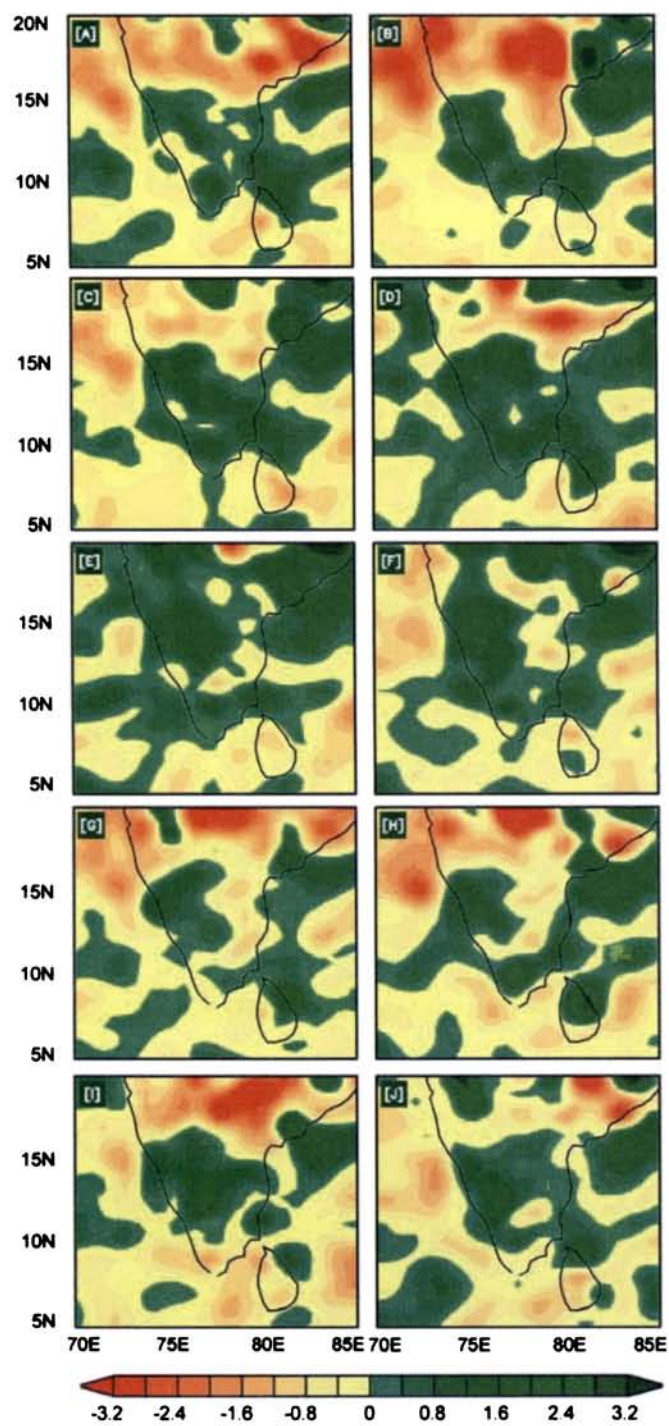
Fig. 5.5. Vertically integrated moisture simulated by RegCM3. Figures are Expt-Ctrl for an SST increment 0.1 to 1.0 in (a) to (j) respectively for the year 1996
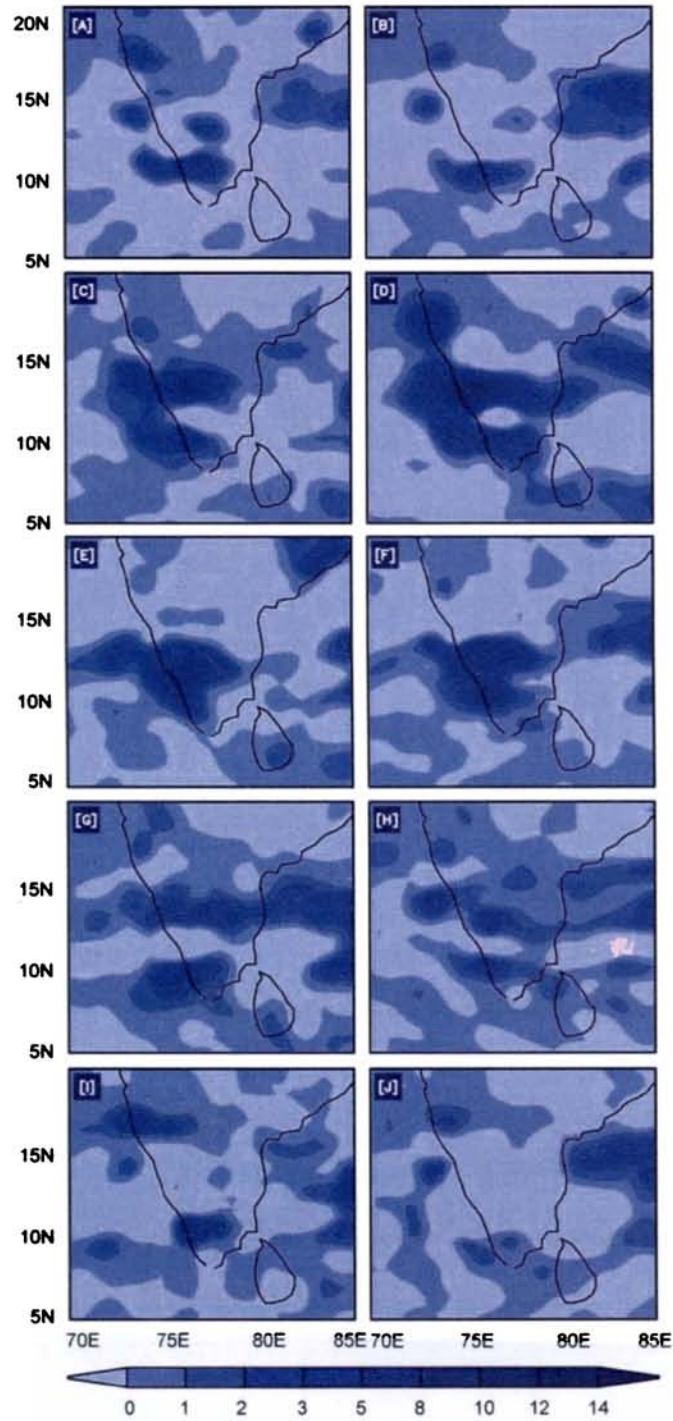
Fig. 5.6. Total precipitation rate (mm/day) simulated. Figures represent Expt-Ctrl for SST increment 0.1 to 1.0 in (a) to (j) respectively for the year 1996
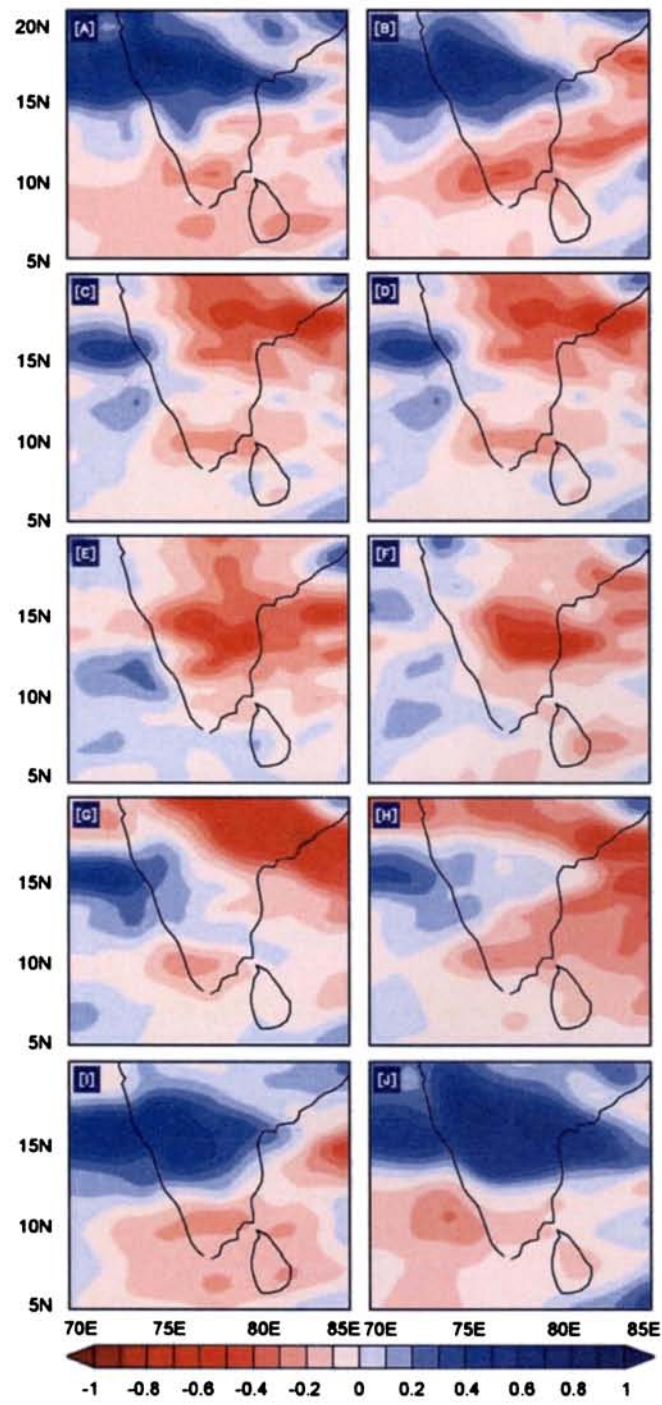
Fig. 5.7 Zonal wind at 850 hPa simulated by RegCM3. Figures represent Expt-Ctrl for SST increment 0.1 to 1.0 in (a) to (j) respectively for the year 1996
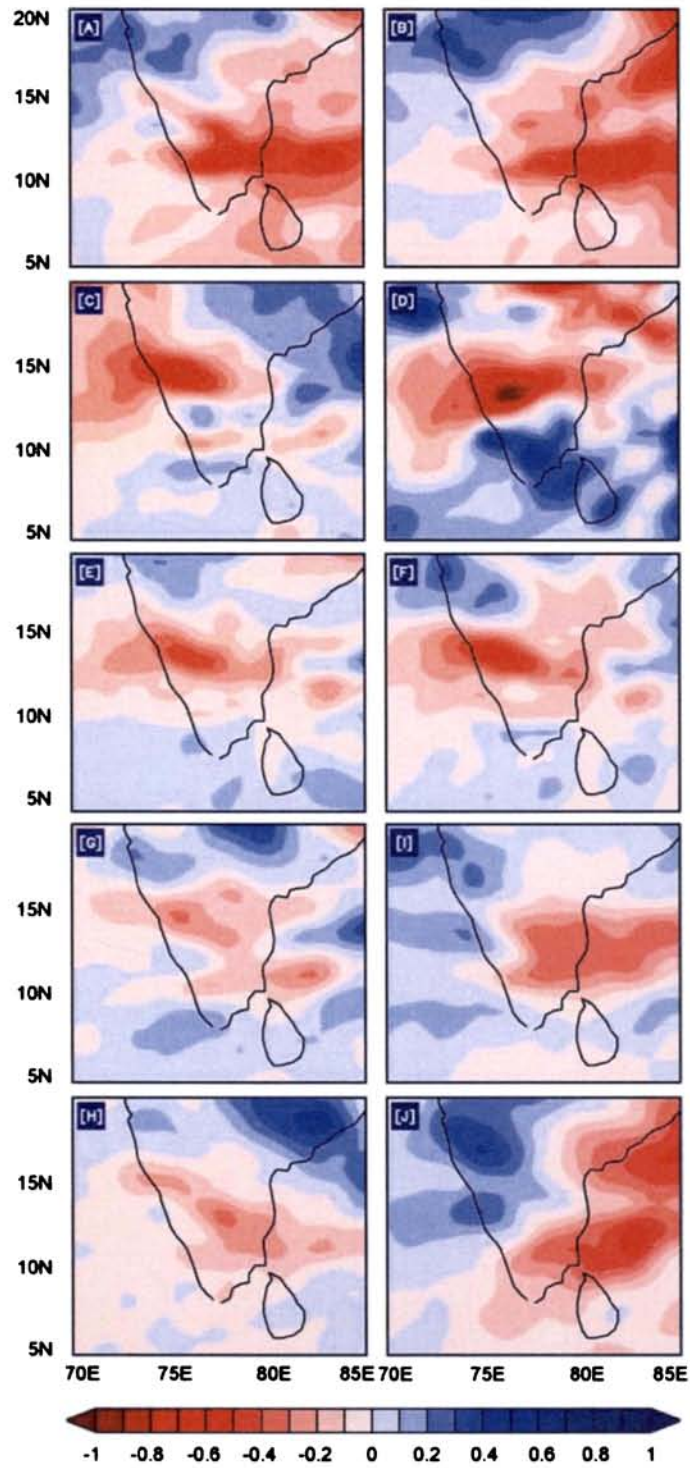
Fig. 5.8. Meridional wind at 850 hPa simulated by RegCM3.Figures represent Expt-Ctrl for an SST increment 0.1 to 1.0°C in (a) to (j) respectively for the year 1996
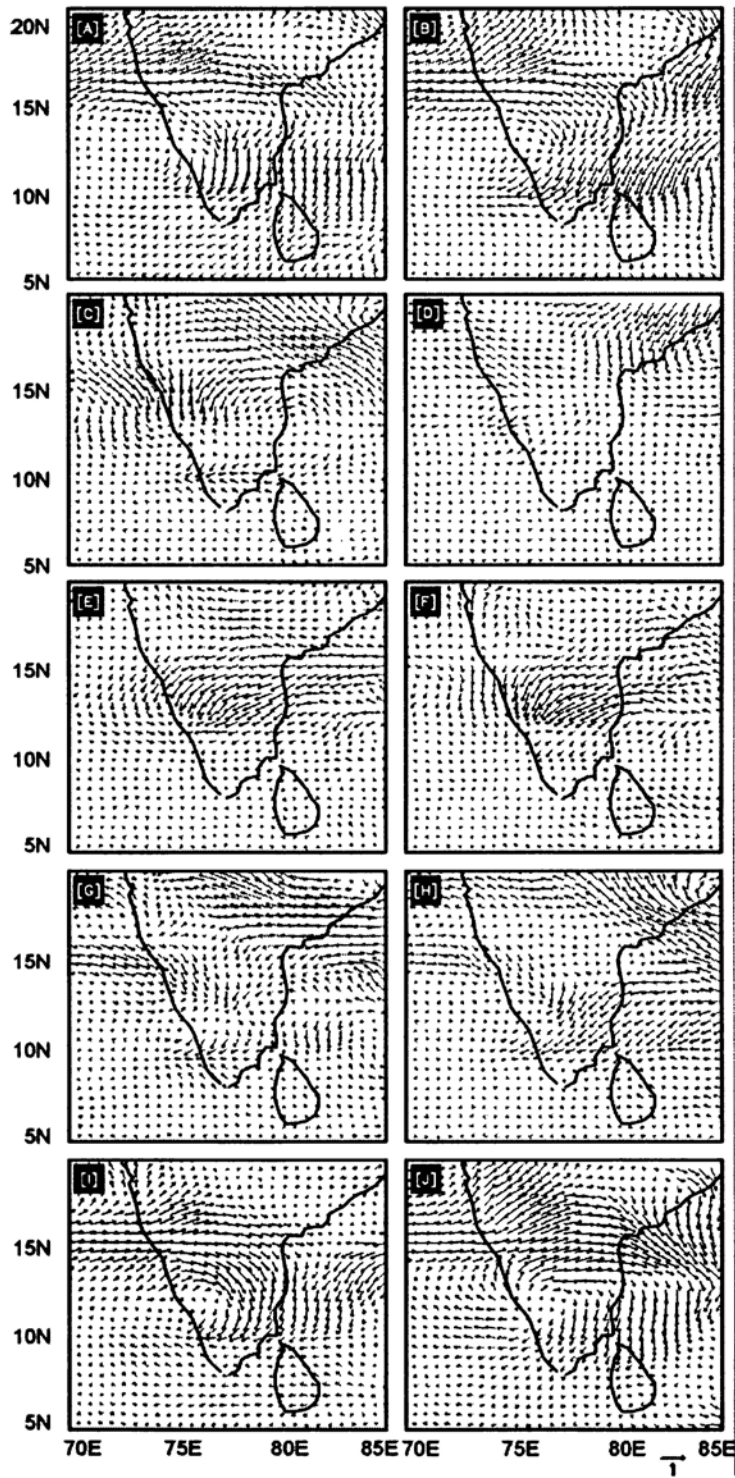
Fig. 5.9. Vector wind at 850 hPa. Simulated Expt-Ctrl for an SST increment 0.1 to 1.0ºC in (a) to (j) respectively for the year 1996

For the anomalously DRY year 2002, the integrated moisture shows (Fig. 5.15) very high negative anomaly over peninsular India north of 15^0 N, though generally positive anomaly patterns exists over south of that. There are no much differences in the amount of total column moisture for the SST experiments. For precipitation (Fig. 5.16), the anomaly patterns are positive over oceanic region leaving the landmass unaffected by increase in SST. However, for SST05 and 0.6, the windward side of the Western Ghats receives increased rainfall.

Zonal wind anomaly shows (Fig. 5.17) negative anomaly over peninsular India for the experiments SST0.1 and this negative anomaly gets replaced by positive values and reaches maximum value of 0.8 m/s by SST0.4 and gradually decreases. From SST0.6 negative wind anomaly spreads over eastern coastal region and reaches a maximum spatial cover by SST1.0.

Meridional wind has positive anomaly to the north of 15^0 N and this anomaly increases to a maximum value by SST0.4 and then decreases (Fig. 4.18). By SST0.9, some negative anomaly over oceanic region reappears as in the spatial pattern of SST0.1. The vector wind shows maximum increases in wind speeds for SST0.4 in 2002 (Fig. 4.19). Here also the precipitation patterns are in accordance with the convergent zones in the wind pattern.

The Hovmöller diagrams of the daily precipitation rate simulated by RegCM3 shows the distinct features for these contrasting rainfall years. For 1996, which is a wet year for peninsular India, the intraseasonal variability shows lesser period than normal or dry years. The period of intraseasonal variability is of the order of 10 days and the increased SST modifies the intraseasonal variability well for the wet year 1996 (Fig 5.20).
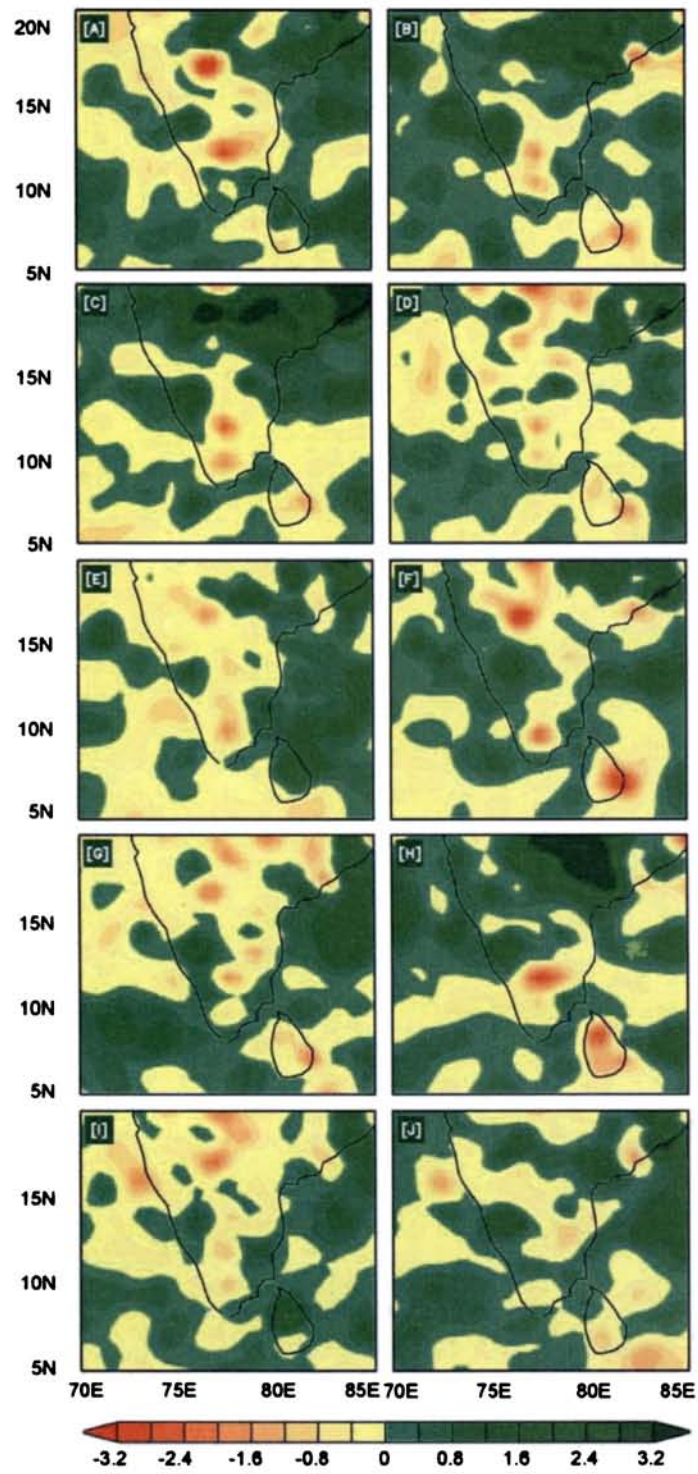
Fig. 5.10. Vertically integrated moisture simulated by RegCM3. Expt-Ctrl for an SST increment 0.1 to 1.0°C in (a) to (j) respectively for the year 1997 are shown

113

Fig. 5.11. Total precipitation rate (mm/day) simulated Expt-Ctrl for SST increment 0.1 to 1.0 in (a) to (j) respectively for the year 1997

114

Fig. 5.12 Zonal wind at 850 hPa simulated Expt-Ctrl for SST increment 0.1 to 1.0 in (a) to (j) respectively for the year 1997.

115

Fig. 5.13. Meridional wind at 850 hPa simulated Expt-Ctrl for SST increment 0.1 to 1.0 in (a) to (j) respectively for the year 1997.

Fig. 5.14. Vector wind at 850 hPa simulated Expt-Ctrl for an SST increment 0.1 to 1.0⁰C in (a) to (j) respectively for the year 1997.
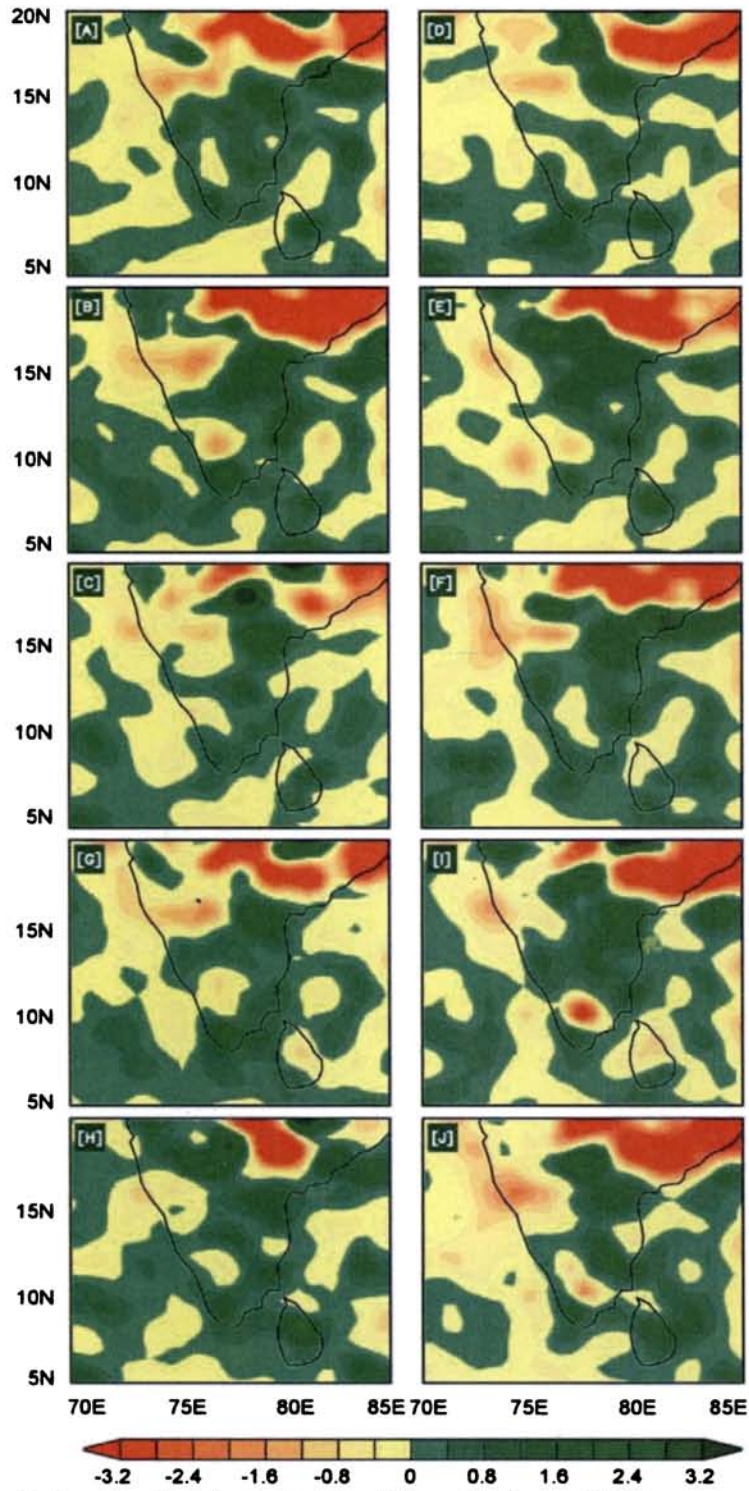
Fig. 5.15 vertically integrated moisture simulated Expt-Ctrl for an SST increment 0.1 to 1.0°C in (a) to (j) respectively for the year 2002
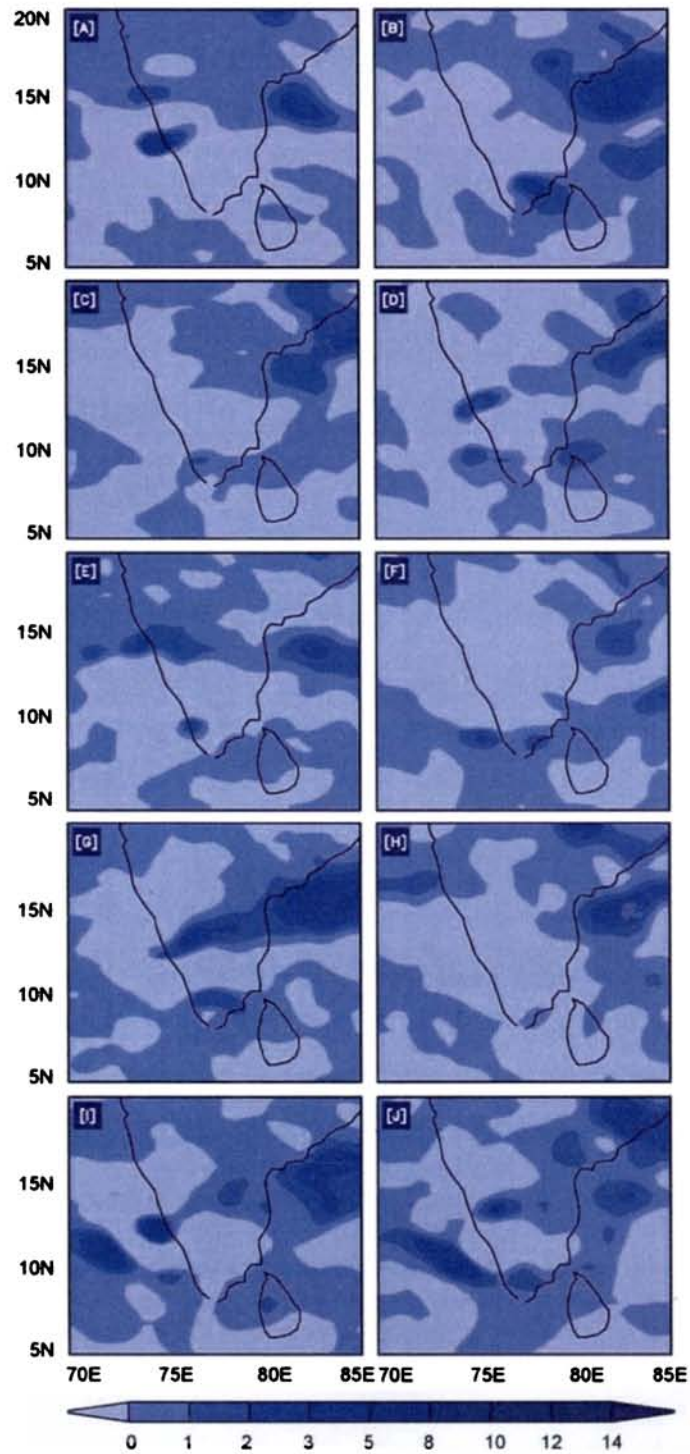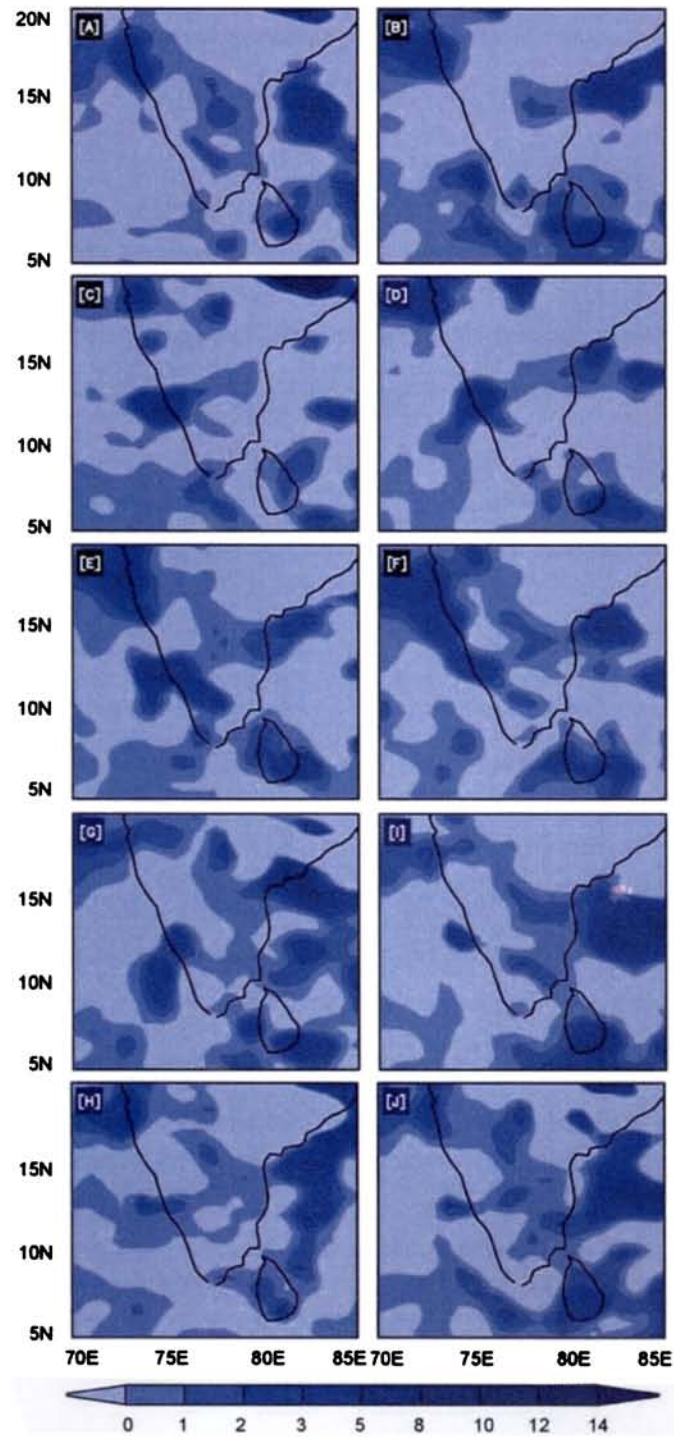
Fig. 5.16. Total precipitation rate (mm/day) simulated Expt-Ctrl for SST increment 0.1 to 1.0 in (a) to (j) respectively for the year 2002.
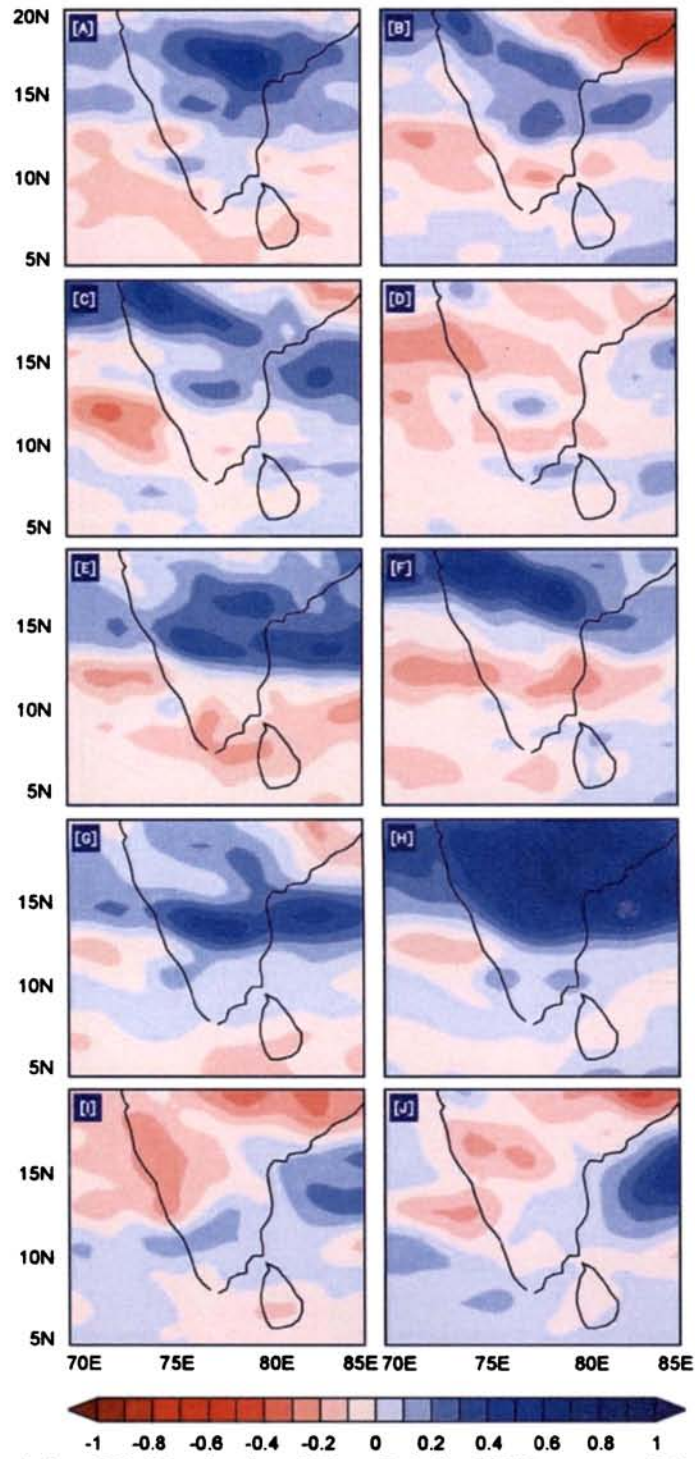
119
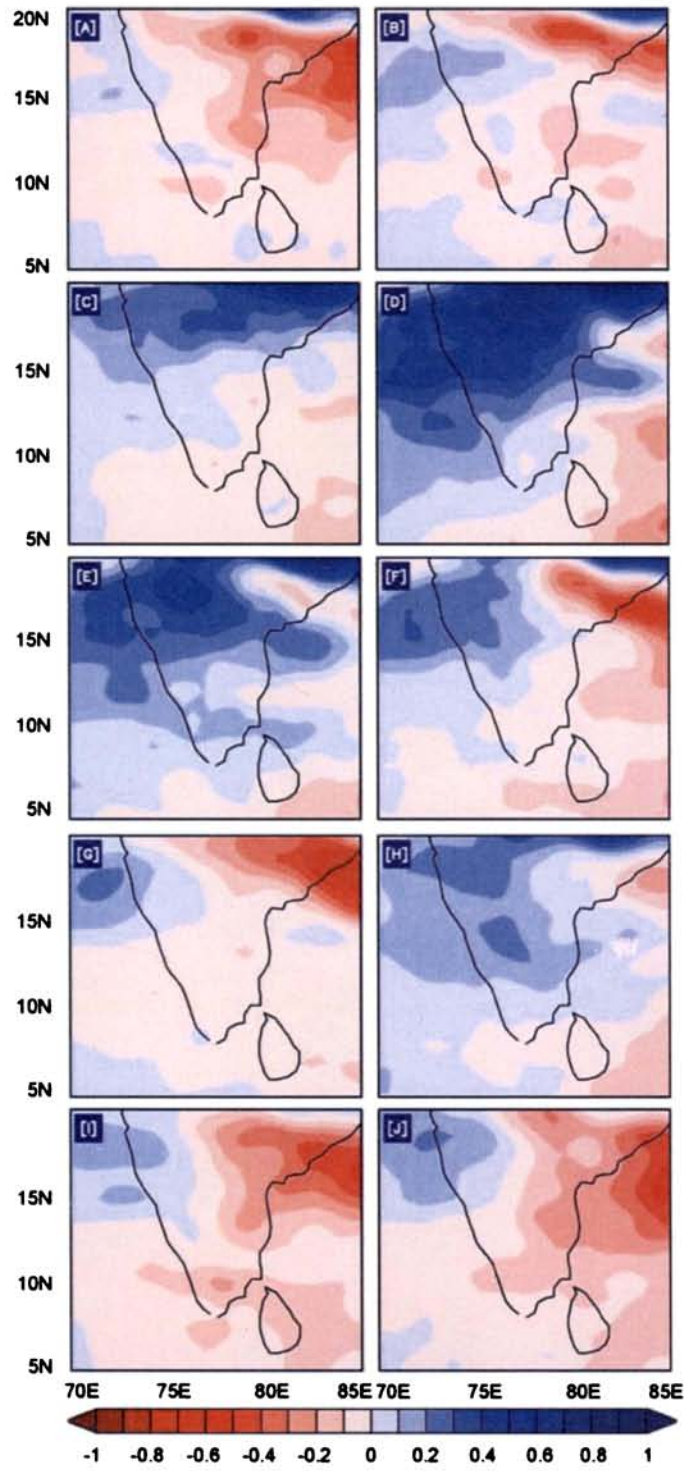
Fig. 5.17. Zonal wind at 850 hPa simulated Expt-Ctrl for SST increment 0.1 to 1.0 in (a) to (j) respectively for the year 2002
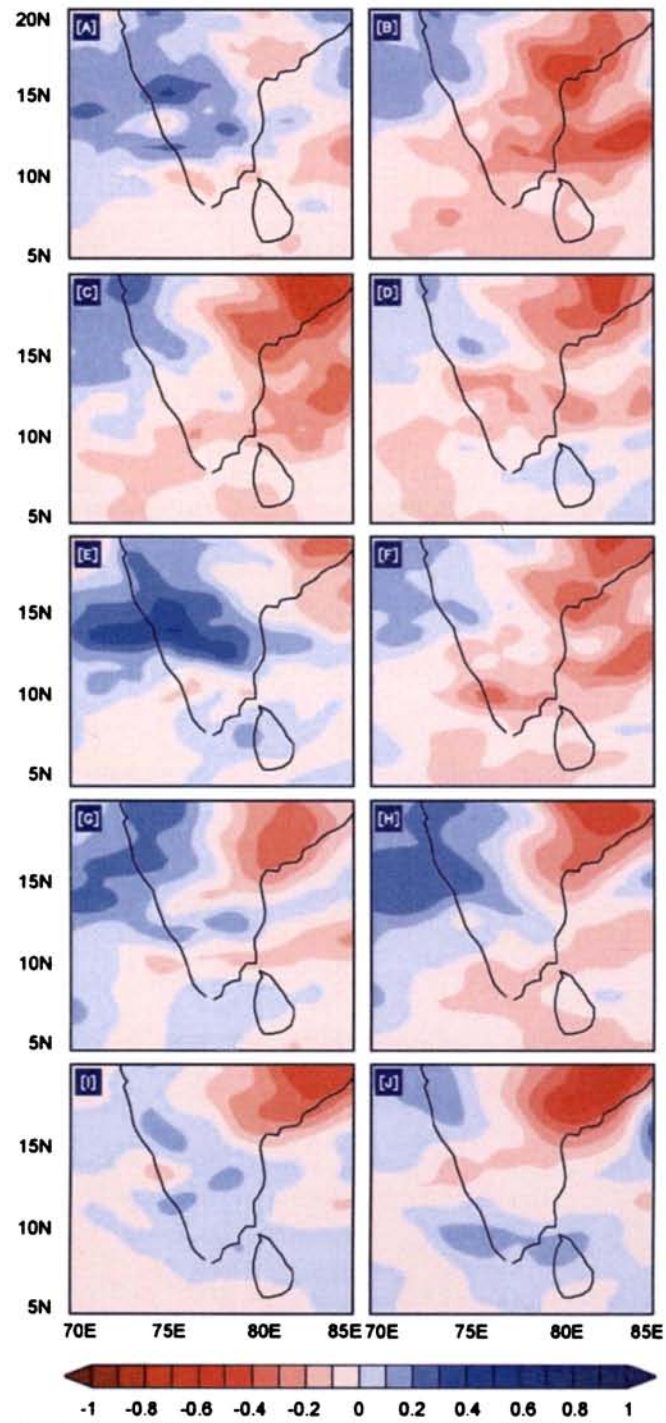
120
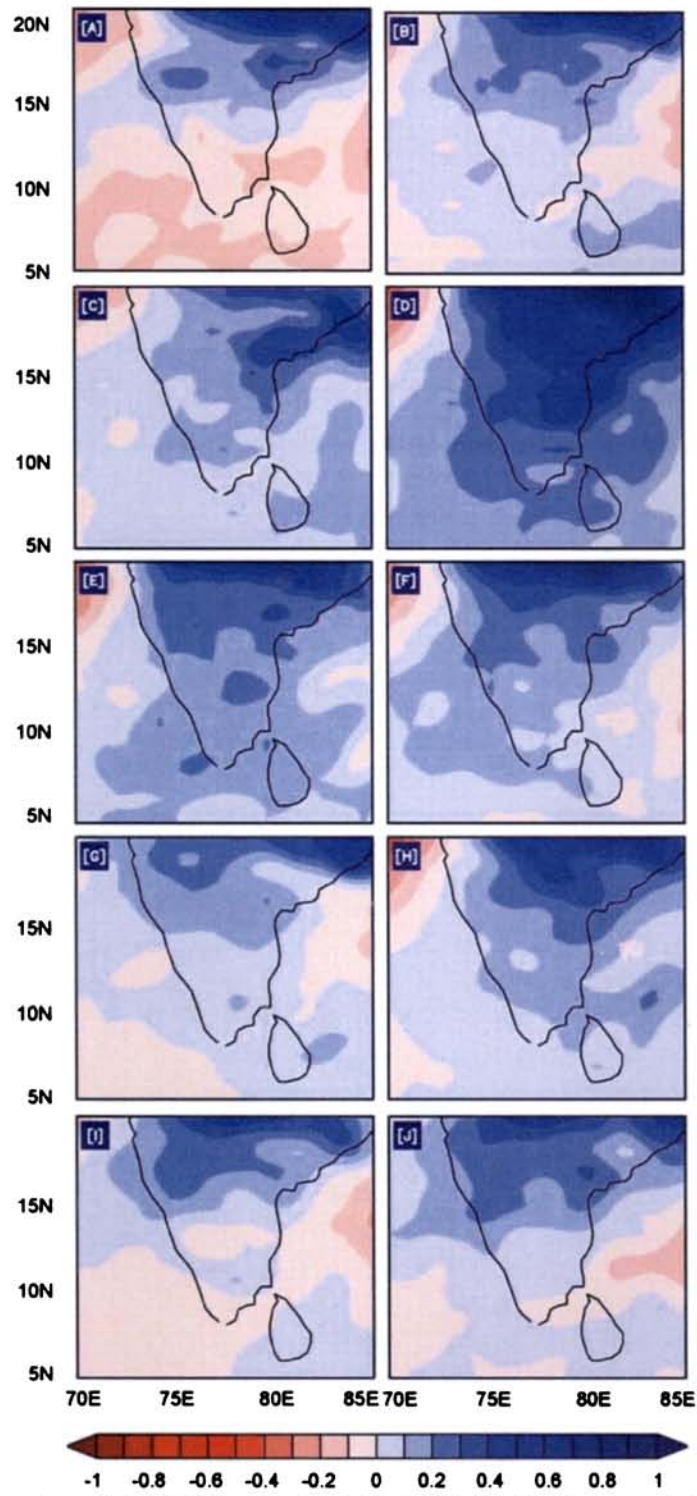
Fig. 5.18 Meridional wind at 850 hPa simulated Expt-Ctrl for SST increment 0.1 to 1.0 in (a) to (j) respectively for the year 2002
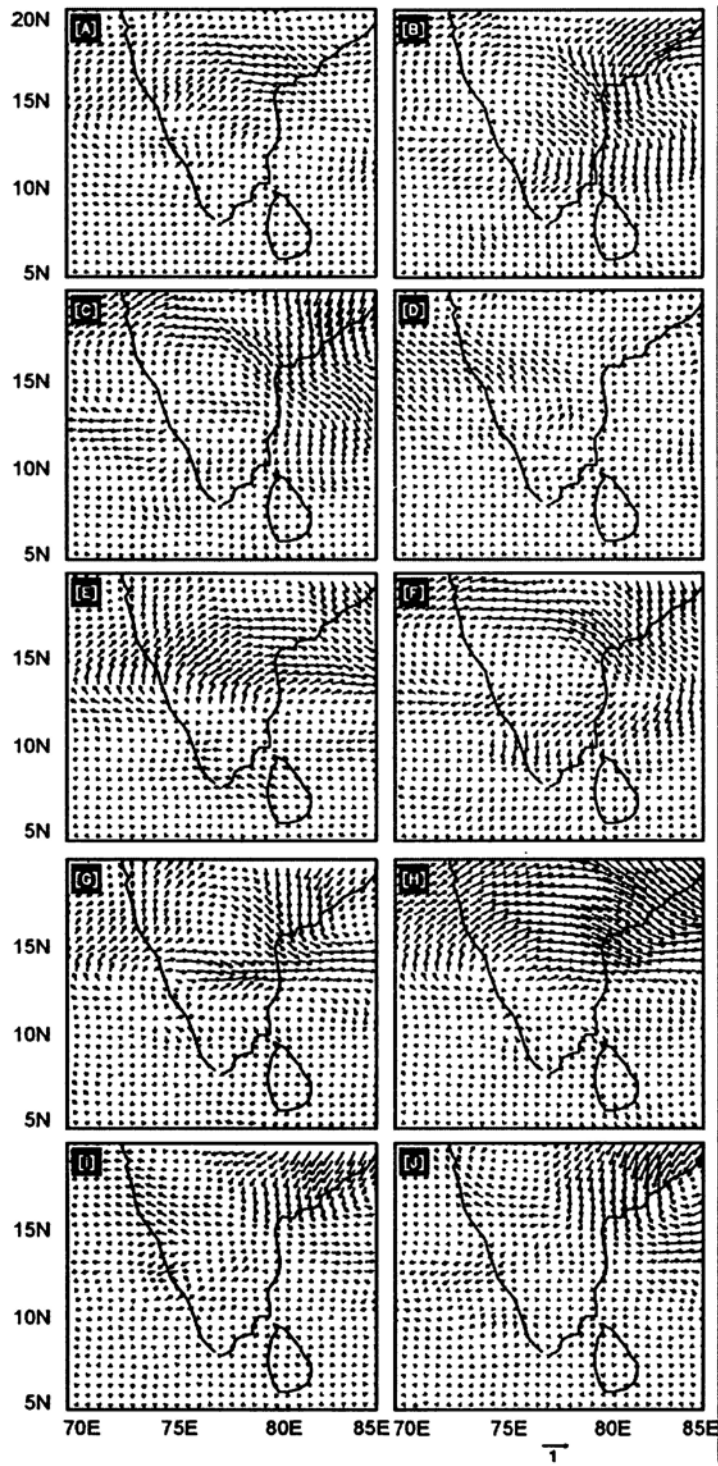
121
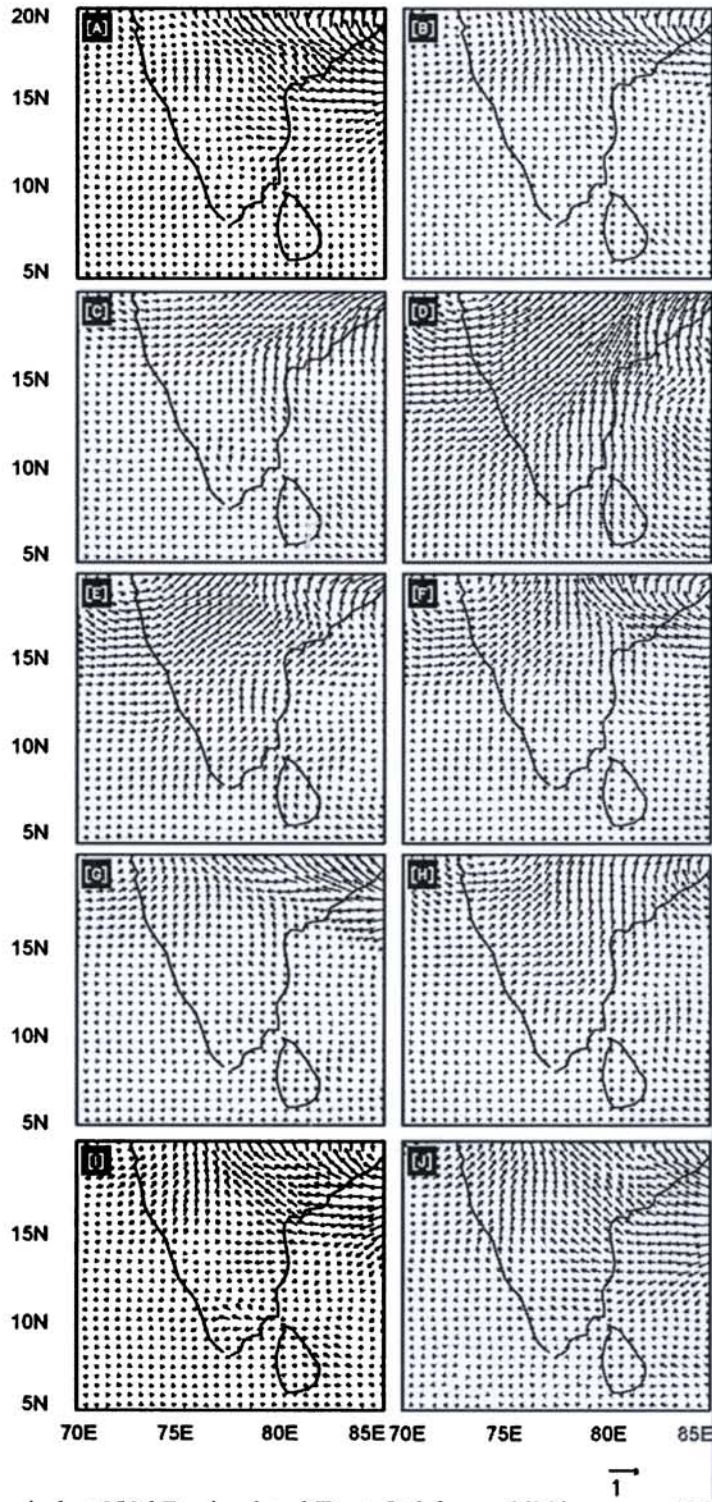
Fig. 5.19. Vector wind at 850 hPa simulated Expt-Ctrl for an SST increment 0.1 to 1.0°C in (a) to (j) respectively for the year 2002.

122
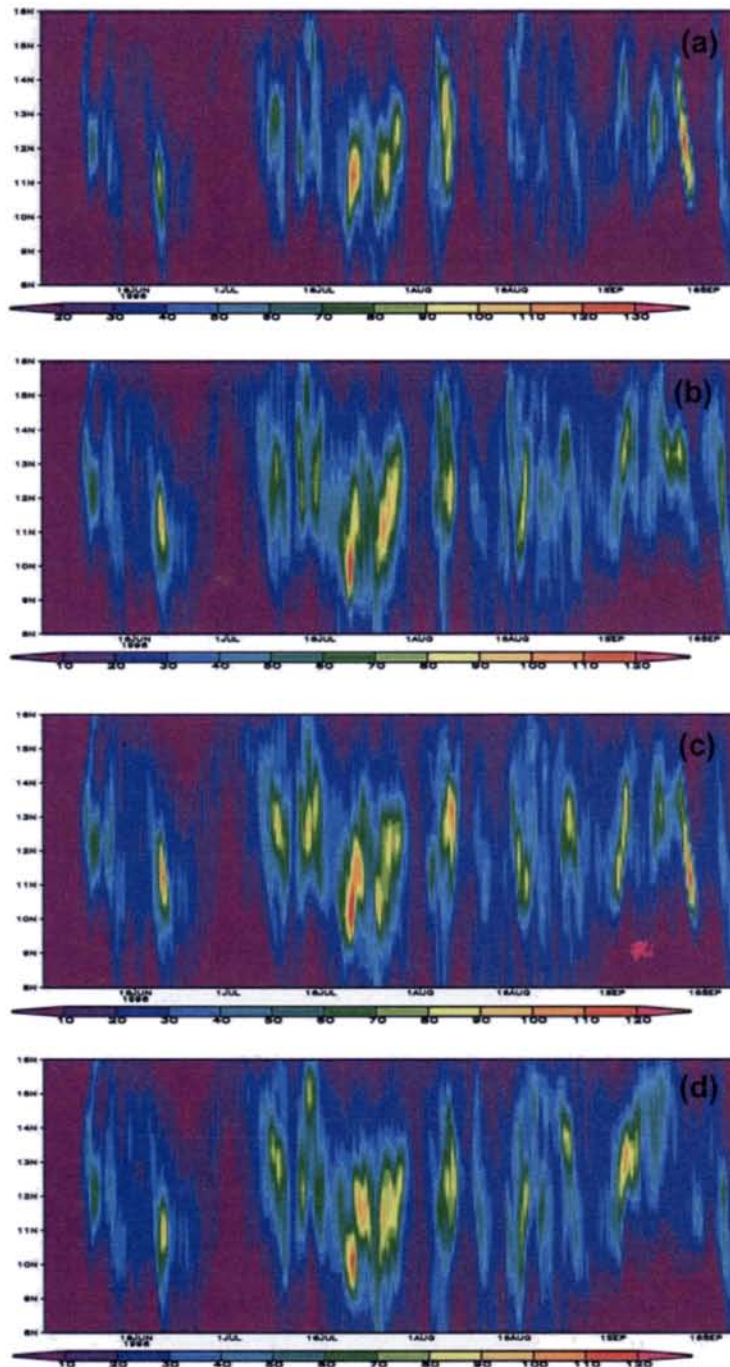
Fig. 5.20. The Hovmöller diagrams of precipitation rate for the summer monsoon 1996 for a) Control experiment b) SST 0.3 c) SST 0.6 d) SST 0.9
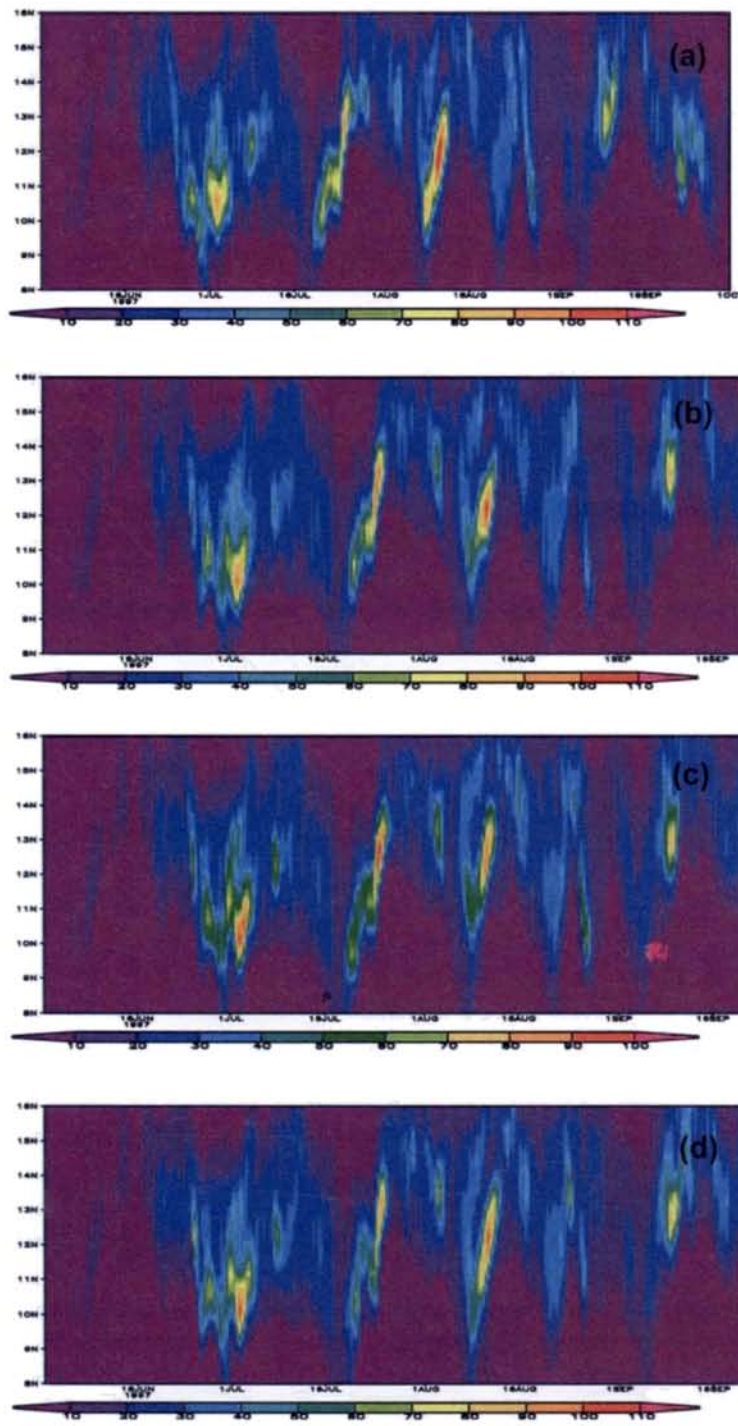
Fig. 5.21 The Hovmöller diagrams of precipitation rate for the summer monsoon 1997 for (a) Control experiment (b) SST 0.3 (c) SST 0.6 (d) SST 0.9
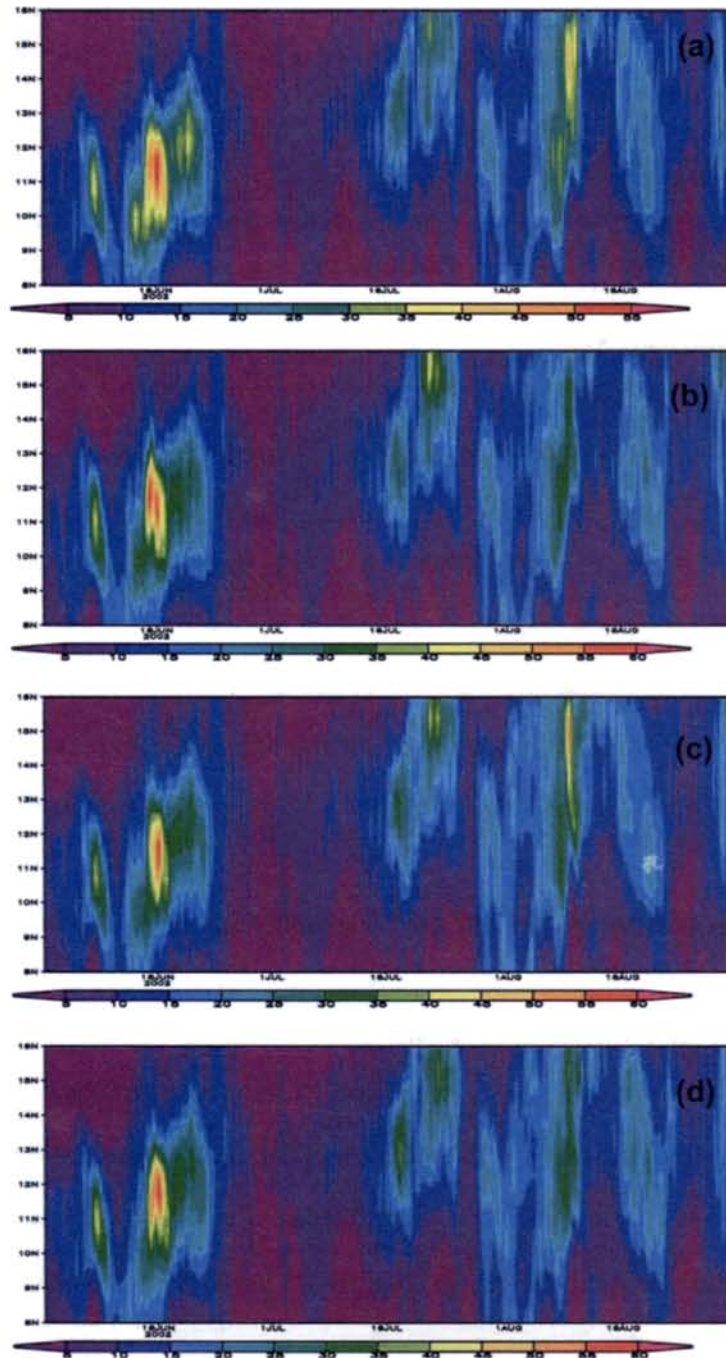
Fig. 5.22. The Hovmöller diagrams of precipitation rate for the summer monsoon 2002 for (a) Control experiment (b) SST0.3 (c) SST0.6 (d) SST0.9

125

For the normal year 1997, (Fig. 5.21) the intraseasonal variability is of a low frequency with average period of 20 days. Here also, the increase in feebly influence the intra seasonal variations in precipitation. For the anomalously dry year 2002 (Fig. 5.22), large gaps in the ISV can be observed. Here also very feeble modifications are seen in the ISV.

5.5 CONCLUSIONS

The study investigates the characteristics of circulation and precipitation during monsoon season over peninsular Indian region, based on the sensitivity experiments performed by a regional climate model for the years 1996, 1997 and 2002. A recent version (Version-III) of National Center for Atmospheric Research (NCAR) Regional Climate Model (RegCM3) was utilised. The planetary boundary layer scheme used is that of Holtslag, cumulus parameterization scheme Grell, SUBEX large scale precipitation scheme and BATS ocean flux parameterization scheme. The model is run from 1st May to 30th September except for 2002 for which the ERA40 data is available only till August. The first month is taken for the spin up. The next four months are taken to study the monsoon. RegCM3 has been integrated at 60 km horizontal resolution over the Indian domain. The experiments are carried out by changing the initial conditions of sea surface temperature by 0.1^0 C steps i.e. 0.1, 0.2 etc. to 1^0 C maximum. The sensitivity experiments showed that the wind strength increases significantly to the northeastern and central parts of India. The change in wind strength is pronounced over the southern peninsula when the sea surface temperature increased by $0.4 - 0.7^0$ C. The response in precipitation over the peninsular Indian region is also studied. The monsoon circulation features simulated by RegCM3 are compared with those of the NCEP/NCAR reanalysis and the simulated rainfall is

validated against observations from the Global Precipitation Climatology Centre (GPCC)

Results indicate that RegCM3 successfully simulates some important characteristics of the Indian summer monsoon circulation, such as the 850-hPa westerlies and precipitation. The seasonal mean summer monsoon rainfall simulated by RegCM3 is close to the corresponding GPCP values although the simulated precipitation is overestimated over Central North India and North Eastern India. Compared with the total precipitation from the GPCP data, the model is found to be capable of simulating the monsoon rainfall to a reasonable degree in spatial distribution, particularly the large-scale precipitation zones owing to the southwesterly monsoon flow.

The intraseasonal variability of the summer monsoon has been captured by the model and the results show that the influence of SST increase is more for WET year than for normal year or DRY year. The periods of ISV is shorter in WET year and very large breaks are observed in the DRY year.

CHAPTER 6

Influence of Moisture over the Northern Indian Ocean on the Climate of Peninsular India

6.1 INTRODUCTION

Joseph and Raman (1966) pointed out the existence of a low-level jet or the Monsoon Low Level Jet stream over peninsular India. The linkage between southwest monsoon wind in the Arabian Sea and India rainfall was studied by *Findlater (1969).* As expected, large-scale monsoon rainfall accumulation over India and Southeast Asia and wind strength over the Arabian Sea and India are strongly correlated *(Ju and Slingo 1995).* The cross-equatorial flux entering the Arabian Sea from the southern hemisphere is one of the most important sources of moisture for the Indian subcontinent during the southwest monsoon season. Surface level moisture flux computation showed that the net positive surface-level moisture flux divergence over the Arabian Sea and negative moisture flux divergence over the Bay of Bengal *(Kishtawal et al 1991).* The evaporation over the Arabian Sea is a variable quantity and forms a significant part of the net moisture budget over the Arabian Sea. The sharp increase between May and June is the combined effect of a sudden increase of the zonal component of the low level wind as well as a sudden increase of atmospheric water vapour over the Arabian Sea during the onset phase of the monsoon *(Kishtawal et al 1991).* Between April and July, there is a systematic transition of high moisture values from equator to upper latitudes *(Kishtawal et al 1994)*

During onset of the monsoon over India, the horizontal flux convergence of heat and moisture, as well as diabatic heating, are enhanced over the Arabian

Sea. These subsequently increase with the evolution and advancement of the monsoon over India *(Raju et al 2005)*. The convection over India is associated with the water vapor amount over the Arabian Sea. The enhancement (suppression) of convection over India during July corresponded to larger (smaller) water vapor amount and to colder (warmer) SST over the Arabian Sea. SST to east of Somalia decrease (increase) with the increase (decrease) of low-level Somali jet. However, the magnitude of SST decrease over the area does not directly correspond to the magnitude of low-level Somali jet *(Toshiro, 1997)*.

The origin and amount of moisture being transported to the Indian subcontinent during the southwest monsoon season was also studied by many investigators. *Pisharoty (1965)* utilizing the data collected during International Indian Ocean Expedition (IIOE), examined the moisture budget and found that evaporation from Arabian Sea to be the main contributor for summer monsoon rainfall. *Saha and Bavadekar (1973)* using additional upper air data concluded that 70% of moisture flux from the south Indian ocean accounts for the bulk of moisture needed for summer monsoon rainfall. The intraseasonal variations of moisture budget have also been examined by several scientists *(Ghosh et al 1978 and Cadet and Reverdin 1981)*. While the importance of evaporation over the Arabian Sea is suggested by *Ghosh et al (1978)* and *Murakami et al (1984)*, the role of cross equatorial flux has been emphasized by *Cadet and Reverdin 1981; Howland and Sikdar (1983) and Sadhuram and Ramesh (1988)*. Most of these studies suggest that the cross equatorial moisture flux provides an important source of moisture for the Indian Summer Monsoon rainfall though the evaporation from the Arabian Sea is quite significant. The monsoon activity is directly linked to the amount of moisture is transported to the Indian subcontinent during the monsoon period. Active periods of rainfall are characterised by stronger low

129

level flow directed to Indian subcontinent transporting more moisture in to the Indian subcontinent between latitudes 5°N to 15°N. During break and weak rainfall periods, the low level flow is diverted to equator and hence the moisture is transported south of the Indian peninsula, leading to below normal rainfall over India.

The importance of the Arabian Sea, which acts as a moisture source, and its role in the onset and maintenance of summer monsoon have been studied by *Mohanty et al. (1983)*. Moisture availability and advection by prevailing monsoonal wind are precursors of subsequent rainfalls over the Indian Continent. In a series of studies, *Mohanty et al (1983, 1994, 2002)* tried to establish the relation of moisture and surface heat budget over the Indian seas to the Indian summer monsoon. It has been found by *Cadet and Greco (1987)* that the moisture flux entering through the western coast is positively correlated with the coastal rainfall. For June, July, August and September, the amount of moisture crossing the western coast was estimated as $(1.5, 2.7, 1.5$ and $0.37) \times 10^{12}$ Kg. The volume of water precipitating over the land by estimation from the ISMR normal was $(1.95, 3.0, 2.3$ and $1.7) \times 10^{12}$ Kg for each of June, July, August and September. This agreement between ISMR and moisture across the continent indicated that a major source of moisture for the ISMR was transported across the western coast *(Valsala and Ikeda, 2005)*. Correlation between the ISMR anomalies and the Arabian Sea moisture convergence anomalies is 0.46, much higher than that between the moisture transport and the moisture convergence (0.25) in their study. The high correlation found between the ISMR and convergence anomaly in the study of *Valsala and Ikeda (2005)* also indicates that the moisture anomalies arising over the Arabian Sea has a significant contribution to the subsequent rainfall.

A possible reason of the moisture divergence and suppressed convection over the Arabian Sea are speculated to be related to the existence of the high sea level pressure (SLP) anomaly over the Arabian Sea. The usual breaks in ISMR often occur following a propagation of high SLP anomalies from the eastern Indian Ocean to the west as fast moving Rossby waves. From the modeling experiments *Krishnan et al (2000)* proposed that the life of the high SLP increases as the background westerly winds dominant over the westward propagation of the Rossby waves.

In a diagnosis study of surface wind vector patterns in the Arabian Sea to a degree of great detail, *Halpern and Woiceshyn (1999)* showed that eastward expansion of the Somali Jet raised the intensity of surface wind convergence and, consequently, increased the amount of integrated cloud liquid water in the eastern Arabian Sea, which, presumably, influence the rainfall of the west coast of India. *Shukla (1975)* suggested colder SST anomalies over western Arabian Sea tend to reduce monsoon rainfall over India. The important factor in explaining the fluctuations in monsoon circulation and precipitation rate is the air-sea interaction *(Saha 1974)*. SST anomaly may influence Monsoon rainfall through their effects on evaporation and the resultant moisture transport *(Meehl 1997; Chang and Li 2000)*. A large amount of water vapor is carried from over the ocean to the monsoon region by the Asian Summer Monsoon flow. The water vapor transport, therefore, is greatly affected by the monsoon circulation, which in turn has a significant influence on the rainfall in the monsoon region.

The possible effects of the SST anomaly as postulated by several workers *(viz. Saha, 1970a, b, 1974)* may be qualitatively described as follows: 1) Warmer SST anomalies and stronger winds may cause higher evaporation and the monsoon current may be more moist and unstable. Colder SST anomalies may cause

131

higher surface pressures and less evaporation over the Arabian Sea and this may reduce the cross-equatorial moisture flux and thus reduce the rainfall over India. 3) Higher pressures over the western Arabian Sea and lower pressures over the eastern Indian Ocean may set up east-west circulation.

Moisture availability and advection by prevailing monsoonal wind are precursors of subsequent rainfalls over the Indian Continent. In a series of studies, *Mohanty et al (1983, 1994, 2002)* tried to establish the relation of moisture and surface heat budget over the Indian seas to the Indian summer monsoon. A contrast is made on meteorological fields over the Indian seas between the extreme monsoon years (WET vs. DRY) based on monthly reanalysis data sets of the last 42 years *(Mohanty et al 2002)*. They reported a statistically significant region between air sea fluxes and wind over the Arabian Sea in the pre and summer monsoon epochs. For a last few decades, relative contributions of moisture from the Arabian Sea and cross-equatorial flow to the Indian summer monsoon have provided a controversial topic *(Hastenrath and Lamb 1980)*. The importance of the Arabian Sea, which acts as a moisture source, and its role in the onset and maintenance of summer monsoon have been studied by *Mohanty et al (1983)*.

During the summer monsoon epochs, large scale moisture convergence usually occurs below 800 hPa, and moisture turns into clouds above 800 hPa as explored by *Mohanty et al (1983)*. Thus, the surface moisture convergence yields accumulation of water in the low level of the atmosphere.

The physical processes by which the Indian Ocean responds to intraseasonal forcing are the same as those of the Pacific, but differences in the background conditions have a large influence on the oceanic effect. The shape of the Indian Ocean basin has an important effect because it is closed in the northern

subtropics. In the Pacific (or Atlantic) equatorial Kelvin waves reflect along the eastern boundary to coastal signals that propagate poleward; as a result intraseasonal wind forcing is lost to the tropics in those basins. In the Indian Ocean, by contrast, coastal waves are directed into the Bay of Bengal (and from the Bay around the southern tip of India into the Arabian Sea), providing an important source of remote forcing to the off-equatorial tropics originating in equatorial winds *(Potemra et al 1991; McCreary et al 1993; Schott et al 1994; Somayajulu et al 2003; Yu 2003).*

From the earlier studies it has been shown that the role of moisture, surface temperature and the geographic coastal boundaries of the northern Indian Ocean in modulating the climate of the Indian region during monsoon. This necessitates investigating the role of Arabian Sea rather the remotely brought moisture in distributing and modulating the climatic features over Indian Region.

In this study, a regional climate model RegCM3 has been used to study how the water vapour flux through the southern and western boundaries (as defined in the following section) to the Arabian Sea affects the climate of Peninsular India. The moisture through the western and southern boundary of the model domain were shut down in two different sensitivity experiments while keeping the evaporative flux from the Arabian Sea surface unaltered. Thus the difference in the control experiment and sensitivity experiments give an indication whether the moisture flux from the Arabian Sea surface can compensate, to an extend, the moisture reduction in the monsoon flow through lateral boundaries at the south and west. The parameters such as Vertically integrated moisture, moisture transport, precipitation and surface air temperature, which is having a direct

effect from moisture in the atmosphere has been studied for three contrasting years.

6.2   MODEL DESCRIPTIONS

The Regional Climate Model RegCM3 used in the present study is originally developed by *Giorgi et al (1993 a, b)* and then augmented and described by *Giorgi and Mearns (1999) and Pal et al (2000)*. The model includes cumulus parameterization schemes, large-scale precipitation scheme, planetary boundary layer (PBL) parameterization, surface vegetation soil hydrology package, the Biosphere-Atmosphere Transfer Scheme (BATS), Ocean flux parameterization, pressure gradient scheme, explicit moisture scheme, the radiative transfer scheme and the ocean-atmosphere flux scheme.

The model was set up as in the previous chapter. So details are not mentioned in this section.
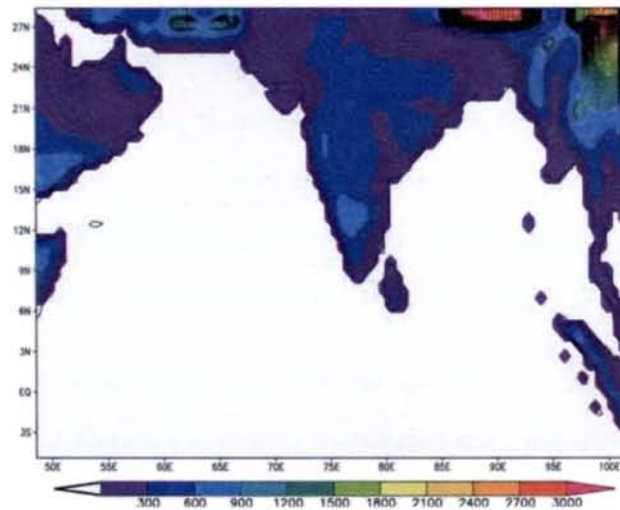
Fig. 6.1 the model domain for the experiment and control run.
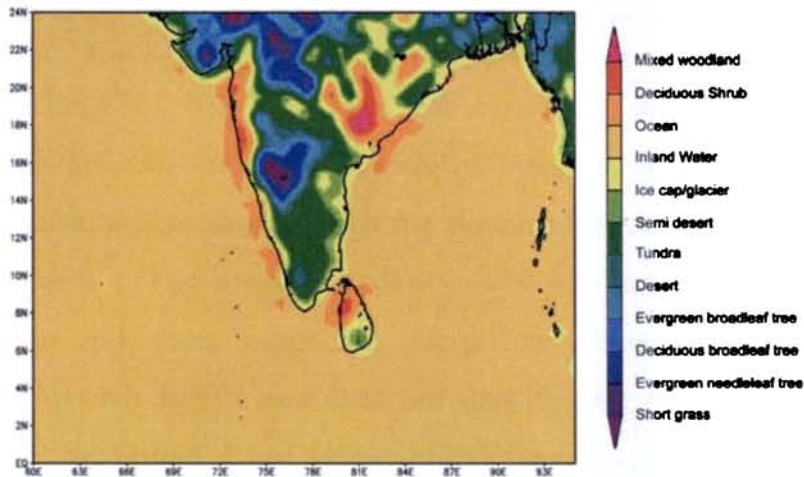
Fig. 6.2. The Landuse Data used in the RegCM3 model for the experiment and Control Run

6.3   OBJECTIVES

During the period of the Asian summer monsoon (ASM), a large amount of water vapor is brought to the Asian continent by the monsoonal flows. However, the origin of the water vapor carried by the streams is uncertain, and there are two possible kinds of source. One is the contribution from some distant sources outside the monsoon region due to the large-scale flows. Some literature (*Li 1999; Ding 2004*) suggest that the water vapor source of the ASM is in the oceanic regions of the Southern Hemisphere or the Arabian Sea, as most of the monsoon region in summer is a moisture sink (i.e., evaporation is less than precipitation). The second kind of water vapor source is the evaporation of water vapor when the low-level monsoon flows pass over the oceans.

The objective of this study is to determine whether the monsoon rainfall over India during boreal summer is mainly associated with the distant sources due to the long-distance transport of water vapor by the low-level monsoonal streams, or with the water vapor provided by the adjacent oceans.

135

6.4   DATA AND METHODOLOGY

In this study, RegCM3 has been used for simulating the Indian summer monsoon circulation and associated rainfall for three characteristic years with and without moisture advection through the Western and Southern boundaries of the model domain. The lateral boundary conditions for wind, temperature, surface pressure and water vapor are interpolated from 6 hourly NCEP reanalysis. The terrain height and land-use data for the given domain are generated from the United States Geographical Survey (USGS) global 5 min resolution terrain and land-use data. The original weekly averaged optimum interpolated Sea Surface Temperature (OISST) available from the National Oceanic and Atmospheric Administration (NOAA) for the whole year is horizontally interpolated into the specified domain and also in each time step for the model integration. The model domain covers the area approximately 50^0 E to 110^0 E and 5^0 S to 40^0 N with a horizontal grid distance of 60 km. The grid is defined on a Normal Mercator Projection. The CONTROL Run results are compared with GPCP precipitation and NCEP winds (shown in the previous chapter; Fig. 5.3 & 5.4). The difference in wind vectors and precipitation for the CONTROL Run and the Experiments (EXP_WB-CTL and EXP_SB-CTL) are analyzed to get a spatial perspective of the results. In this study, a control simulation is made over the domain and topography as shown in Fig. 6.1 & 6.2

6.4.1 CONTROL EXPERIMENT

In the control Run the model was integrated for five months from May to September for three years 1996, 1997 and 2002, which are considered as the three recent typical years designated as wet, normal and dry for peninsular Indian rainfall. The lateral boundary conditions are updated and supplied every 6 hours into the model and the time step of the integration has been kept at 150 seconds. The model resolution is 60 km.

6.4.2 SENSITIVITY EXPERIMENT

In this study we design the sensitivity experiments such that the moisture advection through the lateral boundaries through which the monsoon flow fetches moisture to the subcontinent are cut down for successive experiments. Since during the summer monsoon season, the zonal flow is southwesterly, moisture advection through south and west lateral boundaries of the model domain are closed for different experiments. They are termed as EXP-SB and EXP-WB respectively. In the third experiment the moisture through West, East and South boundaries were shut down (EXP-AB). Despite letting moisture though the boundary, the values at the model domain boundary are relaxed through a buffer zone of eight model grids. All the experiments are conducted for three years. The model is integrated from May to September for each of these experiments. The first month is taken as the spin up time for the model. The rest four months averaged to get the seasonal averaged values of Vertically Integrated moisture, precipitation and air temperature.

6.5   RESULTS

Fig. 6.3a indicates while shutting down the moisture over the southern boundary, that the vertically integrated moisture over peninsular India still increases. This means that the Arabian Sea acts as a source region for the

137

moisture. But while the western boundary has been closed, there is a decrease in the total column moisture over the entire peninsular India and Arabian Sea. But over Bay of Bengal, the compensation of moisture by evaporation is higher in both the experiments. The anomaly of peninsular Indian and west coastal precipitation for the EXP-SB is positive (Fig. 6.4a). But for EXP-WB, there is a large decrease in the western coastal region and Arabian Sea (Fig. 6.4b). Similarly the southeastern coastal region and Bay of Bengal also experiences a reduction in the precipitation. The rainfall which has an orographic component over the west coast of India suffers a reduction when the western boundary moisture has been shut down. For the EXP-AB, similar results are observed for moisture except a redistribution of the anomalies over the Bay of Bengal.

Fig. 6.5. shows the surface air temperature difference for the three experiments for the year 1996. The air temperature over the landmass has been reduced for EXP-SB, while for EXP-WB the air temperature over the pathway over the Indian subcontinent has reduced. Similarly for EXP-AB also there is a sharp decrease (1.5^0 C) in the temperature over Peninsular India and Bay of Bengal.

Fig. 6.3. The difference (EXP-CTRL) in the vertically integrated moisture seasonally averaged for June to September 1996 for (a) EXP-SB, (b) EXP-WB and (c) EXP-AB

Fig. 6.4. Difference (EXP-CTRL) in the seasonal mean precipitation (mm/day) for June to September 1996 for (a) EXP-SB, (b) EXP-WB and (c) EXP-AB

139

Fig. 6.5. Difference (EXP-CTRL) in the seasonal mean surface temperature for June to September 1996 for (a) EXP-SB, (b) EXP-WB and (c) EXP-AB
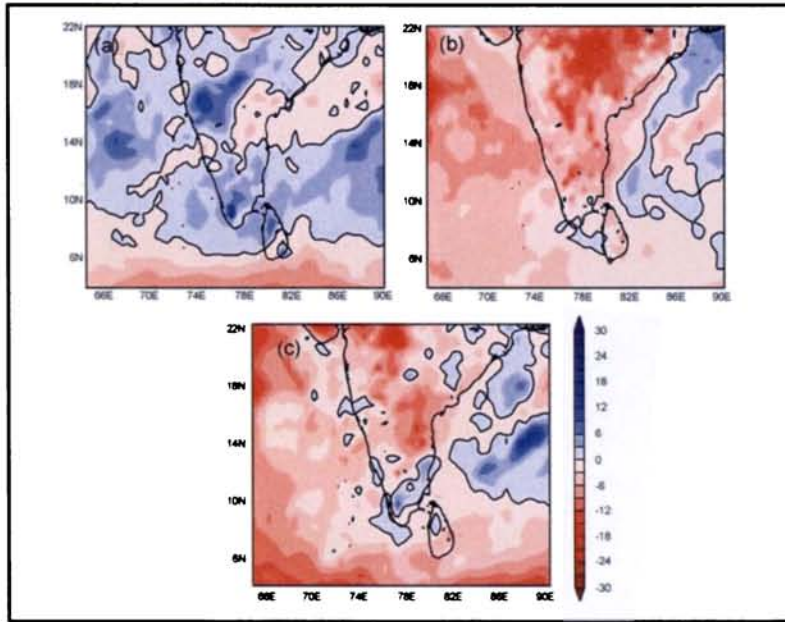

Fig. 6.6. The difference (EXP-CTRL) in the vertically integrated moisture seasonally averaged for June to September 1997 for (a) EXP-SB, (b) EXP-WB and (c) EXP-AB
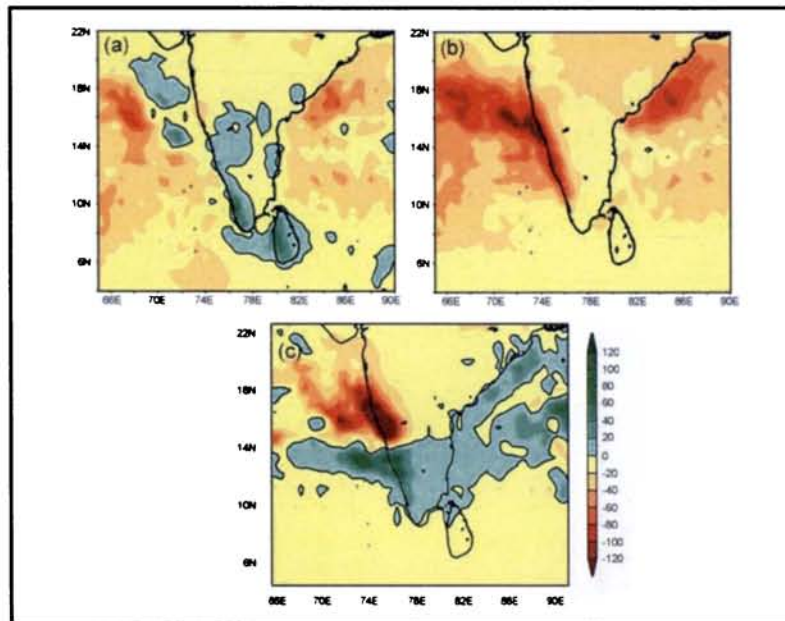
140

As in the case of 1996, for 1997 also shows increase of Total Column moisture for EXP-SB (Fig. 6.6). A supporting feature could also be seen in precipitation (Fig. 6.7a, 6.7b and 6.7c). Though there is spatially a large reduction in precipitation, the southern Peninsular India south of 12^0 N experiences an increased rainfall in the two experiments. This has an implication that the southern peninsular India is fed significantly by the moisture flux over the Arabian Sea and Bay of Bengal. A reduction in the moisture field is associated with more evaporation from the Oceanic region in the experiment domain and eventually a decrease in the surface air temperature (Fig. 6.8). In the three experiments conducted for the year 2002, the vertically integrated moisture is having similar patterns as that of the other years, with an increase in the moisture over peninsular Indian region for the EXP-SB (Fig. 6.9a) and increase over Bay of Bengal and adjoining coastal regions for EXP-WB and EXP-AB (Fig. 6.9b and 6.9c). But the excess in the peninsular Indian rainfall has decreased over western coast and oceanic region (Fig. 6.10). A simultaneous reduction in the air temperature also is noted (Fig. 6.11).

The vertically integrated moisture transport has also been analysed for the three years. In all the three cases, the western boundary experiment and southern boundary experiment showed divergent anomalies over peninsular India and the western coastal region. For the EXP-AB, the anomalies are even stronger and the convergent pattern over Bay of Bengal and Arabian Sea has weakened too. Over the southern Peninsular India, for the EXP-AB, weak anomalies shows that the moisture transport over this region is compensated by evaporative moisture from the adjacent oceanic regions (Fig. 6.12c). The main difference in these three sets of experiments is that the EXP-WB and EXP-AB moisture transport anomaly vectors with almost double the magnitude than the southern

141
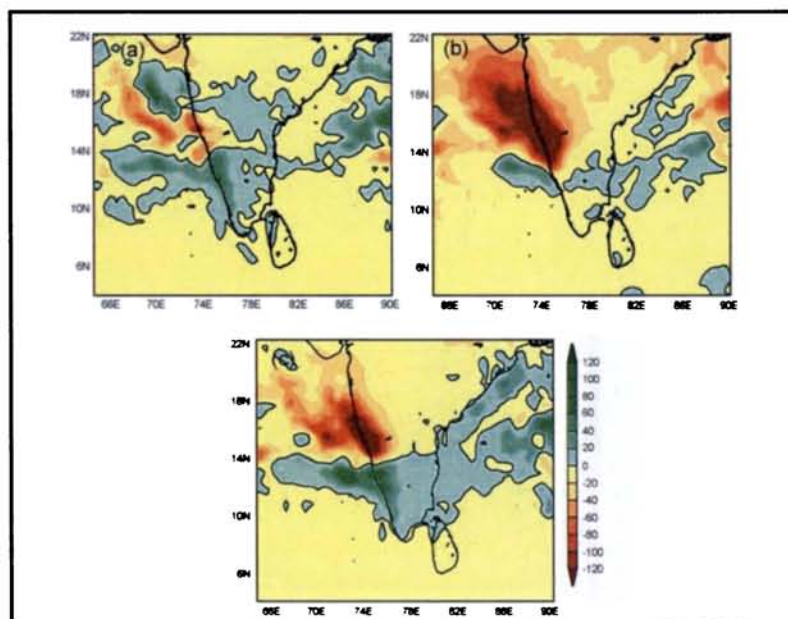
Fig. 6.7. Difference (EXP-CTRL) in the seasonal mean precipitation (mm/day) for June to September 1997 for (a) EXP-SB, (b) EXP-WB and (c) EXP-AB
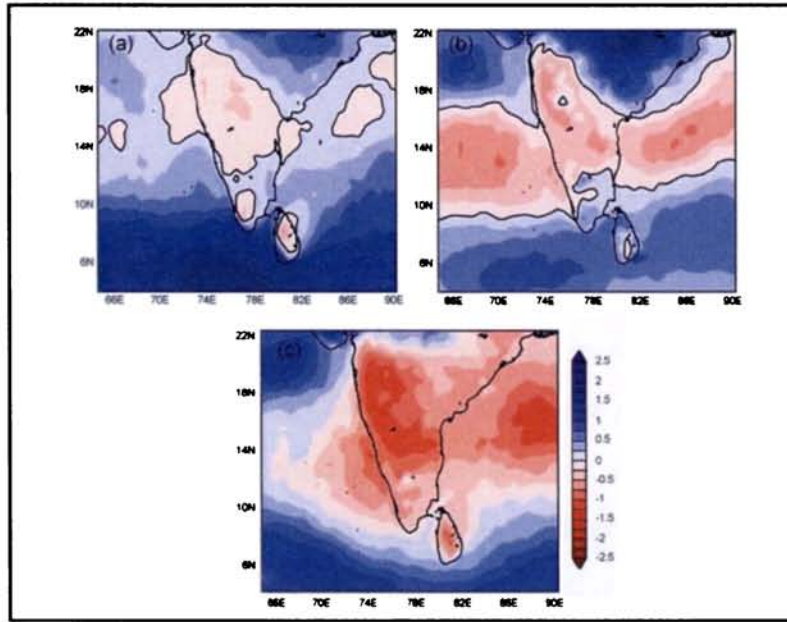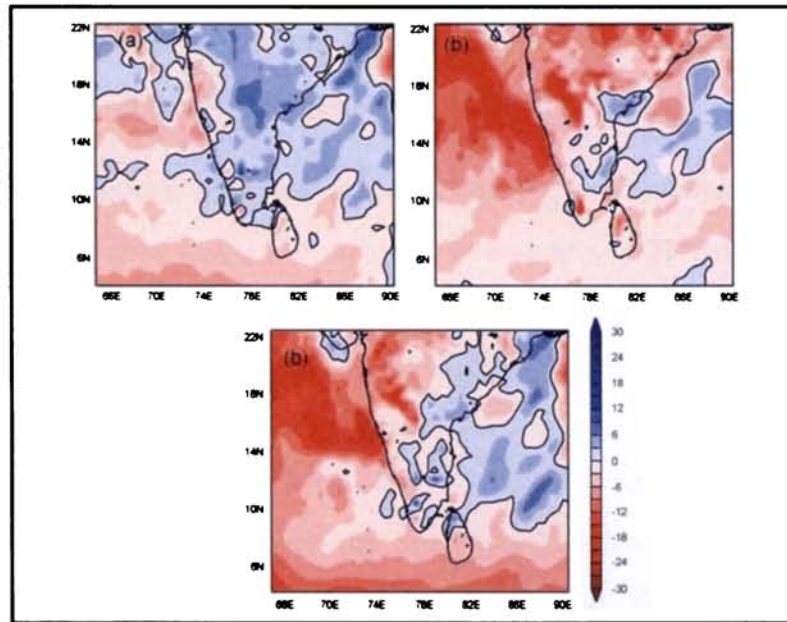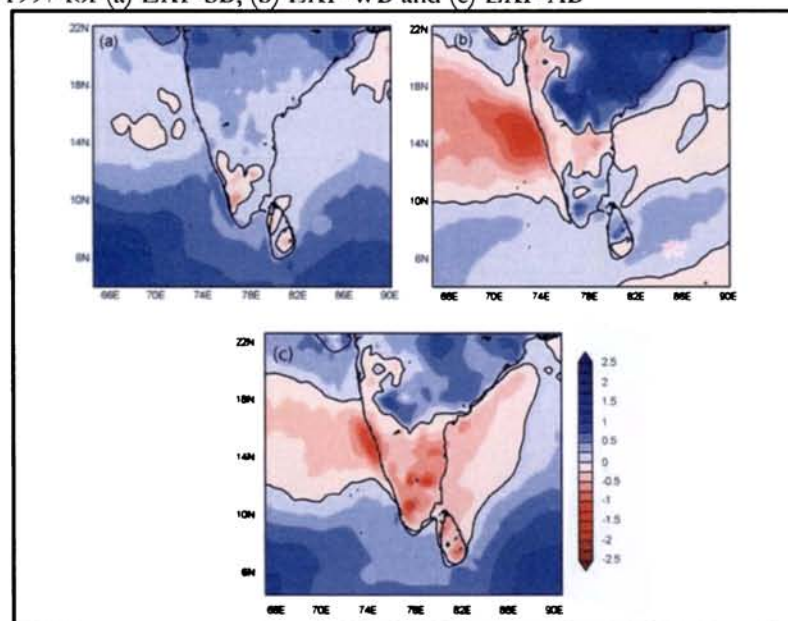

Fig. 6.8. Difference (EXP-CTRL) in the seasonal mean surface temperature for June to September 1997 for (a) EXP-SB, (b) EXP-WB and (c) EXP-AB
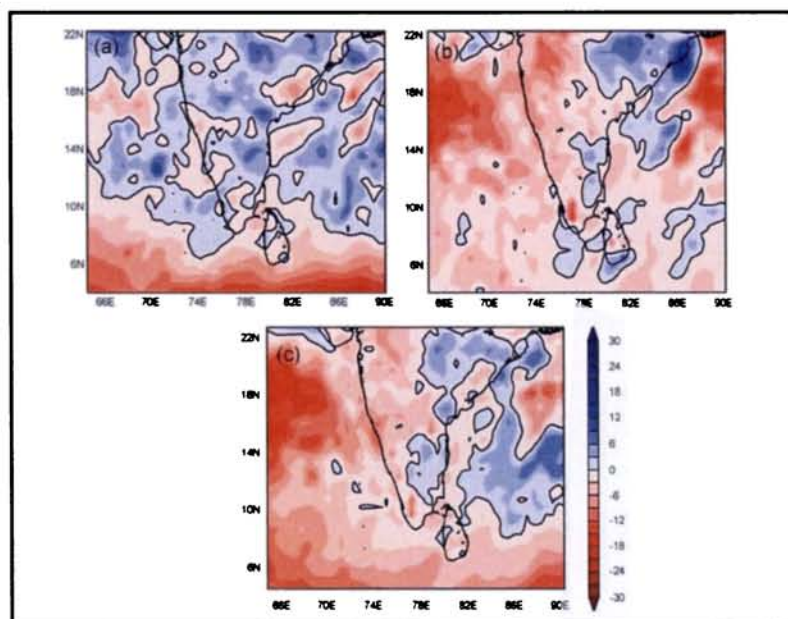
Fig. 6.9. The difference (EXP-CTRL) in the vertically integrated moisture seasonally averaged for June to September 2002 for (a) EXP-SB, (b) EXP-WB and (c) EXP-AB
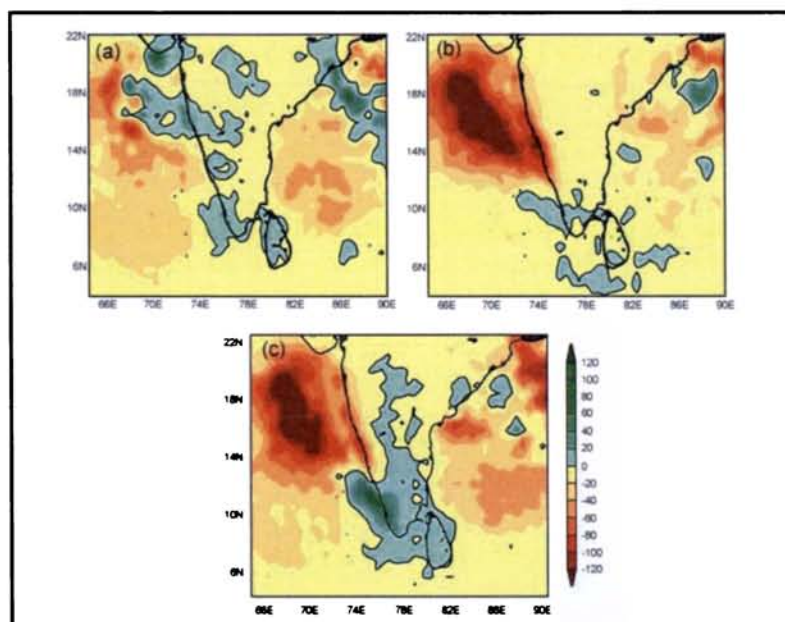
Fig. 6.10. Difference (EXP-CTRL) in the seasonal mean precipitation (mm/day) for June to September 2002 for (a) EXP-SB and (b) EXP-WB and (c) EXP-AB
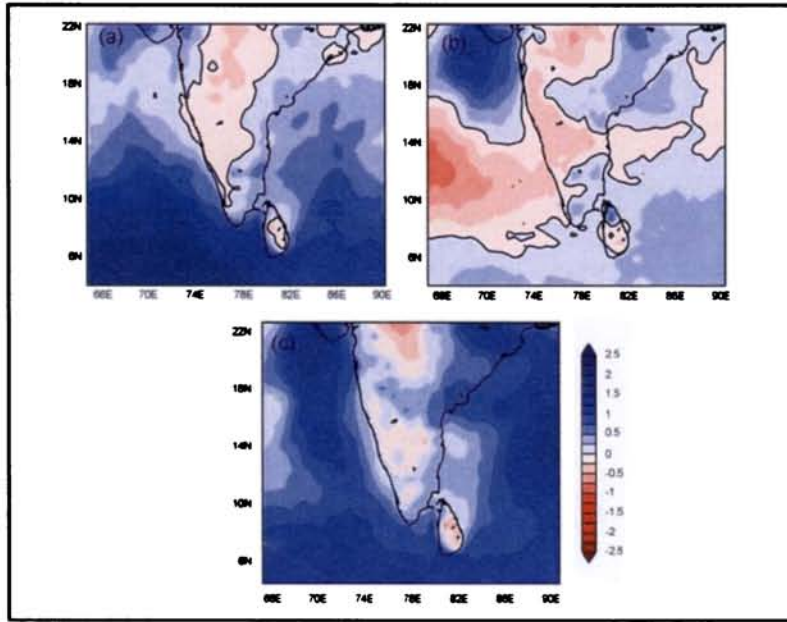
Fig. 6.11. Difference (EXP-CTRL) in the seasonal mean surface temperature for June to September 2002 for (a) EXP-SB, (b) EXP-WB and (c) EXP-AB
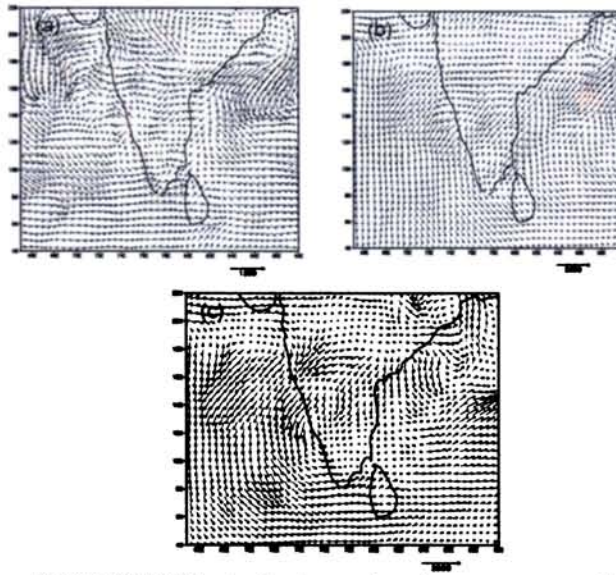
Fig. 6.12. Difference (EXP-CTRL) in the horizontal moisture transport for June to September 1996 for (a) EXP-SB, (b) EXP-WB and (c) EXP-AB.

144
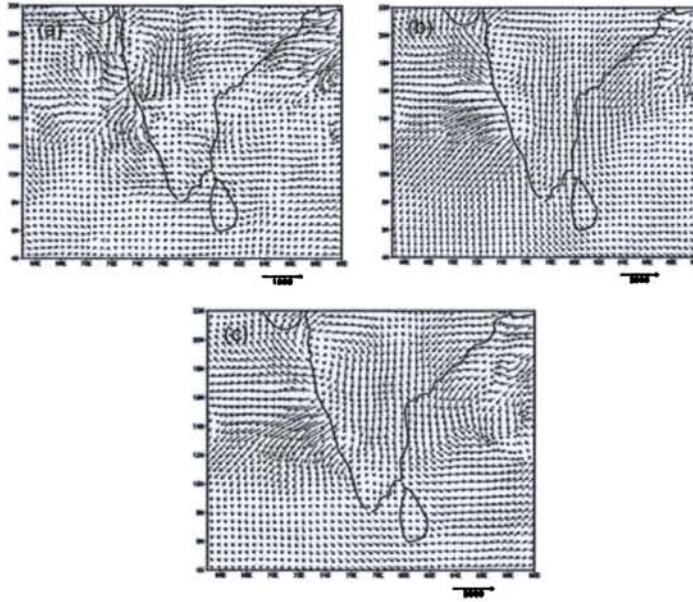
Fig. 6.13. Difference (EXP-CTRL) in the horizontal moisture transport for June to September 1997 for (a) EXP-SB, (b) EXP-WB and (c) EXP-AB.
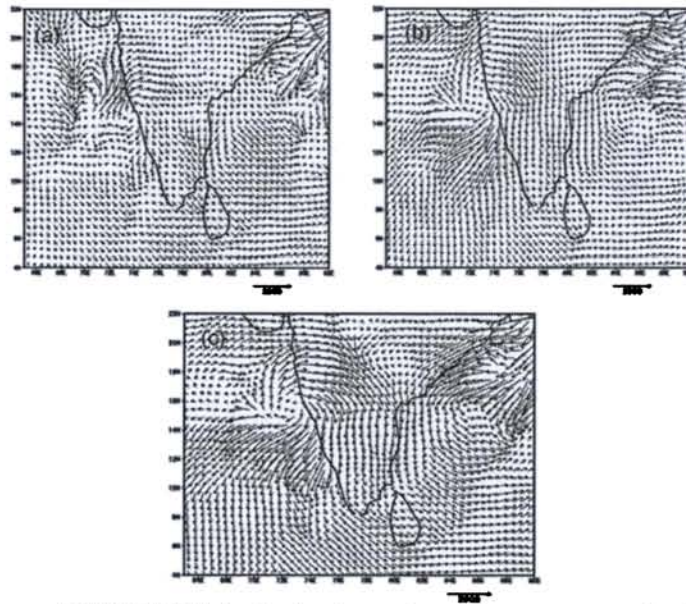
Fig. 6.14. Difference (EXP-CTRL) in the horizontal moisture transport for June to September 2002 for (a) EXP-SB, (b) EXP-WB and (c) EXP-AB.

145
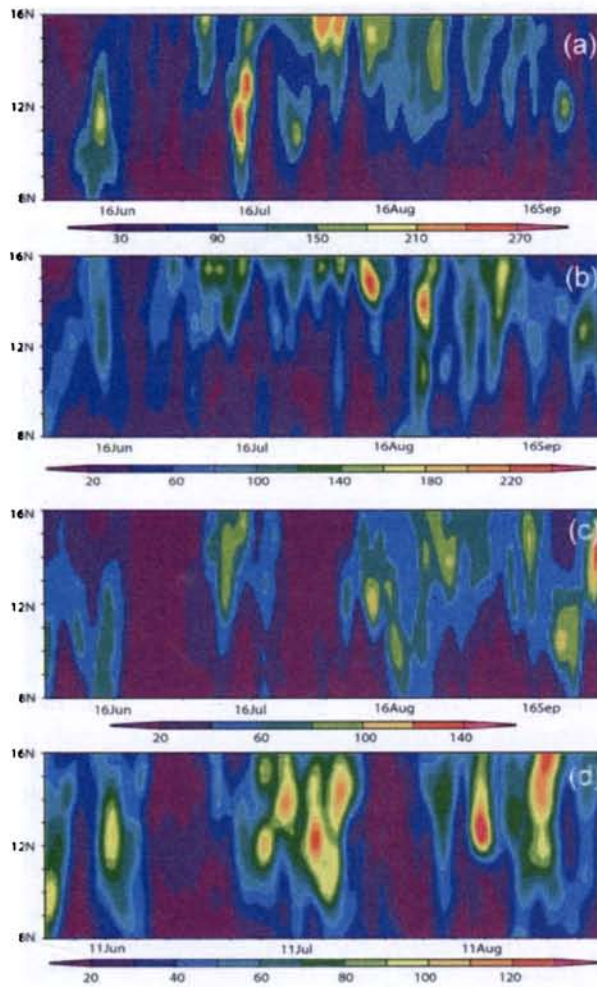
Fig. 6.15 the Hovmöller diagrams of daily Precipitation longitudinally averaged for 70⁰-85⁰E for a period of June to September 1996 for (a) Control Run, (b) EXP-SB, (c) EXP-WB and (d) EXP-AB.

boundary experiment (Fig. 6.12-6.14). Another feature that is to be pointed out from the analysis is that over the southern peninsular India, the moisture transport anomalies are relatively low. The moisture divergent anomalies over the western coastal and Arabian Sea region are marked with highly reduced values of precipitation, especially in the EXP-WB and EXP-AB.

In order to analyze the intraseasonal variations in the precipitation due to this experiments, longitudinally averaged (70-85⁰ E) precipitation for the monsoon

season is represented in Hovmöller plots (Fig 6.15-6.17). There is a clear indication that the intraseasonal variation in the peninsular Indian rainfall is sensitive to the moisture advection through the western and southern boundary of the model domain. The analysis shows that for a WET year 1996, the reduced moisture in all the experiments has redefined the spatial (meridional) and intraseasonal distributions in the rainfall over peninsular India during active months (June and July, see Fig. 6.15). For the EXP-AB, for the WET year 1996, the southern peninsular rainfall has increased (6.15d) while for the normal and DRY years the precipitation has decreased (Fig. 6.16d and 6.17d).

For normal year 1997, the distribution of rainfall has not varied much in time or region, but obviously the amount has decreased considerably. Here also, during June and July, there is a sharp decrease in the precipitation. For the year 2002 which is typically a dry year, the western boundary experiment shows a large decrease in the precipitation during the first half of the season (Fig. 6.15 and 6.17). This has an implication that during the first half of the monsoon season (during June and July), the rainfall depends heavily on the moisture advected through the boundaries of the domain and later depends on local moisture sources from the adjacent oceanic regions.
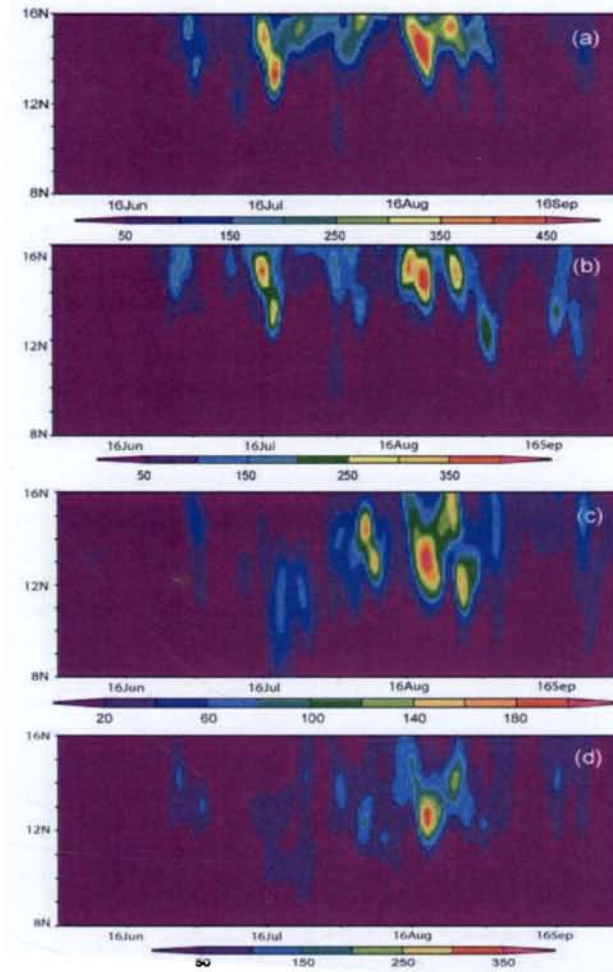
Fig. 6.16. The Hovmöller diagrams of daily Precipitation longitudinally averaged for 70⁰-85⁰ E for a period of June to September 1997 for (a) Control Run, (b) EXP-SB, (c) EXP-WB and (d) EXP-AB.
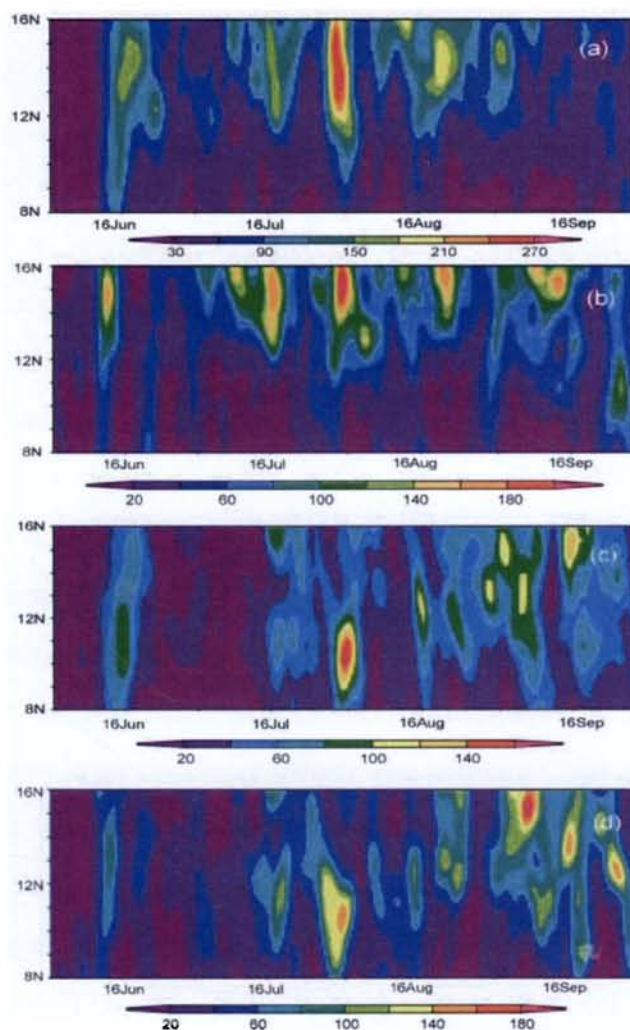
Fig. 6.17. The Hovmöller diagrams of daily Precipitation longitudinally averaged for 70°-85°E for a period of June to September 2002 for (a) Control Run, (b) EXP-SB, (c) EXP-WB and (d) EXP-AB.

6.5 CONCLUSION

In the study using the Regional Climate model RegCM3, the effect of absence of moisture in the low-level monsoon flow through the western and southern lateral boundary of the model domain on the Vertically Integrated moisture, precipitation, surface air temperature and integrated moisture transport are

studied. The southern boundary experiment EXP_SB showed that when the moisture influx to the domain through the southern boundary was shut down, still there is an increase in the vertically integrated moisture over the peninsular India for the wet year 1996, normal year 1997 and dry year 2002. But for the western boundary experiment, EXP_WB, the integrated moisture has substantially reduced implying that the total column moisture is mainly fed by the western boundary stream rather the compensation by evaporation from the Arabian Sea or the meridional transport through the southern boundary. The greatest decrease in moisture fields is for the wet year 1996 and the lowest change is for the dry year. There is sharp decrease in moisture over the Arabian Sea also. For precipitation also greatest decrease is seen for the wet year. Over the Western Ghats and the Adjoining Arabian Sea there is negative anomaly for precipitation for all the three years. Surface temperature anomaly patterns observe a decrease in temperature where the moisture was anomalously low. This could be due to the fact that the dry air allows for greater evaporation and thus facilitating cooling in surface temperature. The Vertically Integrated moisture transport anomaly vectors for EXP_WB are double the order of magnitude larger than the EXP_SB implying a more significant role of moisture through western Arabian Sea than moisture advected meridionally through southern boundary.

The intraseasonal variability in the zonally averaged precipitation over Peninsular India shows that the precipitation pattern and its distribution in time have been mostly modified for the wet year. In all the experiments the EXP_WB showed reduction in precipitation for the first half of the season owing to the reduced moisture.

CHAPTER 7

SUMMARY AND CONCLUSION

The Doctoral thesis focuses on the factors that influence the weather and climate over Peninsular India. Major outcome of the thesis is summarized below:

Vertically Integrated Moisture (VIM) from surface to various levels over the peninsular India for different seasons was studied for the period 1950-2004. The wavelet spectrum of VIM during the summer monsoon (June-August) and post monsoon (September-November) showed an eleven-year mode of variability. The spatial extend of this mode of variability for different seasons was analysed using Fast Fourier Transform (FFT) of the VIM for the region 20^0S-50^0N and 0-160^0 E. The spectral power corresponding to 10 and 11 years for the winter season - December, January and February- (DJF) show high values over the Peninsular India and extending over Bay of Bengal to Indo-China peninsula. This also has a southeastward spread towards Indonesian region. Similar analyses for September, October and November (SON) season show high spectral power for 12-year period over Peninsular India. The spectrum for June, July and August (JJA) season shows highest spectral powers concentrated over regions other than Peninsular India.

The variability of this mode is studied quantitatively using the Empirical Orthogonal Function (EOF) analysis of VIM over the same region. The amplitude for DJF of first EOF shows similar patterns as that of the FFT power corresponding to 11 years over the aforesaid area. The second EOF shows patterns as that of the spectral power for 10 years over the southern Peninsular India region. The first EOF gives 21.2% of the total moisture variability over the

study area, which corresponds to 11-year mode, and the second EOF gives 12%, which corresponds to the 10-year mode. For SON season, the EOF analysis shows that the first EOF corresponds to 12 years but with negative phase and explains a variability of 19.4%.

A possible association with moisture and air temperature in connection with solar activity is also suggested by computing the correlation of monthly solar flux and tropospheric air temperature along vertical sections of 80^0 E and 10^0 N. The meridional cross-section shows that in the northern hemisphere up to 25^0 N, the correlation extends down to about 850 hPa whereas for the zonal cross section the correlations are significant up to 800 hPa in the eastern hemisphere. Thus it seems that the influence of solar flux on the tropospheric temperature be the driving force behind the principal modes of variability.

The wavelet analysis of PCs of VIM for various seasons and various years shows that the intraseasonal variability in the integrated moisture over the Arabian Sea and Peninsular India is around 16-24 days. The EOF patterns show that the third greatest variability over the Indian domain regarding the VIM is over the Arabian Sea and Peninsular India, though the variabilities account for a small percentage.

Spectral analysis of seasonal VIM shows significant intraseasonal variability in the 12-32 days band and the principal modes of variability in the EOF analysis shows zonal coherence over peninsular India and adjoining Seas.

The wavelet analysis of high frequency removed KSMR showed a significant mode of decadal variability corresponding to 11-12 year period. The cross-spectral analysis of subdivisional rainfall over peninsular India also showed spectral peeks at a decadal frequency scale. Significant correlations were obtained between 4-year running mean Indian summer monsoon rainfall and F 10.7 for concurrent time (lag0), lag1 and lag2. A positive relation is observed over the western coastal

region and a negative relation is noticed over the entire leeside of the Western Ghats.

The regressed vectors between F10.7 and zonal wind indicate that the monsoon flow in the months of July and August is influenced by solar flux and the convection also is very much influenced by solar flux, though there have been significant changes in the regions and intensity in these relations after 1976.

A linear regression model was developed and tested for the seasonal rainfall prediction of Peninsular India using immediate regional parameters such as (i) lower tropospheric temperature during May over the Peninsular India and adjoining Bay of Bengal (ii) Sea Surface Temperature during the month of March over the Mid-Indian Basin over the Indian Ocean (iii) Zonal wind at 700 hPa during February and (iv) meridional wind at 700 hPa during January. The period of analysis was from 1975-2006 of which last nine years were tested against the observed rainfall. These parameters were arrived from a larger set of candidate predictors, which had statistically significant relation with PIR. The empirical model could explain 77.7 % of the total variance in the PIR and has a RMS error of 7.8%, BIAS of 0 mm and an absolute error of 40.2 mm. Except 2002, the model could capture the extreme years reasonably good. It is noteworthy that in 2002, a prolonged 30-day break in summer rains had lead to an extremely dry monsoon season whereas IMD models in use at the time had predicted normal rains in 2002.

The characteristics of circulation and precipitation during monsoon season over Peninsular Indian region are also investigated on the basis of the sensitivity experiments performed by a regional climate model for the years 1996, 1997 and 2002. A recent version (Version-III) of National Center for Atmospheric

Research (NCAR) Regional Climate Model (RegCM3) was used. The planetary boundary layer scheme used is that of Holtslag, cumulus parameterization scheme Grell, SUBEX large scale precipitation scheme and BATS ocean flux parameterization scheme. The model was run from 1st May to 30th September except for 2002 for which the ERA40 data is available only up to August. The first month is taken as the spin up for the model. The next four months are taken to study the monsoon. RegCM3 has been integrated at 60 km horizontal resolution over the Indian domain. The experiments are carried out by changing the initial conditions of sea surface temperature by 0.1^0 C steps ie. 0.1, 0.2 etc. to 1^0 C maximum. The sensitivity experiments showed that the wind strength increases significantly to the northeastern and central parts of India. The change in wind strength is pronounced over the southern peninsula when the sea surface temperature is increased by 0.4 - 0.7^0 C. The response in precipitation over the peninsular Indian region is also studied. The monsoon circulation features simulated by RegCM3 are compared with those of the NCEP/NCAR reanalysis and the simulated rainfall is validated against observations from the Global Precipitation Climatology Centre (GPCC)

The RegCM3 model successfully simulates some important characteristics of the Indian summer monsoon such as the 850-hPa westerlies and precipitation. Even though the observed precipitation is underestimated over Central North India and North Eastern India, the model is found to be capable of simulating the monsoon rainfall to a reasonable degree in both spatial distribution and quantity, particularly the large-scale precipitation zones owing to the southwesterly monsoon flow.

The intraseasonal variability of the summer monsoon also has been captured by the model. The results indicate that the influence of SST increase is more for

WET year than for normal year or DRY year. The periods of ISV is shorter in WET year and very large breaks are observed in the DRY year.

The effect of the absence of moisture in the low-level monsoon flow through the western and southern lateral boundary of the model domain on the Vertically Integrated moisture, precipitation, surface air temperature and integrated moisture transport is also studied using the RegCM3. In the southern boundary experiment EXP_SB, when the moisture influx to the domain through the southern boundary was shut down; an increase in the vertically integrated moisture is noted over the peninsular India for the wet year 1996, normal year 1997 and dry year 2002. But for the western boundary experiment, EXP_WB, the integrated moisture has substantially reduced implying that the total column moisture is mainly fed by the moisture through western boundary rather than the moisture by evaporation from the Arabian Sea or the meridional transport through the southern boundary. The greatest decrease in moisture fields is for the wet year 1996 and the lowest change is for the dry year. A sharp decrease in moisture over the Arabian Sea is also observed. For precipitation, a negative anomaly is noticed for all the three years over the Western Ghats and the Adjoining Arabian Sea, with the greatest decrease for the wet year. Surface temperature anomaly patterns are observed with a decrease in temperature where the moisture was anomalously low. This could be due to the fact that the dry air allows for greater evaporation and thus facilitating cooling in surface temperature. The Vertically Integrated moisture transport anomaly vectors for EXP_WB (Expt-Ctl) are double the order of magnitude larger than the EXP_SB (Expt-Ctl) implying a more significant role of moisture through western Arabian Sea than moisture advected meridionally through southern boundary.

The intraseasonal variability in the zonally averaged precipitation over Peninsular India shows that the precipitation pattern and its distribution in time have been

mostly modified for the wet year. In all the experiments the EXP_WB showed reduction in precipitation for the first half of the season owing to the reduced moisture.

REFERENCES

Annamalai H, Slingo JM, Sperber KR, Hodges K; (1999) The mean evolution and variability of the Asian summer monsoon: comparison of ECMWF and NCEP--NCAR reanalyses. *Monthly Weather Review*, **127**:1157-1186.

Annamalai H, Slingo JM; (2001) Active break cycles: Diagnosis of the intraseasonal variability of the Asian summer monsoon. *Climate Dynamics*, **18**: 85-102.

Anthes, R. A., 1977: A cumulus parameterization scheme utilizing a one-dimensional cloud model, Mon. Wea. Rev., 105, 270–286.

Ardanuy PE, Kyle HL, Hoyt D; (1992) Global relationships among the Earth's radiation budget, cloudiness, volcanic aerosols, and surface temperature. *Journal of Climate*, **5**: 1120–1139.

Balachandran NK, Rind D, Lonergan P, Shindell DT; (1999). Effects of solar cycle variability on the lower stratosphere and troposphere. *Journal of Geophysical Research*, **104**: 27321-27339.

Baldwin MP, Dunkerton TJ; (1989) Observations and statistical simulations of a proposed solar cycle/QBO/weather relationships. *Geophysical Research Letters*, **16**: 863–866

Barnett TP; (1991) The interaction of multiple timescales in the tropical climate system. *J. Climate*, *4*, 269-285

Barnett, T.P., 1989 : The effect of snow cover on regional and global climate variations. J. of Atmos. Sci. Vol. 46. No. 6, p. 662-685.

Bell GT; (1977) Changes in sign of the relationship between sunspots and pressure, rainfall and the monsoon. *Weather* **32**: 26–32

Bhaskaran BR, Jones G, Murphy JM, Noguer M; (1996) Simulations of the Indian summer monsoon using a nested regional climate model: Domain size experiments. Climate Dynamics **12**: 573–578

Bjerknes J; (1969) Atmospheric teleconnections from the equatorial Pacific, *Monthly Weather Review*, **97**: 163-172

Blanford HH; (1884) On the connection of Himalayan snowfall and seasons of drought in India. *Proceedings of Royal Society*, London, **37**: 3-22

Bradley RS, Jones PD; (1993) "Little Ice Age" summer temperature variations: Their nature and relevance to recent global warming trends. *The Holocene*, **3**: 367–376

Cadet DL and Greco S; (1987); Water Vapour Transport over the Indian Ocean, during 1979 Summer Monsoon. Part II: Water Vapour Budgets, *Monthly Weather Review*, **115**: 2358–2366

Cadet DL and Reverdin G; (1981) Water Vapour Transport over the Indian Ocean, during Summer 1975. *Tellus*, **33**: 476–487

Chandrasekar A and Kitoh A; (1998) Impact of localised sea surface temperature anomalies over the equatorial Indian Ocean on the Indian Summer Monsoon. *Journal of the Meteorological Society of Japan*, **76**: 841–853

Chang CP and Li T; (2000) A theory for the tropical tropospheric biennial oscillation. *Journal of Atmospheric Sciences*, **57**: 2209–2224

Charney JG and Shukla J; (1981) Predictability of monsoons. *Monsoon dynamics* (Lighthill J, Pearce RP, eds). Cambridge University Press, pp 99–109

Chen TC and Murakami M; (1988) The 30-50 day variation of convective activity over the western Pacific ocean with the emphasis on the northwestern region. *Monthly Weather Review*, **116**: 892-906

158

Clemens, S. C., and R. J. Oglesby (1992), Interhemispheric Moisture Transport in the Indian Ocean Summer Monsoon: Data-Model and Model-Model Comparisons, *Paleoceanography*, 7: 5, 633–643.

Cocke, S., and T.E. LaRow, 2000: Seasonal Predictions Using a Regional Spectral Model Embedded within a Coupled Ocean–Atmosphere Model. **128**, 689–708

Crooks SA and Gray LJ; (2005) Characterisation of the 11-year solar signal using a multiple regression analysis of the ERA-40 dataset. *Journal of Climate*, **18**: 996–1015

Crowley TJ and Kim KY; (1995) Comparison of proxy records of climate change and solar forcing. *Geophysical Research Letters*, **22**: 933–936.

Dakshinamurti J and Keshavmurty RN; (1976) On oscillations of period around one month in the Indian summer monsoon. *Indian Journal Meteorology Hydrology Geophysics* **27**: 201-203

Dash SK., Shekhar MS and Singh GP; (2006) Simulation of Indian summer monsoon circulation and rainfall using RegCM3. *Theoretical and Applied Climatology*, **86**: 161–172.

Delsole T, Shukla J 2002: linear prediction of Indian Monsoon rainfall. *Journal of Climate*, **15**, 3645-3658

Dickinson RE, Erico RM, Giorgi F and Bates GT; (1989) A regional climate model for the western United States. *Climate Change*, **15**: 383–422.

Ding Y (2004) Seasonal march of the East-Asian summer monsoon. In: Chang CP (ed) East Asian Monsoon. World Scientific, Singapore, 564pp

Draper NR and Smith H; (1981) Applied Regression Analysis, 2nd edn. John Wiley and Sons: New York: Wiley.

Dudhia J; (1993) A nonhydrostatic version of the Penn State NCAR mesoscale model: Validation tests and simulation of an Atlantic cyclone and cold front. *Monthly Weather Review,* **121**: 1493–1513.

Dunbar, R. B., G. M. Wellington, M. W. Colgan, and P. W. Glynn. 1994. Eastern Pacific sea surface temperature since 1600 A.D.: the $\delta^{18}O$ record of climate variability in Galapagos corals. *Paleoceanography,* 9: 291–315

Emanuel KA; (1991) A scheme for representing cumulus convection in large-scale models. *Journal of Atmospheric Sciences,* **48**: 2313–2335

Findlater J; (1969) A major low-level air current near the Indian Ocean during the northern summer. *Quarterly Journal of Royal Meteorological Society,* **95**: 362–380

Fleitmann D, Burns SJ, Mudelsee M, Neff U, Kramers J, Mangini A and Matter A; (2003) Holocene forcing of the Indian monsoon recorded in a stalagmite from southern Oman. *Science,* **300**: 1737-1739

Folland CK and Rowell DP (Eds); (1995) Workshop on simulations of the Climate of the Twentieth Century using GISST. *Hadley Centre Climate Research Technical Note,* **56**

Fox J; (1991) Regression Diagnostics: An Introduction, Sage University Paper series on Quantitative Applications in the Social Sciences, Series No. 07-079. Sage: Newbury Park, CA.

Gadgil S and Asha G; (1992) Intraseasonal Variation of the Summer Monsoon .1. Observational Aspects, *Journal of the Meteorological Society of Japan,* **70**: 517-527

Gadgil S, Guruprasad A, Sikka DR and Paul DK; (1992) Intra-seasonal variations and simulation of the Indian summer monsoon. Simulation of Interannual and Intraseasonal Monsoon Variability Report of Workshop, National Center for Atmospheric Research, Boulder, Colorado, USA. 21-24

Ghosh SK, Pant PC and Dewan BN; (1978) Influence of Arabian Sea on the Indian Summer Monsoon, *Tellus*, **30**: 117–125

Giorgi F and Mearns LO; (1999) Introduction to special section: regional climate modeling revisited. *Journal of Geophysical Research*, **104**: 6335–6352

Giorgi F, Bi X and Qian Y; (2003) Indirect vs. direct effects of anthropogenic sulfate on the climate of East Asia as simulated with a regional coupled climate-chemistry/aerosol model. *Climatic Change*, **58**: 345–376

Giorgi F, Marinucci MR and Bates GT; (1993b) Development of a second-generation regional climate model (RegCM2). Part II: Convective processes and assimilation of lateral boundary conditions. *Monthly Weather Review*, **121**: 2814–2832

Giorgi F, Marinucci MR, Bates GT; (1993a) Development of a second-generation regional climate model (RegCM2). Part I: Boundary layer and radiative transfer processes. *Monthly Weather Review*, **121**: 2794–2813

Giorgi F, Shields BC, Bates GI; (1994.) Regional climate change scenarios over the United States produces with a nested regional climate model. *Journal of Climate*, **7**: 375–399

Giorgi F; (1990) Simulation of regional climate using a limited area model nested in a general circulation model. *Journal of Climate*, **3**: 941–963

Gleisner H and Thejll P; (2003) Patterns of tropospheric response to solar variability. *Geophysical Research Letters*, **30**: 17129

Goswami BN and Ajayamohan RS; (2001) Intraseasonal oscillations and interannual variability of the Indian summer monsoon, *Journal of Climate*, **14**: 1180-1198

161

Goswami BN and Xavier PK; (2005) Dynamics of 'Internal' Interannual Variability of Indian Summer Monsoon in a GCM *Journal Geophysical Research,* 110: D24104, doi:10.1029/2005JD006042.

Goswami BN; (1998) Interannual variations of Indian summer monsoon in a GCM: External conditions versus internal feedback. *Journal of Climate,* **11**: 507–522

Goswami BN; (2005) South Asian Monsoon, in Intraseasonal Variability of the Atmosphere-Ocean Climate System, edited by W. K. M. Lau and D. E. Waliser, Praxis, Springer Berlin Heidelberg, pp. 19-61

Gowariker V, Thapliyal V, Kulshrestha SM, Mandal GS, Sen RN and Sikka DR; (1991) A power regression model for long range forecast of southwest monsoon rainfall over India, *Mausam,* **42**:125-130

Gowariker V, Thapliyal V, Sarker RP, Mandal GS and Sikka DR; (1989) Parameteric and power regression models: New approach to long-range forecasting of monsoon rainfall in India. *Mausam,* **40**: 115-122

Gregory S; (1989) Macro-regional definition and characteristics of Indian summer monsoon rainfall 1871-1985. *International Journal of Climatology,* **9**:465-483.

Grell GA, Dudhia J and Stauffer DR; (1994) A description of fifth generation Penn State/NCAR Mesoscale Model (MM5). *NCAR Technical Notes,* NCAR/TN-398+STR, 21.

Grell GA; (1993) Prognostic evaluation of assumptions used by cumulus parameterizations. *Monthly Weather Review,* **121**: 764 -787.

Haigh JD, Austin J, Butchart N, Chanin ML, Crooks S, Gray LJ, Halenka T, Hampson J, Hood LL, Isaksen ISA, Keckhut P, Labitzke K, Langematz U, Matthes K, Palmer M, Rognerud B, Tourpali K and Zerefos C; (2004) Solar variability and climate: selected results from the SOLICE project. *SPARC Newsletter No.* 23

Haigh JD, Blackburn M and Day R; (2005) The response of tropospheric circulation to perturbations in lower stratospheric temperature. *Journal of Climate.* 18(17): 3672

Haigh JD; (1999) A GCM study of climate change in response to the 11-year solar cycle. *Quarterly Journal of Royal Meteorological Society,* 125: 871-892

Haigh JD; (2003) The effects of solar variability on the Earth.s climate. *Philosophical Transactions of the Royal Society,* London. 361: 95-111

Halpern D and Woiceshyn PM; (1999) Onset of the Somali Jet in the Arabian Sea during June 1997. *Journal of Geophysical Research,* 104: 18041–18046

Hansen JA, Lacis D, Rind G, Russell P, Stone I, Fung R, Ruedy and Lerner J; (1984) Climate sensitivity: Analysis of feedback mechanisms. *Climate Processes and Climate Sensitivity,* Geophysical Monograph, 29: American Geophysical Union, 130–163.

Hastenrath S and Greischar L; (1993) Changing predictability of Indian monsoon rainfall anomalies? *Proceedings of the Indian Academy of Science,* 102: 35–47

Hastenrath S and Lamb P; (1980) On the heat budget of hydrosphere and Atmosphere in the Indian Ocean. *Journal of Physical Oceanography,* 10: 694-708

Hastenrath S; (1987) On the prediction of India monsoon rainfall anomalies. *Journal of Climate and Applied Meteorology,* 26: 847–857

Hastenrath S; (1991) Climate Dynamics of the Tropics. Kluwer Academic Publishers, Dordrecht, The Netherlands, 488 pp

Hastenrath, S. and Lamb, PJ. 1980. On the heat budget of the hydrosphere and atmosphere in the Indian Ocean. Journal of Physical Oceanography, 10, 694-708.

Hazallah A and Sadourny R; (1995) Internal versus SST forced atmospheric variability simulated by an atmospheric general circulation model. *Journal of Climate*, **8**: 474–495

Herman JR and Goldberg RA; (1978) Sun, Weather and Climate, Washington: NASA

Hircmath KM and Mandi PI; (2004), New Astronomy, **9**: 651.

Hiremath KM; (2006) The Influence of Solar Activity on the Rainfall over India: Cycle-to-Cycle Variations. *Journal of Astrophysics and Astronomy*, **27**: 367–372

Holtslag AAM, Bruijin EIF de and Pan HL; (1990) A high resolution air mass transformation model for short range weather forecasting. *Monthly Weather Review*, **118**: 1561–1575

Houghton JT, Mcira FLG, Bruce J, Hoesung Lee, Callander BA, Haites E, Harris N, and Maskell K, Eds., (1995) Climate Change 1994: Radiative Forcing of Climate Change

Howland MR and Sikdar DN; (1983) The Moisture Budget over the North Eastern Arabian Sea During the Pre-monsoon and Monsoon onset 1979, *Monthly Weather Review*, **111**: 2255–2268.

Hoyt DV, Schatten KH; (1993) A discussion of plausible solar irradiance variations, 1700–1992. Journal of Geophysical Research **98**: 18895–18906

Hsie EY, Anthes RA, Kiyser D; (1984.) Numerical simulation of frontogenesis in a moist atmosphere. Journal of the Atmospheric Sciences **41**: 2581–2594

Hsu HH, Weng CH and Wu CH; (2004) Contrasting characteristics between the northward and eastward propagation of the intraseasonal oscillation during the boreal summer. *Journal Climate*, **17**: 727-743

164

Hudgins L, Friehe CA and Mayer ME; (1993) Wavelet transforms and atmospheric turbulence. *Physical Review Letters*, **71**: 3279–3282

James IN and James PM; (1989) Ultra-low-frequency variability in a simple atmospheric circulation model. *Nature*, **342**: 53–55

Ji Y and Vernekar AD; (1997) Simulation of the Asian summer monsoons of 1987 and 1988 with a regional model nested in a global GCM. *Journal of Climate*, **10**: 1965–1979

Jiang XN, Li T and Wang B; (2004) Structures and mechanisms of the northward propagating boreal summer intraseasonal oscillation. *Journal of Climate*, **17**: 1022-1039

Jones R, Murphy GJM and Noguer M; (1995) Simulation of climate change over Europe using a nested regional climate model. Part- I: assessment of control climate, including sensitivity to location of lateral boundaries. *Quarterly Journal of the Royal Meteorological Society*, **121**: 1413–1449.

Joseph PV and Pillai PV; (1984) Air-sea interaction on a seasonal scale over North Indian Ocean - Part I: Inter-annual variations of sea Surface Temperature and Indian summer monsoon rainfall. *Mausam*, **35**: 323-330

Joseph PV and Raman PL; (1966) Existence of low-level westerly jet stream over peninsular India during July; *Indian Journal of Meteorology and Geophysics*, 407-410

Ju J and Slingo JM; (1995) The Asian Summer Monsoon and ENSO. *Quarterly Journal of the Royal Meteorological Society*, **121**: 1133-1168

Kalnay E, Kanamitsu M, Kistler R, Collins W, Deaven D, Gandin L, Iredell M, Saha S, White G, Woollen J, Zhu Y, Leetmaa A, Reynolds R, Chelliah M, Ebisuzaki W, Higgins W, Janowiak J, Mo KC, Ropelewski C, Wang J, Roy Jenne and Dennis

Joseph; (1996) The NCEP/NCAR 40 year reanalysis project. *Bulletin of American Meteorological Society*, **77**: 437 – 471

Kemball-Cook S and Wang B; (2001) Equatorial waves and air-sea interaction in the Boreal summer intraseasonal oscillation. *Journal of Climate*, **14**: 13, 2923-2942

Kida, H., T. Koide, H. Sasaki, and M. Chiba, (1991) A new approach for coupling a limited area model to a GCM for regional climate simulations. *J. Meteor. Soc. Japan*, **69**, 723–728

Kishtawal CM, Gautam N, Jaggi S and Pandey PC, (1994) Surface-level moisture transport over the Indian Ocean during southwest monsoon months using NOAA/ HIRS data. *Boundary Layer Meteorology*, 69, 159–171

Kishtawal CM, Pal PK and Narayanan MS; (1991) Water Vapour Periodicities over Indian Ocean during Contrasting Monsoons from NOAA Satellite Data, *Proceedigs of the Indian Academy of Science*, (Earth Planet. Sci.), 100, 341–359

Kripalani RH, Kulkarni A and Sabade SS; (1999) Characteristic features of intraseasonal MJOs over the Indo-Pacific region as revealed by NCEP/NCAR Reanalysis data. Proc Second WCRP Int Conf on Reanalysis, Reading, UK, WCRP-109, WMO/TD No. 985: 294-297

Kripalani RH, Singh SV and Arkin PA; (1991) Large scale features of rainfall and outgoing long wave radiation over India and adjoining regions. *Contributions to Atmospheic Physics*, **64**: 159-168

Krishnamurthy V and Shukla J; (2000) Intraseasonal and interannual variability of rainfall over India. *Journal of Climate*, **13**: 4366-4377.

Krishnamurti TN and Ardunay P; (1980) The 10 to 20 day westward propagating mode and "breaks in the monsoons." *Tellus*, **32:** 15–26

166

Krishnamurti TN and Bhalme HN; (1976) Oscillations of monsoon system. Part I. Observational aspects. *Journal of Atmospheric Sciences*, **33**: 1937–1954

Krishnan R, Zhang C and Sugi M; (2000) Dynamics of Breaks in the Indian Summer Monsoon, *Journal of Atomospheric Science*, **57**: 9, 1354-1372

Kumar KK, Rupa KK and Pant GB; (1997) Pre-monsoon maximum/minimum temperatures over India in relation to the summer monsoon rainfall. *International Journal of Climatology*, **17**: 1115-1127

Kumar KK, Soman MK and Rupa KK; (1995) Seasonal forecasting of Indian summer monsoon rainfall. *Weather*, **50**: 449–467

Labitzke K and van Loon H; (1993a) Some recent studies of probable connections between solar and atmospheric variability. *Annales Geophysicae*, **11**: 1084–1094

Labitzke K and van Loon H; (1993b) Aspects of a decadal sun–atmosphere connection. The Solar Engine and its Influence on Terrestrial Atmosphere and Climate, E. NesmeRibes, Ed., ASI Series I: Global Environmental Change **25**: 381–393.

Labitzke K; (2002) The solar signal of the 11-year sunspot cycle in the stratosphere: differences between the northern and southern summers. *Journal of Meteorological Society of Japan*, **80**: 963-971

Lau KM and Shen S; (1988) Dynamics of Intraseasonal Oscillations and ENSO. *Journal of Atmospheric Sciences*, **45**: 1781-1797.

Lawrence DM and Webster PJ; (2002) The boreal summer intraseasonal oscillation: Relationship between northward and eastward movement of convection. *Journal Atmospheric Sciences*, **59**: 1593-1606

Lean J and Rind D; (1998) Climate forcing by changing solar radiation. *Journal of Climate*, **11**: 3069-3094

Li WP (1999) Moisture flux and water balance over the South China Sea during late boreal spring and summer. Theor Appl Climatol 64:179–187

Liu F. Yang G, Wang h, Chen Z and Zhou Y 2006. Thermochem. Acta 443, 212pp

Lockyer N and Lockyer WJS; (1904) The behaviour of the short-period atmospheric pressure variation over the earth's surface. *Proceedings of Royal Society*, London **73**: 457-470

Ma Lihua, Han Y and Yin Z; (2007) The possible influence of solar activity on Indian monsoon. *Applied geophysics*, **4**: 231-237

Makridakis S, Wheelwright SC, Hyndman RB 1998. Forecasting Methods and applications *John Wiely and sons* 241-310 pp

Mann ME and Park J; (1994) Global-scale modes of surface temperature variability on interannual to century timescales. *Journal of Geophysical Research*, **99**: 25819–25833

Mc Cuen RH; (1985) Statistical Methods for Engineers. Prentice Hall: New Jersey; 439.

McCreary JP, Kundu PK and Molinari R; (1993) A numerical investigation of dynamics, thermodynamics and mixed-layer processes in the Indian Ocean. *Progress in Oceanography*, **31**: 181–244

Mearns LO, Schneider SH, Thompson SL and McDaniel LR; (1990) Analysis of climate variability in general circulation models: comprasion with observations and changes in variability in 2xCO2 experiments. *Journal of Geophysical Research*, **95**: 20469–20490

Meehl GA and Arblaster JM; (2002) Indian monsoon GCM sensitivity experiments testing tropospheric biennial oscillation transition conditions. *Journal of Climate*, **15**: 923–944

Meehl GA; (1987) The tropics and their role in the global climate system. *Geographical Journal*, **153**: 21–36

Meehl GA; (1993) A coupled air-sea biennial mechanism in the tropical Indian and Pacific regions: Role of the ocean. *Journal of Climate*, **6**: 31–41

Meehl GA; (1994) Influence of the land surface in the Asian summer monsoon: External conditions versus internal feedbacks. *Journal of Climate*, **7**: 1033–1049

Meehl GA; (1997) The South Asian monsoon and the tropospheric biennial oscillation. *Journal of Climate*, **10**: 1921-1943

Mehta VM and Delworth T; (1995) Decadal variability of the tropical Atlantic ocean surface temperature in shipboard measurements and in a global ocean–atmosphere model. *Journal of Climate*, **8**: 172–190

Mesinger F; (1984) A blocking technique for representation of mountains in atmospheric models. *Riv Meteor Aeronaut*, **44**: 195–202

Mitra, K., and Dutta, S. N., 1992, 18.6-year luni-solar nodal and 10-11-year solar signals in rainfall in India: International Journal of Climatology, **12**: 839–851.

Mohanakumar K; (2008) Stratosphere Troposphere Interactions; An Introduction, XVII, 416 p. ISBN: 978-1-4020-8216-0

Mohanty UC, Bhatla R, Raju PVS, Madan OP and Sarkar A; (2002) Meteorological fields variability over the Indian seas in pre and summer monsoon months during extreme monsoon seasons. *Procedings of Indian Academy Sciences (Earth and Planet Sciences)*, **111**: 3, 365-378

Mohanty UC, Dube SK and Singh MP; (1983) A study of heat budget over the Arabian Sea and their role in the onset and maintenance of Summer monsoon. *Journal of Meteorological Society Japan*, **61**: 208-221

Mohanty UC, Kumar NM and Potty KVJ; (1994) Variability of Indian summer monsoon in relation to oceanic heat budget over the Indian seas. *Dynamics of Atmospheres and Oceans*, **21**: 1-22

Murakami T, Nakazawa T and J He; (1984) On the 40–50 day oscillations during the 1979 Northern Hemisphere summer. I: Phase propagation. *Journal of the Meteorological Society of Japan*, **62**: 440–468

Murakami T; (1976) Analysis of summer monsoon fluctuations over India. *Journal Meteorological Society Japan*, **54**: 15-31

Murakami T; (1977) Spectrum analysis relevant to Indian monsoon. *Pure Applied. Geophysics*, **115**: 1145-1166

Nair VG and Mohanakumar K; (2009) A modeling study in mountain Meteorology: Impact of Western Ghats Orography on the Weather and Climate of South India-a meso-scale modeling study. VDM Verlag.

Nayagam LR, Rajesh J and Ram Mohan HS; (2007) An empirical model for the seasonal prediction of southwest monsoon rainfall over Kerala, a meteorological subdivision of India, *International Journal of Climatology*, **28**: 6, 823 – 831

Neff U, Burns SJ, Mangini A, Mudelsee M, Fleitmann D and Matter A; (2001) Strong coherence between solar variability and the monsoon in Oman between 9 and 6 kyr ago. *Nature*, **411**: 290-293

Neter J, Wasserman W and Kutner MH; (1990) Applied Linear Statistical Models, 3d edn Homewood, Illinois: Richard D. Irwin, Inc; 1181.

170

Nicholls N; (1984) The stability of empirical long-range forecast techniques: A case study. *Journal of Climate and Applied Meteorology*, **23**: 143–147

Overpeck JT, Anderson DM, Trumbore S and Prell WL; (1996) The southwest monsoon over the last 18,000 years. *Climate Dynamics*, **12**: 213-225

Pal JS, Small EE and Eltahir EAB; (2000) Simulation of regional-scale water and energy budgets: Representation of subgrid cloud and precipitation processes within RegCM. *Journal of Geophysical Research Atmospheres* **105**: 29579 –2594

Palmer TN, Brankovic C, Viterbo P and Miller MJ; (1992) Modelling interannual variations of summer monsoons. *Journal of Climate*, **5**: 399-417

Palmer TN and Anderson DLT; (1994) The prospect for seasonal forecasting- a review paper. Quarterly Journal of Royal Meteorological Society. **120**: 755-793

Pant GB and Rupa Kumar K; (1997) Climates of South Asia, John Wiley and Sons, Chichester, ISBN: 0471949485

Parthasarathy B and Mooley D; (1978) Some Features of a Long Homogeneous Series of Indian Summer Monsoon Rainfall. *Monthly Weather Review*, 106: 771–781

Parthasarathy B and Sontakke NA; (1988) El-Nino/SST of Puerto Chicama and Indian summer monsoon rainfall - Statistical relationships. *Geofisica Internacionale*, **27**: 37-59

Penner JE; (1995) Carbonaceous aerosols influencing atmospheric radiation: Black and organic carbon. *Proceedings of the Dahlem Workshop on Aerosol Forcing of Climate*, R.J. Charlson and J. Heintzenberg (eds.). John Wiley & Sons, Chichester.

Percival DP; (1995) On estimation of the wavelet variance. *Biometrika*, **82**: 619–631

Perrier V, Philipovitch T and Basdevant C; (1995) Wavelet spectra compared to Fourier spectra. *Journal of Mathematical Physics*, **36**: 1506–1519

171

Perry CA; (1994) Solar-irradiance variations and regional precipitation fluctuations in the western USA. *International Journal of Climatology*, **14**: 969–983

Pisharoty PR; (1965) Evaporation from the Arabian Sea and the Indian South West Monsoon, *Proceedings of Symposia on Meteorological Results*, I.I.O.E., Bombay, 43–54

Pittock AB; (1979) Solar cycles and the weather: Successful experiments in autosuggestion? Solar-Terrestrial Influences on Weather and Climate, B. M. McCormac and T. A. Selida, Eds., D. Reidel, 181–191

Potemra JT, Luther ME and O'Brien JJ; (1991) The seasonal circulation of the upper ocean in the Bay of Bengal; *Journal of Geophysical Research*, **96**: 12667-12683

Prasad KD and Singh S; (1992) Possibility of Indian monsoon rainfall prediction on reduced spatial and temporal scale. *Journal of Climate*, **5**: 1357-1361

Qian Y and Giorgi F; (1999) Interactive coupling of regional climate and sulfate aerosol model over eastern Asia. *Journal of Geophysical Research*, **104**: 6477–6500

Rajeevan M, Bhate J, Kale JD and Lal B; (2005) Development of a high resolution daily gridded rainfall data for the Indian region 2005, *IMD Met Monograph Climatology*. 22

Rajeevan M, Guhathakurta P and Thapliyal V; (2000) New Models for Long Range Forecasts of Summer Monsoon Rainfall over North West and Peninsular India. *Meteorology and Atmospheric Physics*, **73**: 211-225

Rajeevan M, Pai DS and Thapliyal V; (2002) Predictive relationships between Indian Ocean Sea surface temperatures and Indian summer monsoon Rainfall *Mausam*, **53**: 337-348

Rajeevan M, Pai DS, Dikshit SK and Kelkar RR; (2004) IMD's new operational models for long-range forecast of southwest monsoon rainfall over India and their verification for 2003. *Current Science*, **86**: 422-431

Rajeevan M, Guhathakurta P and Thapliyal V; (2000) New Models for Long range forecasts of summer monsoon rainfall over NW India and Peninsular India. *Meteorology and Atmospheric Physics*, **73**: 211-225

Rajeevan M; (2001) Prediction of Indian summer monsoon: Status, problems and prospects, *Current Science*, **81**: 1451-1457

Raju PVS, Mohanty UC and Bhatla R; (2005) Onset characteristics of the southwest monsoon over India, *International Journal of Climatology*, **25**: 2, 167 – 182

Rakhecha PR and Pisharoty PR; (1996) Heavy rainfall during monsoon season: Point and spatial distribution. *Current Science*, **71**: 179-186

Ramage CS; (1971) Monsoon Meteorology. New York: Academic Press, 296pp

Kumar RMR and Sastry JS; (1990) Relationship between sea surface temperature, Southern Oscillation, position of the 500 mb ridge along 75°E in April and the Indian monsoon rainfall. *Journal of the Meteorological Society of Japan*, **68**: 741–745

Rao KG and Goswami BN; (1988) Interannual Variations of sea Surface Temperatures over the Arabian Sea and the Indian Monsoon: A New Perspective. *Monthly Weather Review*, **116**: 558-568

Rasmusson EM, Wang X and Ropelewski CF; (1990) The biennial component of ENSO variability. *Journal of Marine Systems*, **1**: 71-96

Rind D, Goldberg R and Ruedy R; (1989) Change in climate variability in the 21st century. *Climatic Change*, **14**: 5–37

Robock, A., and M. P. Free. 1995. Ice cores as an index of global volcanism from 1850 to the present. *Journal of Geophysical Research* 100:11549-11567

Sadhuram Y and Ramesh Kumar MR; (1988) Does Evaporation over the Arabian Sea Play a Crucial Role in Moisture Transport Across the West Coast of India during an Active Monsoon Period? *Monthly Weather Review*, **116**: 307–312

Sadhuram Y, Ramesh BV, Gopalakrishna VV and Sharma MSS; (1991) Association between Pre-monsoonal Sea Surface Temperature anomaly field in the eastern Arabian sea and subsequent monsoon rainfall over the west coast of India. *Indian Journal of Marine Sciences*, **20**: 106-109

Saha KR and Bavadekar SN; (1973) Water vapour budget and precipitation over the Arabian Sea during the northern summer. *The Quarterly Journal of the Royal Meteorological Society*, **99**: 420, 273 - 278

Saha KR and Bavadekar SN; (1977) Moisture flux across the west coast of India and rainfall during the southwest monsoon. *Quarterly Journal of the Royal Meteorological Society*, **103**: 370-374

Saha KR; (1970a) Zonal anomaly of sea surface temperature in equatorial Indian Ocean and its possible effect upon monsoon circulation. *Tellus*, **22**: 403-409

Saha KR; (1970b) Air and water vapor transport across the equator in western Indian Ocean during northern summer. *Tellus*, **22**: 681-687

Saha KR; (1974) Some aspects of the Arabian sea summer monsoon. *Tellus*, **26**: 464-476

Sahai AK, Grimm AM, Satyan V and Pant GB; (2003) Long-lead prediction of Indian summer monsoon rainfall from global SST evolution. *Climate Dynamics*, **20**: 855–863

Salby ML and Shea DJ; (1991) Correlations between solar activity and the atmosphere: An unphysical explanation. *Journal of Geophysical Research*, **96**: 22579–22595

Schneider D; (2005) Living in sunny times. *American Sciences*, 93: 22–24

Schott F, Reppin J, Fischer J and Quadfasel D (1994) Currents and transports of the monsoon current south of Sri Lanka, *Journal of Geophysical Research*, **99**(C12): 25127–25141

Shekhar MS and Dash SK; (2005) Effect of Tibetan spring snow on the Indian summer monsoon circulation and associated rainfall. *Current Science*, **88**: 11 – 10

Shen, S. H., and K. M. Lau; 1995: Biennial Oscillation Associated with the East Asian Summer Monsoon and Tropical Sea Surface Temperature. *J. Met. Soci. Japan*, 73, 105-124.

Sheperd T G; (2002) Issues in Stratosphere-troposphere Coupling. *Journal of the Meteorological Society of Japan*, **80**: 4B, 769-792

Shindell DT, Rind D, Balachandran N, Lean J and Lonergan P; (1999). Solar cycle variability, ozone and climate. *Science*, **284**: 305-308

Shindell DT, Schmidt GA, Mann ME, Rind D and Waple A; (2001b) Solar forcing of regional climate change during Maunder minimum. *Science*, 294: 2149 – 2152

Shindell DT, Schmidt GA, Miller RL, Rind D; (2001a) Northern hemisphere winter climate response to green house gas, ozone, solar and volcanic forcing. *Journal of Geophysical Research*, **106**: 7193-7210

Shukla J and Mishra BM; (1977) Relationships between sea surface temperature and wind speed over the central Arabian Sea and monsoon rainfall over India. *Monthly Weather Review*, **105**: 998–1002

Shukla J; (1975) Effect of Arabian Sea surface temperature anomaly on Indian summer monsoon: a numerical experiment with GFDL model. *Journal of the Atmospheric Sciences*, **32**: 503–511

Shukla J; (1987) In Interannual Variability of Monsoons, Fein JS, Stephens PL (eds). Monsoons. Wiley: Chichester; 399–464.

Sikka DR and Gadgil S; (1980) On the maximum cloud zone and the ITCZ over Indian longitudes during the southwest monsoon. *Monthly Weather Review*, **108**: 1840–1853

Singh G. P., Jai-Ho Oh (2007) Impact of Indian Ocean sea-surface temperature anomaly on Indian summer monsoon precipitation using a regional climate model. *International Journal of Climatology*, Volume 27 Issue 11, Pages 1455 – 1465

Singh R; (1983) Study of sea Surf ace Pressure, sea Surf ace Temperature and cloudiness patterns over Indian ocean region in some contrasting South West monsoon rainfall in India - Part II, *Mausam*, **34**: 205-212

Singh SV and Kripalani RH; (1985) South to north progression of rainfall anomalies across India during summer monsoon season. *Pure and Applied Geophysics*, **123**: 624-637

Singh SV and Kripalani RH; (1986) Application of the extended empirical orthogonal function analysis to interrelationships and sequential evolution of monsoon fields. *Monthly Weather Review*, **114**: 1603-1610

Soman MK and Slingo JM; (1997) Sensitivity of the Asian Summer Monsoon to aspects of the sea surface temperature anomalies in the tropical Pacific Ocean. *Quarterly Journal of the Royal Meteorological Society*, **123**: 309-336

176

Somayajulu YK, Murty VSN and Sarma YVB; (2003) Seasonal and inter-annual variability of surface circulation in the Bay of Bengal from TOPEX/Poseidon altimetry, Deep Sea Research Part II: *Topical Studies in Oceanography*, 50: 5, 867-880

Thapliyal V; (1987) Prediction of Indian monsoon variability evaluation and prospects including development of a new model. In Climate of China and global climate (D. Ye, C. Fu, J. Chano and M. Yoshino (eds)), ChinaOcean Press, 397–416

Thapliyal V; (1990) Long range prediction of summer monsoon rainfall over India: Evolution and development of new models. *Mausam*, 41: 339-346

Torrence C and Compo GP; (1998) A Practical Guide to Wavelet Analysis, *Bulletin of the American Meteorological Society*, 79: 61–78.

Toshiro I; (1997) Contrast of 87/88 Indian summer monsoon observed by split window measurements, *Advances in Space Research*, 19: 3, 447-455

Valsala VK and Ikeda M; (2005) An Extreme Drought Event in the 2002 Summer Monsoon Rainfall and its Mechanism Proved with a Moisture Flux Analysis, *SOLA*, 1: 173-176.

Vecchi GA and Harrison DE; (2002) Monsoon breaks and subseasonal sea surface temperature variability in the Bay of Bengal, *Journal of Climate*, 15(12), 1485-1493.

Vinayachandran PN and Shetye SR; (1991) the warm pool in the Indian Ocean. Proceedings of the Indian Academy of Science (Earth and Planetary Sciences.) 100: 165-175

Visser H and Molenaar J; (1995) Trend estimation and regression analysis in climatological time series: An application of structural time series models and the Kalman filter. *Journal of Climate*, 8: 969–979

\ on Storch H, Langenberg H and Feser F; (2000) A spectral nudging technique for dynamical downscaling purposes. *Monthly Weather Review*, **128**: 3664-3673

Wajsowicz, R. C. and Schopf 2001: Oceanic influences on the seasonal cycle in evaporation over the Indian Ocean. *Journal of Climate*, **14**: 1199-1226

\ ilker GT; (1908) Correlations in seasonal variations of weather, II. *Memoirs India.Meteorol. Dept.* **20**: 117-124

Walker GT; (1918) Correlation in seasonal variation of weather. *Quarterly Journal of the Royal Meteorological Society*, **44**: 223-224

Walker GT; (1923) Correlations in seasonal variations of weather, VIII. A preliminary study of World Weather I. *Memoirs of India Meteorological Department.* **24**: 75-131.

Walker GT; (1924.) Correlations in seasonal variations of weather, IX, A further study of world weather (World weather II). *Memoirs of India Meteorological Department.* B: 275-332.

Walsh K and McGregor JL; (1995) January and July regional climate simulations over the Australian region using a limited area model. *Journal of Climate*, **8**: 2387–2403

Wang Y, Sen OL and Wang B; (2003) A highly resolved regional climate model (IPRC–RegCM) and its simulation of the 1998 severe precipitation events over China. Part I: Model description and verification of simulation. *Journal of Climate*, **16**, 1721-1738

Washington W, Chervin R and Rao GV; (1977) Effects of variety of Indian Ocean Surface anomaly patterns on the summer monsoon circulation: Experiments with the NCAR GCM. *Pure and Applied Geophysics*, **115**:1335-1356

Weare BC; (1979) A statistical study of the relationships between ocean surface temperatures and the Indian monsoon. *Journal Atmospheric Sciences*, **36**: 2279–2291

178

Webster PJ, Magana VO, Palmer TN, Shukla J, Tomas RA, Yanai M and Yasunari T; (1998) Monsoons: process, predictability and the prospects for prediction. *Journal of Geophysical Research* **103**: 14451–14510.

White WB, Lean J, Cayan DR and Dettinger MD; (1997). Response of global upper ocean temperature to changing solar irradiance. *Journal of Geophysical Research* **102**: 3255–3266.

Wilks DS 1995. Statitsical methods in atmospheric Sciences, an introduction. *Intrenational geophysical series* 59, Academic press, 464pp

Yasunari T; (1979) Cloudiness fluctuation associated with the northern hemisphere summer monsoon. *Journal of Meteorological Society of Japan,* **57**: 227-242

Yasunari T; (1980) A quasi-stationary appearance of 30–40 day period in the cloudiness fluctuation during summer monsoon over India. Journal of Meteorological Society Japan, **58**: 225–229

Yasunari T; (1981) Structure of an Indian summer monsoon system with around 40-day period. *Journal Meteorological Society Japan,* **59**: 336–354

Yokoi S and Satomura T; (2006) Mechanisms of the northward movement of submonthly scale vortices over the Bay of Bengal during the boreal summer. *Monthly Weather Review,* **134**: 2251-2265

Yu L, Weller RA and Liu WT; (2003): Case analysis of a role of ENSO in regulating the generation of westerly wind bursts in the western equatorial Pacific. *Journal of Geophysical Research,* **108**(4): 3128, doi:10.1029/2002JC001498.

179

LIST OF PUBLICATIONS

Refereed Journals

1) Lorna R. Nayagam, **Rajesh Janardanan**, H. S. Ram Mohan: *An empirical model for the seasonal prediction of southwest monsoon rainfall over Kerala, a meteorological subdivision of India.*, International Journal of Climatology,

2) **Rajesh Janardanan**, Lorna R Nayagam and Mohanakumar Kesavapillai. *Solar signal in seasonal moisture fields over peninsular India.*, Journal of Atmospheric and Solar-Terrestrial Physics, (Under Revision)

3) **Rajesh Janardanan**, Lorna R Nayagam and Mohanakumar Kesavapillai. *Relation of some meteorological and oceanic parameters over adjoining oceanic region with the Peninsular Indian rainfall.* Theoretical and Applied Climatology (Submitted)

4) Lorna R. Nayagam, **Rajesh Janardanan**, H. S. Ram Mohan, *Variability and tele connectivity of north east monsoon rainfall over India,* Global and Planetary Change (under revision)

Conference Proceedings

1) Lorna R. Nayagam, **Rajesh J.** and H. S. Ram Mohan: *A Multiple Linear Regression Model for the Seasonal Prediction of Rainfall over Peninsular India,* Proceedings of 10th International Meeting on Statistical Climatology (10IMSC) August 20-24, 2007, Beijing, China.

2) Lorna R. Nayagam, **Rajesh J.** and H. S. Ram Mohan: *Seasonal Prediction of Rainfall over Peninsular India using a Principal Component Regression Model,* Proceedings of 10th International Meeting on Statistical Climatology (10IMSC) August 20-24, 2007, Beijing, China.

3) **J. Rajesh,** Lorna R. Nayagam, K. Mohankumar and H. S. Ran Mohan: *Long Range Forecasting of Monsoon Rainfall over Peninsular India for Recent Years,* Proceedings of 10th International Meeting on Statistical Climatology (10IMSC) August 20-24, 2007, Beijing, China.

4) **J. Rajesh,** Lorna R. Nayagam, H. S. Ran Mohan and K. Mohankumar: *Prediction of Monsoon rainfall over Peninsular India using parameters over Arabian Sea and adjacent seas,* Proceedings of 10th International Meeting on Statistical Climatology (10IMSC) August 20-24, 2007, Beijing, China.

5) **Rajesh J.,** and K. Mohankumar *'Solar signal in the monsoon and post monsoon Total Precipitable Water over Peninsular India region'* International CAWSES Symposium held in Kyoto, Japan, 23-27 October 2007

6) **J. Rajesh,** G. Mrudula and K. Mohan Kumar. *Three-dimensional wind characteristics in the troposphere and lower stratosphere over Gadanki during the 1996 Monsoon,* Workshop on Dynamical Coupling in the Equatorial Atmosphere- Ionosphere System (DYCEAIS – 2002), Tirunelveli, May 1-4, 2002.

7) **Rajesh J.** and K. Mohankumar *'Decadal Variability in the monsoon and post monsoon total Precipitable water over Peninsular India region'* (in JPS001 session

181

Interannual and Interdecadal Climate variability), IUGG 2007 held at Perugia University, Perugia, Italy on 2-13 July 2007

8) **Rajesh J.** and K. Mohankumar *'Solar cycle signal in the seasonal moisture field over the Peninsular Indian region'* (in MS020 session Solar activity and its influences on the Earths Weather and Climate (IRC)), IUGG 2007 held at Perugia University, Perugia, Italy on 2-13 July 2007

9) **Rajesh Janardanan,** Kesavapillai Mohanakumar and Lorna Rajanayagam, *'Effects of warm Arabian Sea surface temperature on the Summer monsoon over peninsular Indian region'*, 37th COSPAR Scientific Assembly, July 13-20, 2008, Montreal, Canada

10) **Rajesh Janardanan,** Kesavapillai Mohanakumar and Lorna Rajanayagam, *'Moisture characteristics over Indian region during summer Monsoon using RegCM3'*, 37th COSPAR Scientific Assembly, July 13-20, 2008, Montreal, Canada.

11) **Rajesh J,** Lorna R. Nayagam and K. Mohankumar, *'Impact of ocean warming over Indian subcontinent'*, GLOWINO 2008, August 22-23 2008, Neyyoor, Tamil Nadu, India

12) K. Mohanakumar, Prasanth A. Pillai and **Rajesh J.,** *'Stratosphere Troposphere interaction over tropical monsoon region'*. SPARC Assembly, September 1-5, 2008, Bologna, Italy.